Stony Brook University

Signaling Interactions During Early Zebrafish Development

A Dissertation Presented

by

Fatma Olcay Kok

to

The Graduate School

in Partial Fulfillment of the

Requirements

for the Degree of

Doctor of Philosophy

In

Molecular and Cellular Biology

Stony Brook University

December 2010

Stony Brook University

The Graduate School

Fatma Olcay Kok

We, the dissertation committee for the above candidate for the

Doctor of Philosophy degree,

hereby recommend acceptance of this dissertation.

Dr. Howard I. Sirotkin, Associate Professor, Department of Neurobiology and Behavior, State University of New York at Stony Brook (Dissertation Advisor)

Dr. Gerald H. Thomsen, Professor, Department of Biochemistry and Cell Biology,State University of New York at Stony Brook (Chairperson of Defense)

Dr. J. Peter Gergen, Professor, Department of Biochemistry and Cell Biology, State University of New York at Stony Brook

Dr. Ken-Ichi Takemaru, Associate Professor, Department of Pharmacology, State University of New York at Stony Brook

Dr. Nurit Ballas, Research Associate Professor, Department of Biochemistry and Cell Biology, State University of New York at Stony Brook

This Dissertation is accepted by the Graduate School

Lawrence B. Martin
Dean of the Graduate School

Abstract of the Dissertation

Signaling Interactions During Early Zebrafish Development

by

Fatma Olcay Kok

Doctor of Philosophy

In

Molecular and Cellular Biology

Stony Brook University

2010

During early embryonic development, a collection of mechanisms regulate the formation of complex structures by temporally and spatially controlling cell fate decisions. This control is largely mediated by intercellular signaling pathways and secreted molecules. In this dissertation, I studied the molecular mechanisms regulating two important patterning processes, somitogenesis and neurogenesis, during vertebrate development.

Somitogenesis is a highly controlled process which segments the mesoderm and outlines the vertebrate body axis. The Notch pathway is vital for the regulation of synchronized gene expression while FGF signaling regulates the ability of presomitic mesoderm to mature and form segment boundaries. It is important to identify the regulators of Notch and FGF signaling to dissect how temporal and spatial cues are established during somitogenesis. Here, I report that the embryonic lethal *SBU2* mutation is a result of a nonsense mutation on *spt6* gene. These mutants have wide variety of developmental problems including severe somite defects. I found that Spt6 is essential for the Notch pathway regulated transcriptional response and that the somite defects in *SBU2* mutants are the result of suppressed Notch signaling.

In a complementary study, I investigated the function of ChCh and Sip1a during zebrafish somitogenesis. Microinjection of *chch* and *sip1a* morpholinos caused formation

of short and narrow somites, suggesting that these genes have indispensable roles in regulating somite formation in zebrafish. Further analysis of *chch* and *sip1a* morphants indicated persistent cyclic *her1* and *her7* expression as well as rostral expansion of *fgf8* expression. These results demonstrated novel roles for ChCh and Sip1a in repression of FGF8 activity during somitogenesis.

Neural development is another important process which generates and shapes the nervous system. This progression is controlled by both negative and positive regulators. Rest is a transcriptional repressor which silences neural promoters in non-neural cell lines but the function of Rest in early neural development *in-vivo* is not studied extensively. Here, I studied the function of Rest in zebrafish neurogenesis. Targeted mutation of *rest* caused de-repression of a subset of Rest target genes during early development and in the long term. Overall, I showed that although Rest is required for regulation of neural genes *in-vivo*, it is not necessary for early neural development.

Table of Contents

List of Figures

List of Tables

Chapter 1: Background and Significance

1.1 Zebrafish as a model organism for embryonic development

Since the early 1970s, zebrafish has become one of the most important model organisms to unravel vertebrate development and gene function. This model organism has unique combination of genetic and experimental advantages that make them easy to maintain, manipulate and examine in the laboratory.

Zebrafish is a vertebrate model organism and has developmental attributes that make them useful for biomedical research. For example, some aspects of development such as somite, vertebra, and neural crest formation is seen exclusively in vertebrates. Moreover, complex organ systems such as heart, kidneys, and brain, are best studied in vertebrate models. Zebrafish has many advantages of invertebrates and lacks some of the disadvantages of other vertebrate models. Thus, it is one of the "ultimate" model organisms that can be used in developmental studies.

1.1.1 Genetic advantages of the zebrafish

The most powerful advantage of using zebrafish as a model organism is their ease of use in genetic analysis. Genetic screens are one of the best approaches to identify novel genes essential for certain physiological and cellular functions during development.

C.elegans and *Drosophila* high throughput mutant screens have been extremely successful however apart from zebrafish, this same level of analysis is not feasible with other vertebrate models.

Zebrafish are easy to raise and maintain. Because of their small size, they can be kept at high density in small tanks. They grow fast and reach sexual maturity in as little as 3 months. Large scale forward genetic screens and complementation analysis are possible because generation time is short and large clutches of embryos can be produced at weekly intervals. Mutants can be screened shortly after fertilization to identify genes essential for certain developmental process because zebrafish embryogenesis is rapid and by 24 hours after fertilization, most of the body plan is established.

Large scale Tubingen and Boston screens described nearly 2000 mutations causing various developmental defects in 1996. These mutations are still studied extensively to determine the functions of genes in important signaling pathways controlling early development. However, owing to the advantages explained before, most of the zebrafish labs can have their own mutagenesis screens. For example, *SBU2* mutation, which will be explained in chapter 2 of this dissertation, is obtained from our laboratory's ENU induced mutation screen.

Since most of the zebrafish genome is sequenced and assembled, reverse genetic techniques can be applied to zebrafish embryos to understand the function of a particular gene during development. Genes can be knocked-down using morpholinos to explore gene function and to understand the vertebrate development and disease states. In addition to morpholinos technology, latest technical advances show great potential to enable researchers for disrupting a specific gene function easily by gene-specific zinc finger nucleases (ZFNs) [1-3].

1.1.2 Experimental advantages of the zebrafish

The biggest advantage of utilizing zebrafish in developmental studies is that the embryo develops outside the mother's body therefore all developmental stages can be screened easily without killing the mother. External fertilization of the embryos makes molecular manipulations such as microinjection of mRNA, plasmid DNA and

morpholinos or physical and pharmaceutical treatments easy. Since embryos develop fairly quickly and they are transparent, the effect of these manipulations on complex developmental and behavioral processes can be studied shortly after fertilization real time at single cell resolution without further manipulation. Alternatively, effects of these manipulations on gene expression patterns can be examined by RNA *in-situ* hybridization. In addition, advanced experimental techniques such as single cell transplantations, ablations, fate mapping are also feasible.

Appreciating the developmental processes in a vertebrate model will provide a basis to understand human developmental disorders. Thus, supplemented with research from higher vertebrate models such as rat and mice, zebrafish play a very crucial role in biomedical research.

1.1.3 Disadvantages of zebrafish as a model organism

The biggest disadvantage of using zebrafish as a model organism to study embryonic development is their "redundant" genome. It is believed that genome duplication occurred on the fish lineage during evolution doubling many zebrafish gene families in size than that of land vertebrates. Some developmentally critical genes may be missed in mutant screens because redundant pathways may mask more severe phenotypes caused by a critical gene mutation during development.

Another disadvantage of utilizing zebrafish in scientific studies is the experimental limitations to efficiently generate targeted mutations. Although zinc finger nucleases are shown to be a feasible way of gene knock-outs, this technology is still not practical enough to be used as widely and frequently as morpholinos.

1.2 Early embryonic development of zebrafish

Since zebrafish embryos are externally fertilized and they are transparent, early embryonic development of the zebrafish can easily be examined with a dissecting microscope in real time. Shortly after fertilization, the first blastomere is separated from the yolk at the animal pole. The first three cell divisions are incomplete, that is, until the 8

cell stage, blastomeres are cytoplasmically continuous with the yolk. This feature of the early embryos provide experimental advantage because anything microinjected in the yolk can be distributed into the entire blastoderm.

During the early blastula, blastomeres continue to divide rather synchronously and rapidly on top of the yolk. After 3 hours, cell divisions become more asynchronous and slow down defining the beginning of the mid-blastula transition. At that stage, zygotic RNA synthesis starts. During late blastula, the blastoderm is separated into 3 domains: Enveloping layer is a superficial monolayer of flattened epithelial cells. These cells cover more loosely organized deep cells. Deep layer cells later will give rise to embryo proper. Yolk syncytial cells are formed from the cells located at the margin of the blastoderm. This layer separates deep layer cells from the yolk. During blastula stage, blastomeres are still pluripotent.

At around 4.3 hours after fertilization, the first morphogenic movements spread the blastoderm vegetally around the yolk, marking the onset of epiboly. Most of the epiboly movements are seen near the margin; cells at the animal pole are mostly stationary. After an hour, half of the yolk is covered by blastomeres, representing 50% epiboly stage. At that point, embryo enters the gastrula period.

The gastrula period typically takes about 4 hours. Through gastrula, involution and convergent extension movements enable separation of the deep layer cells into three distinct germ layers: Mesoderm give rise to muscle, circulatory system, urogenital tract and bones while endoderm give rise to gastrointestinal tract. Ectoderm gives rise to nervous system and epidermis. During gastrulation, the dorsal/ventral axis is also established. Gastrulation continues until yolk is covered with cells. At this time, the dorsal side of the embryo contains most of the cells in the embryo.

After the gastrulation period is completed and the embryo reach tailbud stage, the segmentation period starts. Segmentation is a very long process and takes between 14-15 hours. During segmentation, the embryonic body plan is established and the embryo is segmented into smaller sub-divisions. Besides segmentation of trunk mesoderm (somitogenesis), head mesoderm is subdivided into portions which then give rise to

pharyngeal arches. Anterior neural tissue, specifically hindbrain, is also segmented into rhombomeres. By 24 hours after fertilization, most of the major organs including heart, brain, eye and ear plans are laid out and 24-hour-old embryo mostly resemble adult fish features.

1.2.1 Genetic and molecular control of early development

Development is the process during which one cell embryo gives rise to a highly organized multicellular organism. Through development, cells grow, divide and differentiate. During differentiation, cells change their shape, size, metabolic activity and their ability to interact with and respond to outside cues to become more specialized for specific functions essential in the organism. These changes are largely attributed to highly controlled differential gene expression. Different gene expression profiles can be regulated at transcription initiation, post-transcription, translation, and post-translation levels.

In this dissertation, I am mostly focusing on differential gene transcription and how these differences effect the signaling pathways and different developmental processes in zebrafish embryos. Promoter/enhancer profile, epigenetic characteristics of the gene, nature and the positions of the transcription regulators control how much and when the gene is transcribed. In chapter 4 and 5, how epigenetics govern differential gene transcription during development will be discussed in detail.

As well as temporal and spatial regulation of gene expression, signal transduction pathways regulate many cellular processes including metabolism and locomotion. In response to extracellular stimulation, one of the components of the signal transduction cascade can directly act as transcription factor or induce the expression of transcription factor to regulate gene expression levels during cell differentiation, lineage and germ layer specification, tissue patterning during early development. One of the distinct roles of the signal transduction pathways is to transmit and receive temporal and positional information from cells nearby. This intercellular communication is vital during early stages of development because body plan organization and patterning require highly coordinated processes which involve the crosstalk between large number of cell

functions. Disruption of this communication may cause severe patterning defects during development.

1.3 Somite development in zebrafish

Division of body plan into a series of repetitive segments is a highly conserved developmental process. The segments provide basic landmarks to the embryo while the body plan is further detailed according to this basic blueprint. Segmentation of an animal body is regulated by very complex genetic networks which create synchronized and dynamic gene expression profiles. Although most of the components of these networks were already discovered, their individual roles of how positional and temporal information of the genes at particular locations is converted into segmentation signals are not understood completely.

Formation of somites is a well studied vertebrate segmentation process [4]. Somites are the blocks of paraxial mesoderm within the trunk of the vertebrate embryo, flanking notochord. These structures are transient and differentiate into dermis of the dorsal skin, vertebrae and skeletal muscles of trunk and tail later in the development (Fig 1.1). Somites form by budding off from the rostral presomitic mesoderm (PSM) in a highly regulated fashion at intervals of 30 minutes in zebrafish[5], 1.5 hours in chick and 2 hours in mouse. The temporal and spatial regulation of somitogenesis is crucial for further patterning since other segmental structures such as early blood vessels, axial muscle, and peripheral spinal nerves follow the periodicity of the somite borders. Several theoretical models were proposed to understand the precise molecular nature of this highly controlled rhythmic behavior of PSM [6-14]. According to the widely accepted "clock and wavefront" model [7], somitogenesis is regulated by the crosstalk between a "molecular clock" and "wavefront". In this model, the Notch pathway regulated "molecular clock" controls the timing of the segmentation while fgf8 mediated "wavefront" is responsible for spatial regulation so that uniformly sized mesodermal blocks were segmented at regular intervals.

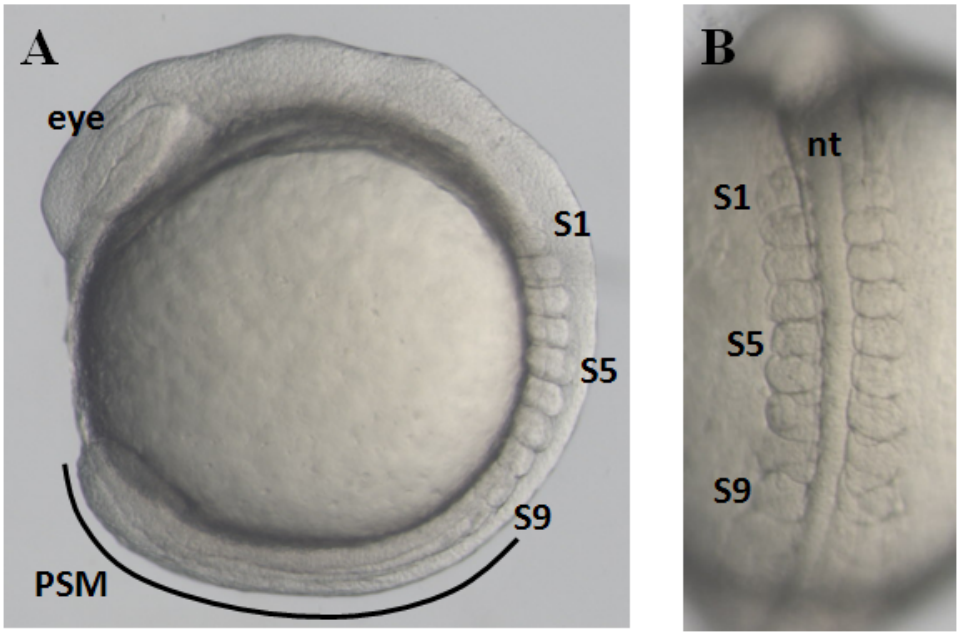

Figure 1.1: Zebrafish somite morphology. Lateral (A) and dorsal (B) view of a living 9-somite stage embryo. Somites are counted beginning with most anterior somite. First somite does not have anterior boundary. Abbreviations S: somite, PSM: Presomitic mesoderm, eye: eye, nt: notochord

1.3.1 Mechanism of the "molecular clock"

The discovery of the oscillatory expression of chick *hairy* homologue *chairy* at PSM is the first indication of the presence of a "molecular clock" during somitogenesis [15]. Later, hairy homologues, *HES1*, Hes7 and c-hey2 are shown to be the additional components of the "clock" in chick and mouse PSM [16-18]. Consistently, two zebrafish hairy homologues *her1* and *her7* and Delta homologue *deltaC* show oscillatory expression in the zebrafish PSM and they are essential for normal segmentation [19-22]. However, expression of Notch pathway modulator *lunatic fringe (lfng)* exhibits oscillating pattern only in chick and mouse but not zebrafish PSM [23-26]. Wnt/β-catenin signaling is cyclic only in mouse PSM but not in chick or zebrafish [27]. Wnt signaling inhibitors Axin2, Nkd1, Dact1 and Dkk1 show oscillating expression patterns [27-30]. In summary, hairy homologues Her/Hes, *lunatic fringe (lfng),* and Wnt inhibitors are three main mechanisms for generation of "molecular clock"/oscillations during somitogenesis. These oscillations exhibit typical striped expression pattern in the PSM and forming somites (Fig 1.2).

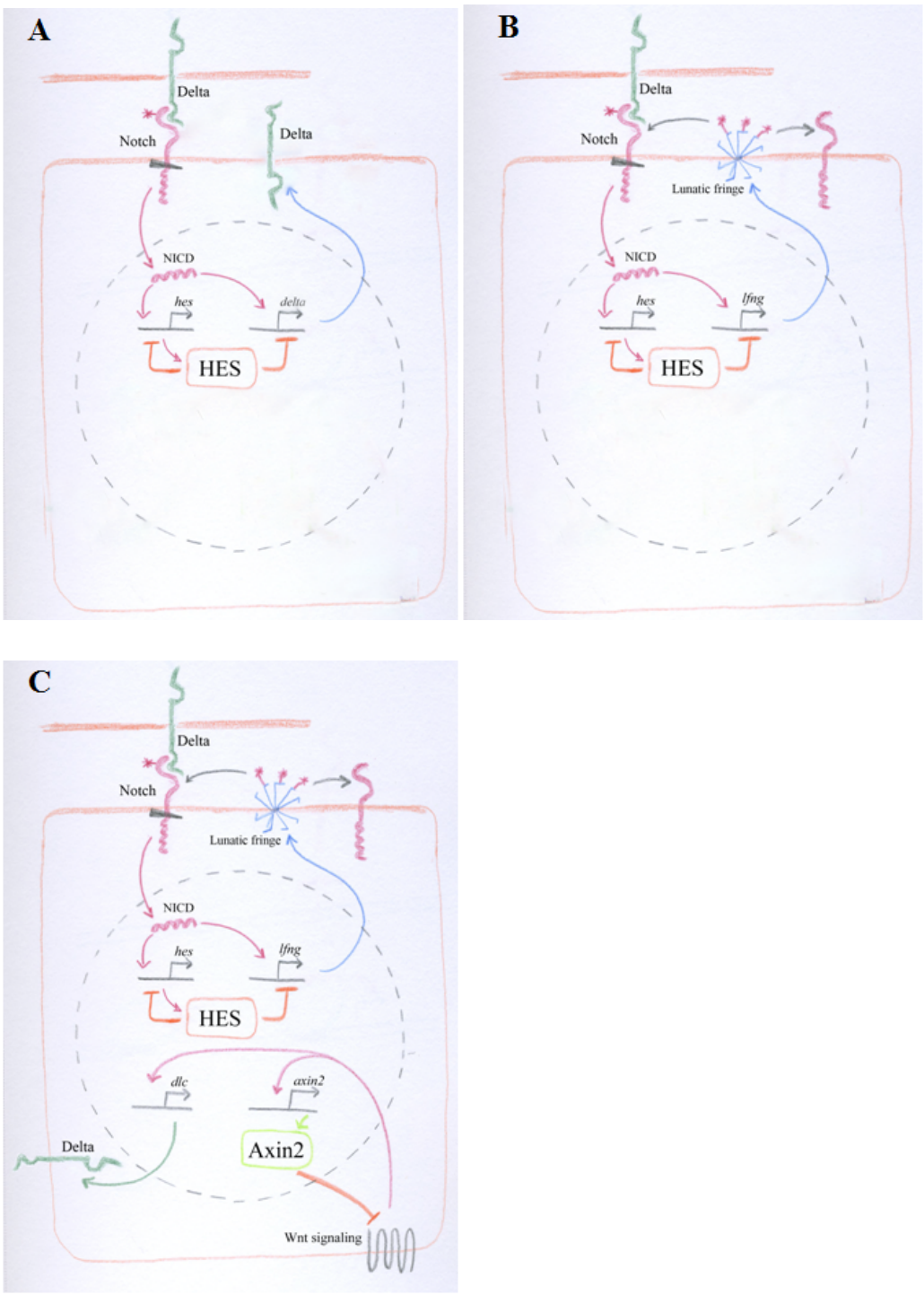

Figure 1.2: Simplified wiring of the zebrafish, chick and mouse clocks. Zebrafish clock is regulated only by Her1/Her7 controlled feedback loop (A). In chick, in addition to zebrafish clock components, Lunatic Fringe regulates molecular clock (B). In mouse, in addition to chick clock components, Wnt inhibitors regulate the molecular clock (C) Zebrafish her1 and her7 genes are summarized as her, chick and mouse hairy, hey, and hes genes are summarized as hes. NICD, Notch intra-cellular domain.

1.3.1.1 Notch Signaling and "Molecular Clock"

Notch signaling depends on direct cell-cell contact: Notch, a large transmembrane receptor, binds to Delta and Serrate families of ligands on the surface neighboring cell. This interaction triggers the proteolytic cleavage of Notch and release of the intracellular domain of Notch protein, NICD. NICD is then translocated to nucleus and act as a transcription regulator in conjunction with Suppressor-of-Hairless (Su(H))/RPB-Jk transcription factors to induce the expression of *hairy/enhancer-of-split (E(spl))* family genes including *her1*, Hes7 and c-hey2 [31-33] (Fig 1.3).

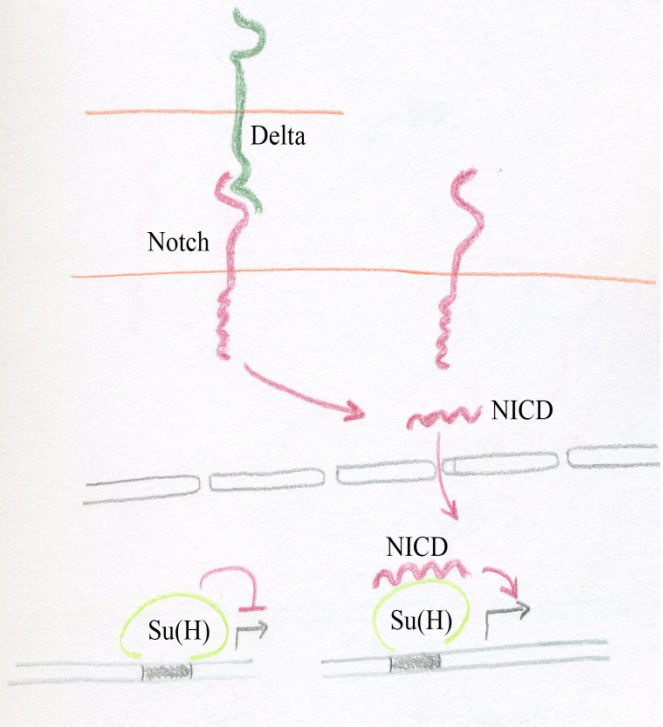

Fig 1.3: Mechanism of Notch activity. Prior to Notch signaling, Suppressor-of-Hairless (Su(H))/RPB-Jk transcription factors bind to Notch regulated genes and recruit repressors of transcription. When Notch is activated by ligands Delta or Serrate, Notch intracellular domain (NICD) is cleaved by γ-proteases. NICD is then translocated to nucleus and interact with Su(H))/RPB-Jk transcription factors and activate the expression of the target gene.

The ligand-receptor affinity between Notch and Delta/Serrate can be moderated by glycosyltransferase function of Fringe on extracellular domain of Notch. Depending on the developmental context, this post-translational modification of Notch can either potentiate or inhibit the pathway [34-36].

The majority of the oscillating genes in PSM are Notch signaling components implicating that Notch pathway plays an important role in generation of "molecular clock". For example, *deltaC* is the ligand and *lfng* is the modulator of the Notch pathway. Moreover, *her1*, Hes7 and other hairy homologs are the Notch pathway target genes. Another indication of the vital role for the Notch pathway in creating the regular gene oscillations and properly segmented somites is the analysis of mouse and zebrafish loss-of-function, zebrafish and Xenopus gain-of-function studies [19, 21, 37-49]. Inhibiting the Notch pathway in mice severely disrupts posterior somite formation. Somitogenesis is highly delayed and disorganized in homozygous *Notch1* mutants in mice [45] while mutation in downstream component of the Notch pathway *Su(H)/RPB-Jk* caused more severe somite phenotype [41]. Similarly, both gain- and loss-of function studies in zebrafish and Xenopus caused formation of defective somites [40, 48-53] suggesting that Notch signaling should be strictly controlled for perfectly ticking "molecular clock".

The Tubingen large-scale genetic screen is the milestone for understanding the components of the Notch regulated "molecular clock" in zebrafish. Five mutations, *fused somites (fss), beamter (bea), after eight (aei), deadly seven (des)* and *white tail/mindbomb (wit/mib),* were identified through this screen. Later, four of those genes were characterized as Notch pathway components: Notch ligands *deltaC* and *deltaD* [54, 55]; Notch receptor *notch1a* [20]; and E3 ubiquitin ligase *mib* [56], which modulates Delta activity in the Notch pathway. The somite phenotype of the Notch mutants is grossly similar. They only form 7-9 (*aei, des, and mib*) or 2-4 (*bea*) anterior somites and more posterior somites fail to segment. Also in each mutant, anterior/posterior polarity of the formed somites is abolished [39, 57]. Importantly, the expression of cycling genes *deltaC, her1* and *her7* is disrupted in these mutants. Instead of displaying highly coordinated oscillating expression pattern, *her1* and *deltaC* exhibit disorganized "salt and

pepper" expression pattern in the rostral PSM [19-22, 51-53, 55] proving that Notch pathway is crucial for the regulation of synchronized and oscillating gene expression.

Studies utilizing Notch pathway mutants and knock-downs lead to a very simple oscillatory model to understand the zebrafish "molecular clock". According to this model, Her1 and Her7 act as a core pacemaker and the *intracellular* oscillations are generated by a negative feedback loop. Mathematical models propose that time delays in the auto-inhibitory circuit is required for generation of oscillations; without such delays, the system will not oscillate. The time interval between the onset of the *her* gene transcription (Fig 1.2A, red arrow) to the Her protein binding to the *her* gene promoter (Fig 1.2A, orange block) is critical since this delay time determines the "ticking" pace of the "clock" [58]. Her1 and Her7 negatively regulate the expression of *deltaC* which in turn activates the Notch ligand in the neighboring cell expressing Notch so that *intracellular* oscillations are transmitted to the neighboring cells in synchrony [58, 59].

1.3.2 Mechanism of the "wavefront"

According to "clock and wavefront" model, spatial periodicity of segment boundaries is regulated by the "wavefront" while the "molecular clock" provides the temporal cues during somitogenesis [7]. However, the molecular mechanisms regulating the "wavefront" remained unknown until recently.

The Fgf receptor 1 (Fgfr1) is thought to be the regulator of somitogenesis since *Fgfr1* is expressed in PSM and anterior half of the segmented somites in zebrafish and mice [60, 61]. Also, homozygous *Fgfr1* knockout mice lack segmented somites [62] suggesting that FGF signaling may have a regulatory role in somitogenesis. However, zebrafish *fgf8 (ace)* mutants do not show a severe somite phenotype [63]. Thus, the precise role of the FGF signaling during somitogenesis remained unknown until Dubrulle *et. al.*[64] and Sawada *et. al*.[65] demonstrated elegantly how Fgf8 regulated the "wavefront" during somitogenesis.

1.3.2.1 FGF signaling and "wavefront"

FGF ligand family has almost two dozen of members. Soluble FGFs bind to extracellular ligand binding domain of FGF receptors on the target cell. This interaction activates the dormant tyrosine kinase domain of the receptor and initiates the auto-phosphorylation of the receptor. This phosphorylation in turn activates Ras. Activated Ras activates Raf kinase. Activated Raf phosphorylates and activates MEK. Activated MEK then activates MAP kinase (MAPK) by phosphorylating it. Activated MAPK is translocated to nucleus and acts as a transcriptional regulator by phosphorylating other transcription factors (Fig 1.4).

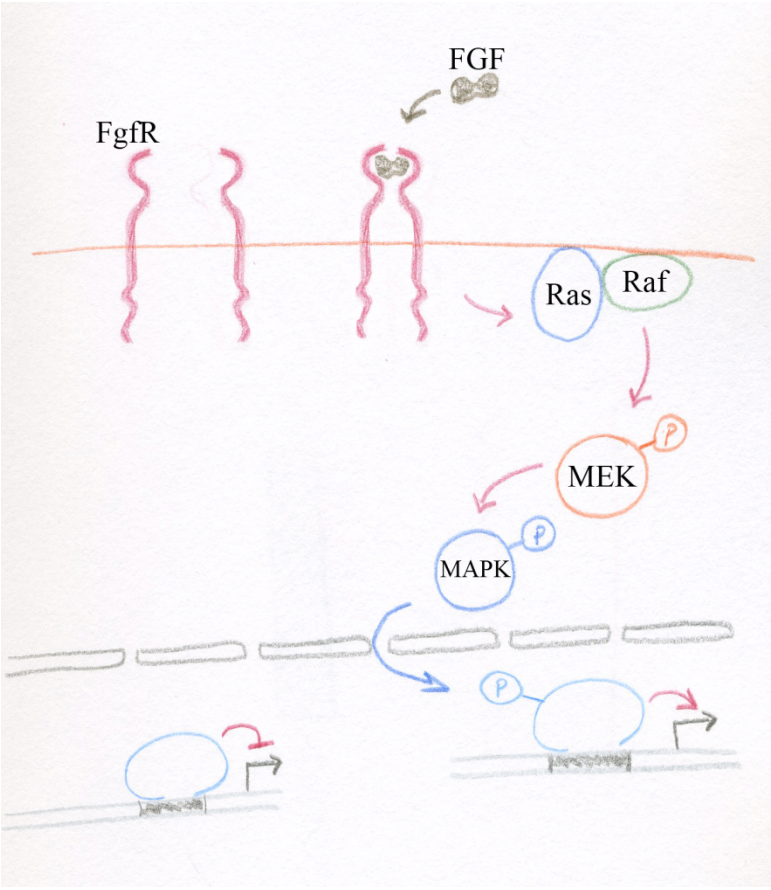

Fig 1.4: Mechanism of FGF activity. Binding of the ligand to the Fibroblast growth factor (FGF) receptor results in receptor dimerization and transphosphorylation of the receptor's cytosolic domain. Phosphorylated protein consecutively activates Ras; Ras activates Raf; Raf activates MEK; MEK activates MAP kinase (MAPK). Activated MAPK is translocated into nucleus and activates target transcription factors.

fgf8 is strongly expressed in posterior PSM and its expression progressively decreases thru anterior PSM, establishing a *fgf8* gradient in the caudal end of the embryo [64, 65]. Activation patterns of the FGF signaling, which is assayed by the levels of the phosphorylated Fgf target MAPK, roughly coincides with the expression pattern of *fgf8* in only caudal PSM where segmental pattern is not yet irreversibly determined [64, 65]. The pattern of this FGF signaling activation suggested a possible role of Fgf in establishment of segmentation pattern. When fgf8 is ectopically expressed in the entire chick PSM or Fgf8 soaked beads were grafted to rostral PSM, segmentation is blocked and caudal identity (immature state) of the PSM is maintained [64]. Moreover, transient repression of the FGF signaling in PSM with the FGF inhibitor SU5402 caused enlarged somite size but the oscillation frequency of *her1* gene expression is not altered [65]. This indicated that FGF signaling does not affect the "molecular clock" but regulates the segmentation program. Therefore, it was proposed that posterior-to-anterior gradient of FGF signaling in the PSM defines a threshold where immature PSM cells become competent to respond to segmentation program and stop the oscillations of the clock genes [64, 65]. After PSM hits the wavefront and segment formation is initiated, Fgf signaling retreats caudally in the PSM and wait for next oscillating "wave" to induce the formation of another somite pair (Fig 1.5).

Although FGF signaling, especially Fgf8, clearly regulates the position of the "wavefront" during somitogenesis, neither zebrafish *fgf8* mutant nor *Fgf8* conditional knockout mouse in PSM exhibits any somite phenotype [63, 66]. In vertebrates, FGF family contains more than 20 ligands. It is possible that other FGF ligands besides Fgf8 can also function in PSM to regulate somitogenesis. Moreover, Wnt signaling can also provide a redundant "wavefront" in the absence of Fgf8 signaling since it was proposed that Wnt signaling either functions upstream of FGF8 gradient[27] or acts in parallel to FGF[67] to regulate the position of the "wavefront".

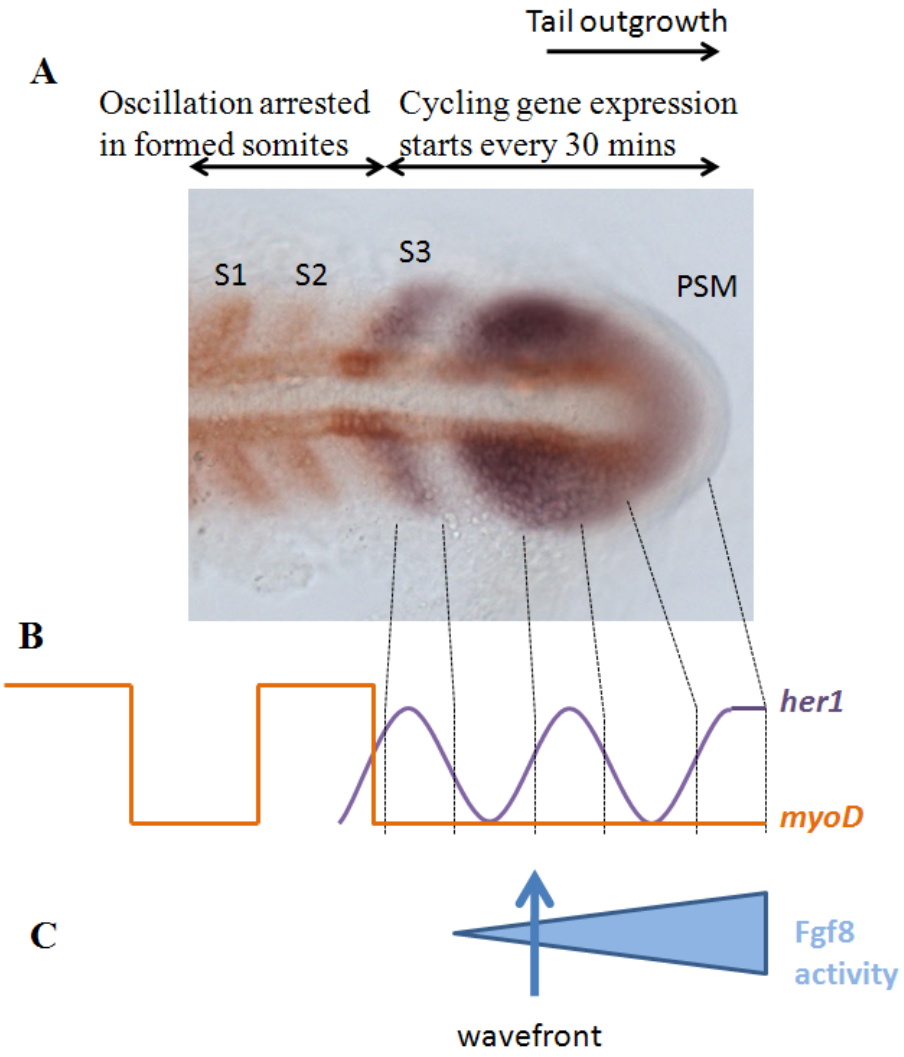

Fig 1.5: The "clock and wavefront" model of somite formation. Flat mounted RNA in situ hybridization of oscillating marker *her1* (purple) and somite marker *myoD*(orange). Dorsal view at 10 somites, anterior to the left, PSM is on the right (A). At PSM, *her1* cycling expression (purple sinusoidal wave in B) is induced every 30 minutes. When Fgf8 activity reduced to a certain level (wavefront) (blue arrow in C), segmentation program is initiated; somites are formed. Somite marker myoD is induced in the formed somites (A).

In this dissertation, I studied the molecular and genetic mechanisms regulating somitogenesis. Here, we characterized the embryonic lethal *SBU2* mutation. This mutation had very severe somite defects as well as other problems in muscle fiber differentiation, pigmentation, neural differentiation and circulatory system. Using positional cloning, a non-sense mutation of the *spt6* gene was identified in *SBU2* mutants. Because somite phenotype of *SBU2* mutants resembled that of Notch pathway mutants, the role of Spt6 in Notch pathway in regulation of somitogenesis was investigated. Spt6 was required for the Notch pathway regulated transcriptional response. Taken together, these results showed that somite defects in *SBU2* mutants are the result of repressed Notch signaling function.

In an additional study, I investigated the function of ChCh and Sip1a during zebrafish somitogenesis. Knock-down of *chch* and *sip1a* resulted in narrow somites throughout the anterior/posterior axis. Although pace of the "molecular clock" was not affected, *chch* and *sip1a* knock-down had persistent her1 and her7 gene expression. Moreover, *fgf8* expression was rostrally expanded. Taken together, we demonstrated that Chch and Sip1a modulate FGF signaling during somitogenesis.

Chapter 2: Genetic and biochemical interactions between Spt6 and Notch

(This chapter is previously published in Developmental Biology 307 (2007) 214–226)

2.1 Introduction

Somites establish the segmental outline of the vertebrate embryo. Bilateral pairs of paraxial mesoderm cells flanking the notochord are first organized into epithelial tissue blocks that then separate from more caudal cells in a regulated fashion, giving rise to highly organized transient structures on the dorsal side of the embryo. These structures then differentiate into dermis of the dorsal skin, vertebrae and skeletal muscles of the trunk and tail.

The process of somitogenesis is regulated by synchronized expression of Notch pathway components in the presomitic mesoderm (PSM) [22]. These include *lunatic fringe* in chick and mouse [24, 25], delta homologs *deltaC* and *deltaD* [22] and several *Hairy and Enhancer of Split–Related (Her)* b-HLH repressor genes *her1* and *her7* in zebrafish [19-21, 55]. Inhibiting the Notch pathway in mice and zebrafish severely disrupts posterior somite formation [19, 21, 37-44, 68].

The first Tubingen large scale genetic screen identified five loci, *fused somites* (*fss*), *beamter* (*bea*), *after eight* (*aei*), *deadlyseven* (*des*) and *white tail/mindbomb* (*wit/mib*), that are required for somite formation in zebrafish [39]. Later, it was shown

that four of those genes, *bea*, *aei, des*, and *wit/mib*, encode the respective Notch pathway components: notch ligands *deltaC* [54], *deltaD* [55], notch receptor *notch1a* [20] and *mib*, an E3 ubiquitin ligase which is required for cellular localization and activity of Delta [56]. The absence of posterior somites is a characteristic phenotype observed in all of the Notch pathway mutants. After forming 1 to 9 anterior somites, segmentation of the posterior PSM is interrupted and no new somites are formed [39]. Furthermore, treatment of zebrafish embryos with DAPT, a γ-secretase inhibitor, phenocopies the Notch pathway mutant phenotype in zebrafish [52]. This observation confirms the crucial role of Notch pathway on the regulation of somitogenesis.

In a genetic screen to isolate mutations disrupting neural patterning and embryogenesis, we identified an embryonic lethal mutation, *SBU2* that has somite defects resembling Notch pathway mutants. In particular, *SBU2* mutants only form 6-7 anterior somites. In addition, *SBU2* embryos have other phenotypes including defects in muscle fiber differentiation, pigmentation, circulatory system development and neural differentiation. RNA *in situ* hybridization with mesodermal markers revealed that *SBU2* mutants have reduced paraxial mesoderm and little lateral plate mesoderm. However, intermediate mesoderm is largely unaltered suggesting that not all mesodermal subtypes are disrupted by the *SBU2* mutation. While early regional neural makers are expressed in *SBU2*, many markers for differentiated neurons and neural crest are absent.

Using positional cloning, we identified a mutation that produces a premature stop codon within the *spt6* gene. The *SBU2* defects could be rescued by microinjection of *spt6* mRNA into *SBU2* mutant embryos. Microinjection of *spt6* morpholino oligonucleotides phenocopied the *SBU2* phenotype. Together, these results demonstrated that the *SBU2* phenotypes are produced by disruption of the *spt6* locus. The *pandora*^{m313} (*pan*) mutation was previously shown to disrupt the *spt6* locus [69]. Since *SBU2* is allelic to pan^{m313}, we designate our allele *pan*^{SBU2}. The phenotypes of *pan*^{SBU2} mutants are apparent at an earlier stage and are more severe than the *pan*^{m313} mutants. This finding demonstrates a broader and earlier requirement for Spt6 in zebrafish embryogenesis then was apparent from characterization of *pan*^{m313}.We present evidence that the phenotypic variations between the two spt6 alleles are the result of genetic background differences.

Spt6 was identified in *Saccharomyces cerevisiae* as a transcription elongation factor which interacts with histone H3 and H4 [70]. Spt6 functions in chromatin disassembly. During transcription, Spt6 allows RNA pol II to pass through the DNA template and re-establishes chromatin structure after RNA pol II passage [71-75]. Hence, Spt6 is required for persistent yet regulated transcription processes in the cell.

In *C. elegans*, EMB-5, the *C.elegans* ortholog of yeast Spt6, genetically interacts with LIN-12 (notch family transmembrane receptor) [76]. EMB-5 augments the penetrance of LIN-12 related defects on vulval morphology. Furthermore, interactions between the ankyrin repeats of EMB-5 and both LIN-12 and GLP-1 were detected in yeast two-hybrid analysis. These findings suggest that EMB-5/Spt6 might function in modulation chromatin structure upon activation of LIN-12/Notch pathway and regulate transcription of Notch pathway genes [76].

We demonstrate that zebrafish Spt6 interacts with Notch. In zebrafish embryos with reduced Spt6 function, activation of target genes by ectopic expression of Notch was suppressed. In addition, we detected a biochemical interaction between Notch and Spt6 in cell culture assays. While the *pan*^{SBU2} phenotype establishes that Spt6 is broadly required for many aspects of development, we also observe somite defects characteristic of Notch mutants. The genetic and physical interactions we have identified between Spt6 and Notch provide the first evidence for a role for Spt6 in notch signaling in vertebrates. These results illustrate a specific developmental requirement for the Spt6 transcription elongation factor in somitogenesis in zebrafish.

2.2 Results:

2.2.1 Identification of a mutant with disrupted somitogenesis

We performed a haploid ENU mutagenesis screen to identify mutations affecting zebrafish embryogenesis. In *SBU2* mutant embryos only 6-7 anterior somites form and further segmentation is severely interrupted (Fig. 2.1). *SBU2* embryos also have a short body length and slightly wide notochord and neural keel which may result from defects in

convergence and extension movements. In addition, other defects including tail elongation, anterior neural, circulatory, and pigmentation defects are apparent in *SBU2* mutant embryos. After about 20 hrs, many of the previously formed structures start to deteriorate (Fig. 2.1J).

The *SBU2* somite defects resemble the Notch pathway mutants. Embryos obtained from *SBU2* intercrosses do not show any morphological abnormalities during gastrulation (data not shown). During early somitogenesis, *SBU2* homozygous embryos can be distinguished from their siblings due to their indistinct and irregularly placed somite boundaries (Fig. 2.1A-A' and 2.1B-B'). At 4-5 somite stage, altered somite boundary formation is evident in *SBU2* embryos (Fig. 2.1D-D'). By the time their heterozygous or wild-type siblings reach the 10-13 somite stage, homozygous *SBU2* embryos exhibit only irregularly and asymmetrically formed 6-7 anterior somites (Fig. 2.1F-F' and 2.1H-H'). After that stage, somitogenesis stops in *SBU2* mutants. In most *SBU2* mutants, previously formed somite boundaries start to degenerate around 4-5 somite stage leaving either incomplete or no somite boundaries by 24 hours post-fertilization (hpf) (Fig. 2.1J).

2.2.2 Mesodermal gene expression is disrupted in *SBU2* mutants

During somitogenesis, the paraxial mesoderm is segmented into highly arranged tissue blocks. Since *SBU2* has segmental defects, we examined the effects of the mutation on specification of mesodermal cells. As somites are specifically derived from paraxial mesoderm cells, we first studied the state of differentiated paraxial mesoderm cells in *SBU2* embryos. RNA *in situ* hybridization with paraxial mesodermal markers *papc* and *spt* revealed that *SBU2* mutants have a reduced expression domain of paraxial mesoderm markers in the A-P dimension (arrowheads, Fig. 2.2A-D). In addition, the boundaries of the expression domain are less distinct in SBU2 mutants. However, this observation does not explain the somitogenesis defects observed in *SBU2*, since *tri; kny* double mutants form very little paraxial mesoderm but somite boundaries still form [77].

The segmentation of the PSM is regulated by the periodic expression of genes including *her1*, *her7* and *deltaC* and disruption of these genes causes somitogenesis defects [21, 22].

To ascertain whether periodic gene expression is altered in *SBU2*, we assayed expression of these markers (Fig. 2.2E-L and data not shown). Whereas distinct stripes of *her7* are observed in wild-type embryos at both the 3 and 10 somite stages, stripes of *her7* are present but exceedingly reduced and diffuse in mutant siblings (arrows, Fig. 2.2E-H). Expression of *deltaD* is similarly altered in *SBU2* mutants (arrows, Fig. 2.2I-L). Therefore, expression of molecular clock components is reduced in *SBU2*, while expression of a gene that is more proximal to somite boundary formation, *papc*, is spatially disrupted. Thus, it is possible that low levels of periodic gene expression may fail to properly specify expression of downstream genes such as *papc* that are critical for somite boundary formation. Muscle differentiation may also be disrupted, as expression of the myogenic regulatory factor MyoD is absent in lateral paraxial mesoderm (Fig. 2.2N).

We also studied differentiation of the other subdivisions of the mesodermal precursors such as lateral plate mesoderm and intermediate mesoderm. An early erythroid lineage marker *gata-1* [78] is not expressed in *SBU2* embryos (Fig. 2.2O, P) suggesting that lateral plate mesoderm in *SBU2* embryos is severely disrupted by the 10 somite stage. *SBU2* embryos have additional defects in lateral plate mesoderm as evidenced by the failure in heart tube formation (data not shown). However, RNA *in situ* hybridization with the nephrogenic marker *pax2a* [79] reveals no difference between wild type and *SBU2* embryos (Fig. 2.2Q, R). This suggests that there is no defect in differentiation of intermediate mesoderm. Together these results suggest that the mutation underlying the *SBU2* phenotype disrupts somite formation, specification of paraxial and lateral plate mesoderm but intermediate mesoderm is relatively unaffected.

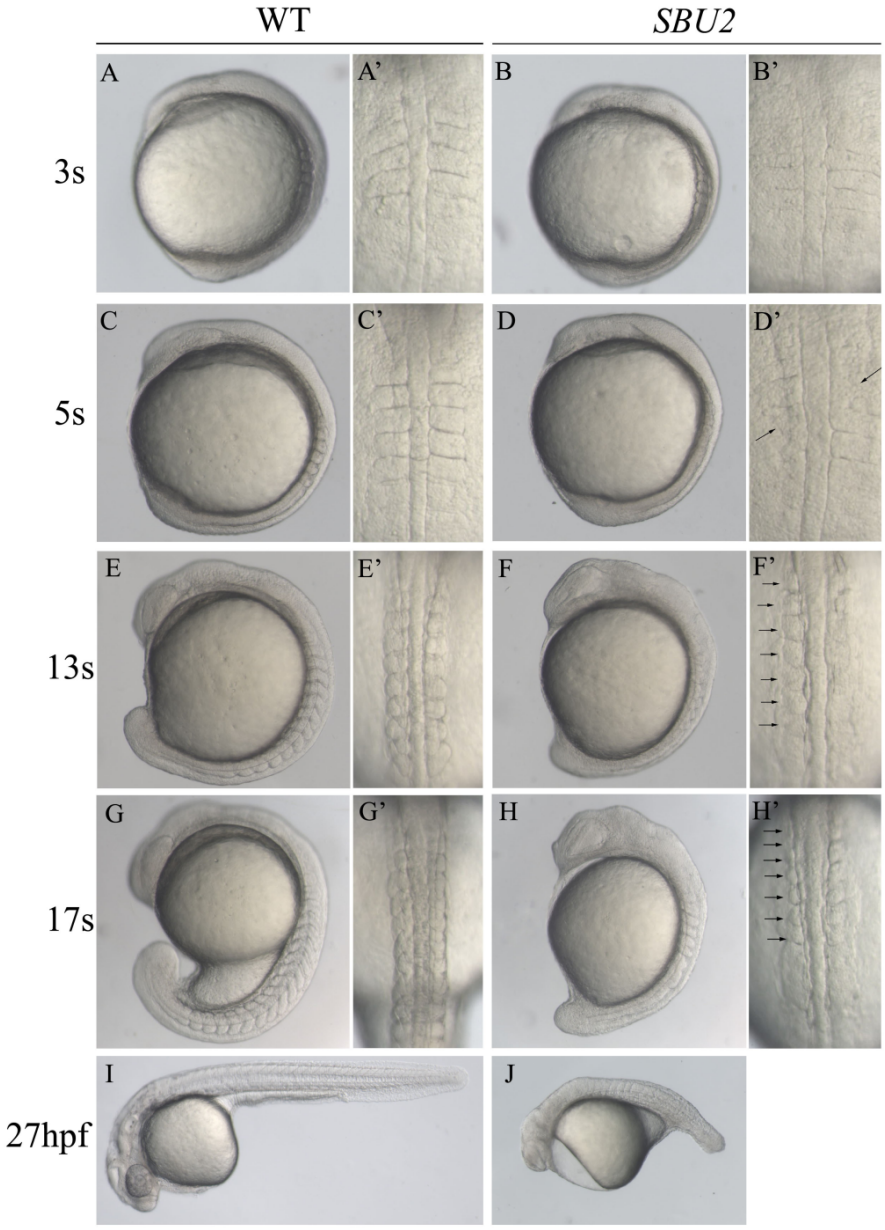

Figure 2.1: Phenotype of *SBU2* mutants. (A-J) Lateral views of living WT and SBU2 embryos, anterior to the top and dorsal to the right. (A'-H') Dorsal views of A-H, anterior to the top. At early somitogenesis, somite boundaries are irregular and indefinite (A' and B') in *SBU2* embryos. At ~5 somite stage, somites are formed asymmetrically while previously formed somite boundaries start to degenerate (arrows) (C' and D'). By the 5somite stage SBU2 mutants have a slightly shorter body length then their wild-type siblings (C and D) and by 13 somite stage, *SBU2* mutants are clearly less extended along AP axis than wild type embryos (E and F). While somites continue to form in wild-type embryos, *SBU2* mutants have only irregularly formed 6-7 somites and lack posterior somites (arrows) (F' and H'). By 24-27 hpf, most of the previously formed structures including somite boundaries are degraded or distorted and the embryos degenerate (J).

2.2.3 Somite boundaries deteriorate in *SBU2* mutants

SBU2 has segmentation defects very similar to Notch pathway mutants. To further characterize these defects in *SBU2* embryos, we examined the somite structure of 29 somite stage *SBU2* mutant embryos using a series of antibodies. Focal adhesion kinase (Fak) is robustly accumulated at somite boundaries during somitogenesis and persists at these boundaries [80-82] (arrows, Fig. 2.3A, A'). In 29 somite stage *SBU2* mutants, Fak fails to accumulate at somite boundaries, even in the anterior of the embryos (Fig. 2.3B, B'). This observation is unexpected, since anterior somite boundaries formed earlier in development morphologically. Therefore, we conclude that somite boundaries that form are not maintained properly in *SBU2* mutants. This result differs from Notch pathway mutant embryos in which irregular posterior somite boundaries eventually form, albeit later in development compared to wild-type embryos [83]. Thus, the initial somite phenotype of *SBU2* and Notch pathway mutant embryos is similar, but the later boundary phenotype of *SBU2* is more severe compared to previously characterized Notch pathway mutants.

It has been hypothesized that migrating slow muscle fibers mediate the belated formation of boundaries in Notch pathway mutant embryos [83]. In *SBU2* mutant embryos, boundaries do not form even later in development. We therefore asked if slow muscle fiber morphology is disrupted in *SBU2* mutant embryos. Staining with the slow muscle antibody F59 revealed a reduced number of differentiated slow muscle fibers in *SBU2* mutants (Fig. 2.3C, D). Furthermore, the initial segmental defects in these embryos are reflected in slow fiber organization; slow fibers are not as well organized as in wild type embryos. In addition, slow muscle fiber staining become fainter and gradually fades away in the posterior (Fig. 2.3C', D'). This result is not surprising because small gaps in adaxial (slow muscle precursor) *myoD* expression (Fig 2.2N) suggest that there may be fewer slow muscle precursors present in *SBU2* embryos which fail to properly differentiate into muscle fibers. The disruption in slow fiber organization at 29 somites in *SBU2* is more severe then that of Notch pathway mutants. In both the Notch pathway

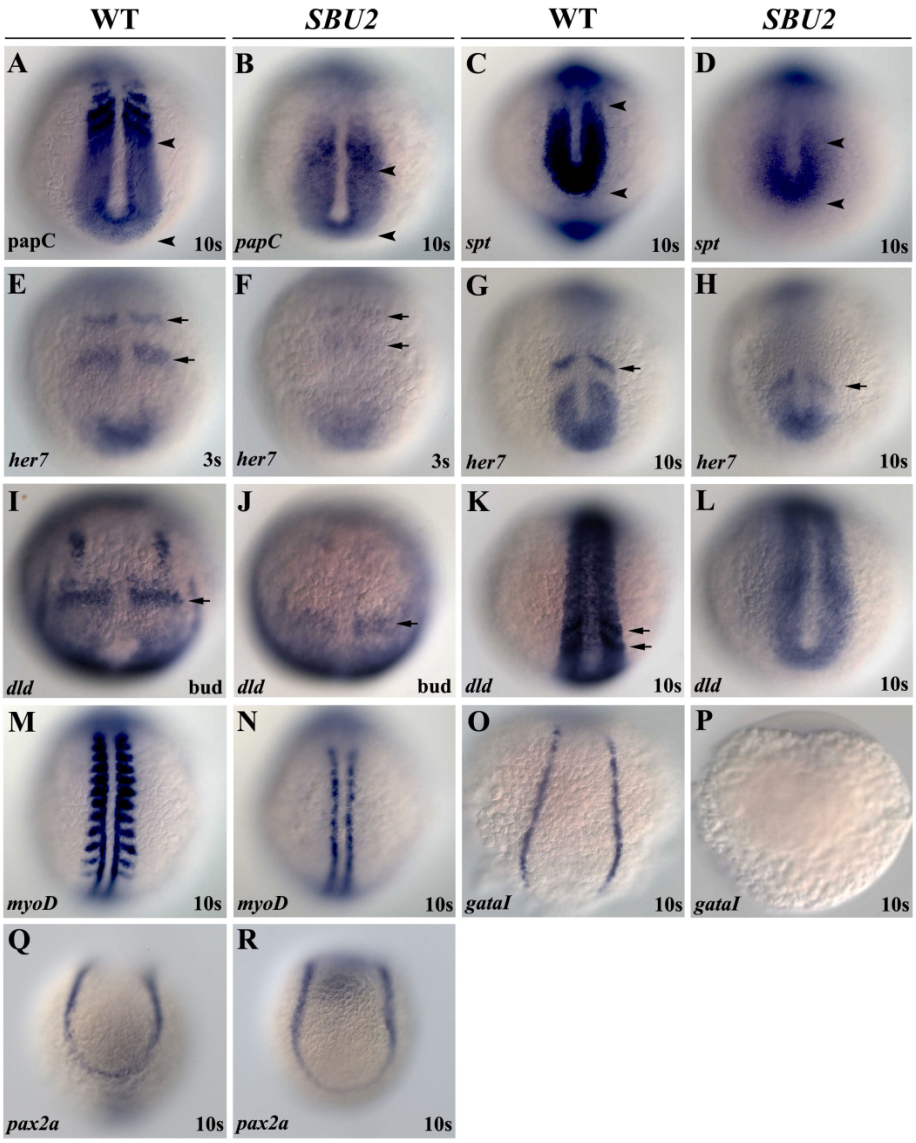

Figure 2.2: *SBU2* mutants have mesoderm defects. Whole mount RNA in situ hybridization of mesodermal markers in wild-type and *SBU2* mutants. All views are dorsal; anterior to the top. The expression domains of presomitic mesoderm markers *papC* and s*pt* are reduced in *SBU2* mutants (A-D). In wild type embryos, periodic activation of notch signaling provides cycling gene expression of Notch pathway genes such as her7 (E and G; I and K). *her7* and *dld* are expressed weakly in presomitic mesoderm as well as presumptive somites and anterior most somites, respectively (F and H; J and L). AP patterning of the somites in *SBU2* embryos is also affected; *myoD* expression at the posterior half of the somites is lost while it is reduced at adaxial cells (M and N). *gataI* expression is diminished in SBU2 mutants (O-P) indicating that lateral plate mesoderm development is highly reduced. There is no apparent difference in *pax2a* expression between wild type and *SBU2* mutants (Q and R); *SBU2* mutants have no defect in intermediate mesoderm formation. The most anterior and posterior *papC* and s*pt* expression is marked by arrowheads. Arrows denote stripes of *her7* or *dld* expression.

mutant embryos *aei/deltaD* and *des/Notch1*, slow muscle fiber morphology is disrupted early but later recovers [83].

Clearly, slow-twitch muscle fiber development is disrupted in *SBU2* mutant embryos. Analysis of *myoD* expression suggests that there might also be a fast muscle defect (Fig. 2.2N). We utilized an antibody against β-catenin that visualizes all cells to ask if fast muscle morphogenesis is disrupted in *SBU2* mutant embryos [84]. In wild-type embryos, the lateral displacement of slow muscle fibers correlates with fast muscle cell elongation [85]. Fast muscle cell elongation is disrupted throughout the axis of *SBU2* mutant embryos. Anteriorly, some cells elongate but elongation is inconsistent and disorganized (Fig. 2.3F). Posteriorly, fast cell elongation is also disrupted (Fig. 2.3F'). Taken together, these data indicate that muscle morphogenesis is more severely disrupted in *SBU2* mutant embryos than in Notch pathway mutant embryos.

2.2.4 *SBU2* mutants have neural defects

Lateral inhibition mediated by Notch signaling regulates neuron number in both vertebrates and invertebrates. In *Drosophila,* Notch pathway mutants are neurogenic. In zebrafish, ectopic neurons or neural progenitors are readily apparent in *mib* [56]. However, the neurogenic defects in *des* are much more subtle [86]. To determine whether *SBU2* embryos are neurogenic, we performed in-situ hybridization with neural markers. RNA *in situ* hybridization with midbrain-hindbrain boundary (arrows) and placode marker (arrowheads) *pax2a* [79] revealed that placode formation is delayed (arrowheads, Fig. 2.4D), the overall midbrain-hindbrain boundary and placode expression of *pax2a* is reduced but the general spatial pattern of *pax2a* is largely unaffected in *SBU2* embryos (Fig. 2.4B, D). However, the midbrain-hindbrain boundary is not morphologically apparent in living embryos (Fig 2.1J). This suggests that although these cells initiate proper gene expression at the midbrain-hindbrain, the boundary does not form. Similarly, expression of the hindbrain marker *krox20* [87] is also delayed in *SBU2* embryos. However, as development progresses, *krox20* recovers and the overall pattern become similar to that of wild type embryos (Fig. 2.4E-H).

The neural marker *huC*, reveals the number of the differentiated neurons in zebrafish embryo during development [88]. *SBU2* embryos express very little, if any,

huC (Fig. 2.4I-I' and 2.4J-J'). Similarly, epibranchial neuron marker, *phox2a* expression is weak or completely absent in *SBU2* embryos (data not shown). Together these data indicate that SBU2 embryos generate few differentiated neurons and are not neurogenic. In zebrafish, somitogenesis is more sensitive to disruptions in notch signaling than neurogenesis as evident by the weak neurogenic phenotype in *des* [86]. Potential neurogenic effects of *SBU2* may be masked by additional requirements for the protein in neurogenesis. Alternatively, *SBU2* might not influence Notch-mediated lateral inhibition in neural tissue.

2.2.5 Disruption of *spt6* causes the *SBU2* phenotype

To identify the gene that is responsible for the *SBU2* phenotype, a large genetic mapping panel comprising 6928 meioses was assembled. *SBU2* was mapped to a ~5 cM interval in the centromeric region of linkage group 21 between Z7809 and Z10432 Because of the proximity to the centromere, recombination is suppressed in this region. Therefore, the genetic distance corresponds to a larger then average physical distance. Using the sequence information from the Sanger Ensembl genome assembly (www.ensembl.org/Danio_rerio) a series of polymorphic markers was generated to narrow the interval (Fig. 2.5A). Sequence analysis of the genes at that region revealed a C to T transition at nucleotide 3931 of the coding sequence of the *spt6* gene (Fig. 2.5B, bottom panel). This sequence change was detected in 75/75 mutants analyzed using restriction analysis of a PCR product generated from the locus (see Materials and Methods). 0/95 phenotypically wild-type sibling were homozygous for the sequence change. This mutation creates a premature stop codon in exon 30 (Fig. 2.5B). The truncated Spt6 protein lacks the C-terminal 415 amino acids which includes a Src homology 2 domain important for recognition and binding to phosphorylated tyrosine [89] (Fig. 2.5C).

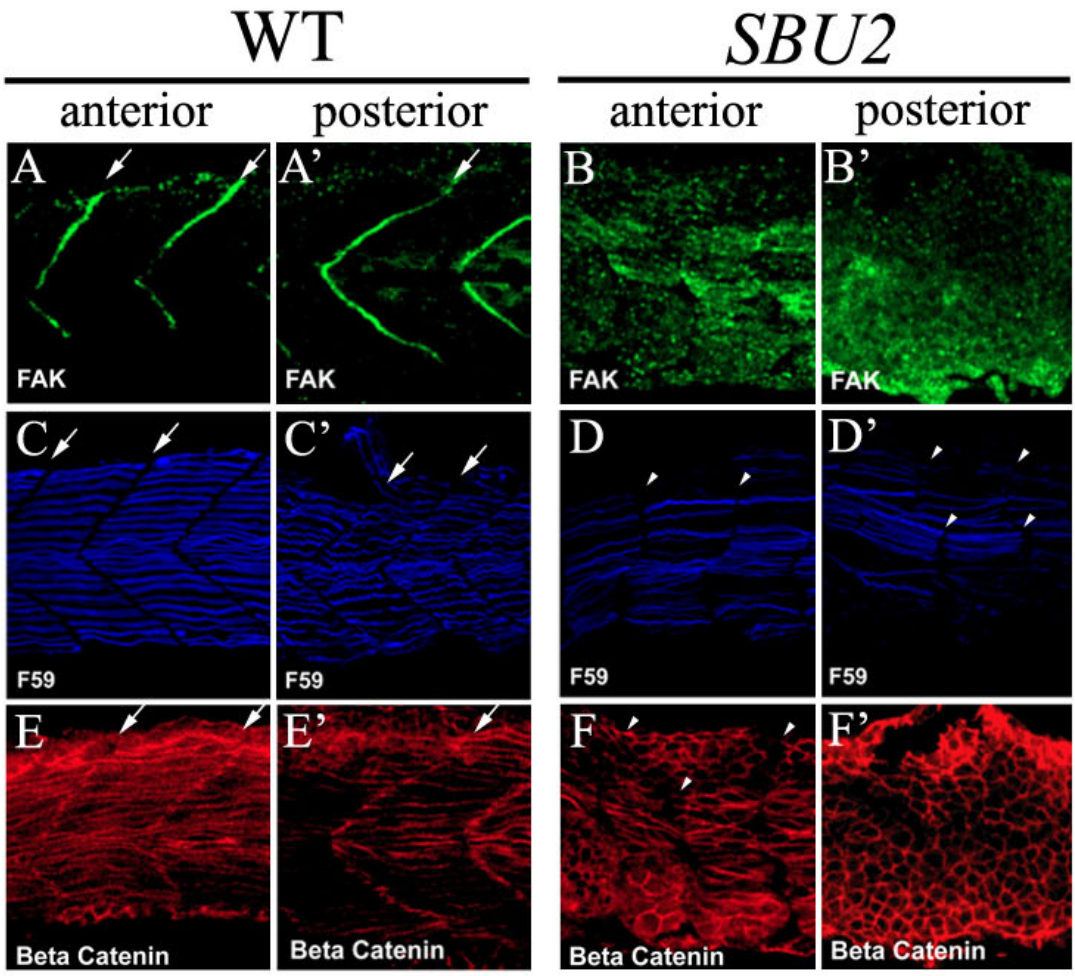

Figure 2.3: Somite boundaries formation and muscle fiber differentiation is disrupted in *SBU2* mutants. Confocal sections of anterior (A-H) and posterior (A'-H') portions of the trunk region 29 somite stage embryos at approximately same medial-lateral and anterior-posterior locations; anterior to the left. Focal adhesion marker phosphorylated Fak is in green; slow muscle marker F59 is in blue; β-catenin which outlines the cell is in red. In wild type embryos, phosphorylated Fak accumulates at myotome borders, revealing regularly formed somite boundaries (A and A'). On the other hand, there is no specific accumulation of phosphorylated FAK in *SBU2* mutants (B and B'). The number of the slow muscle fibers is lower both in anterior and posterior (D and D') compared to wild type muscle fibers (C and C'). In wild-type embryos, fast muscle precursors elongate and attach to the anterior and posterior somite borders (E). In *SBU2* mutant embryos, some fast cells elongate in the anterior of the embryos (F). However, in the posterior, few, if any, fast cells elongate (F'). Therefore, fast muscle fiber morphogenesis is severely disrupted in *SBU2* mutant embryos. Arrows denote somite boundaries. Arrowheads denote improper and degenerated somite boundaries.

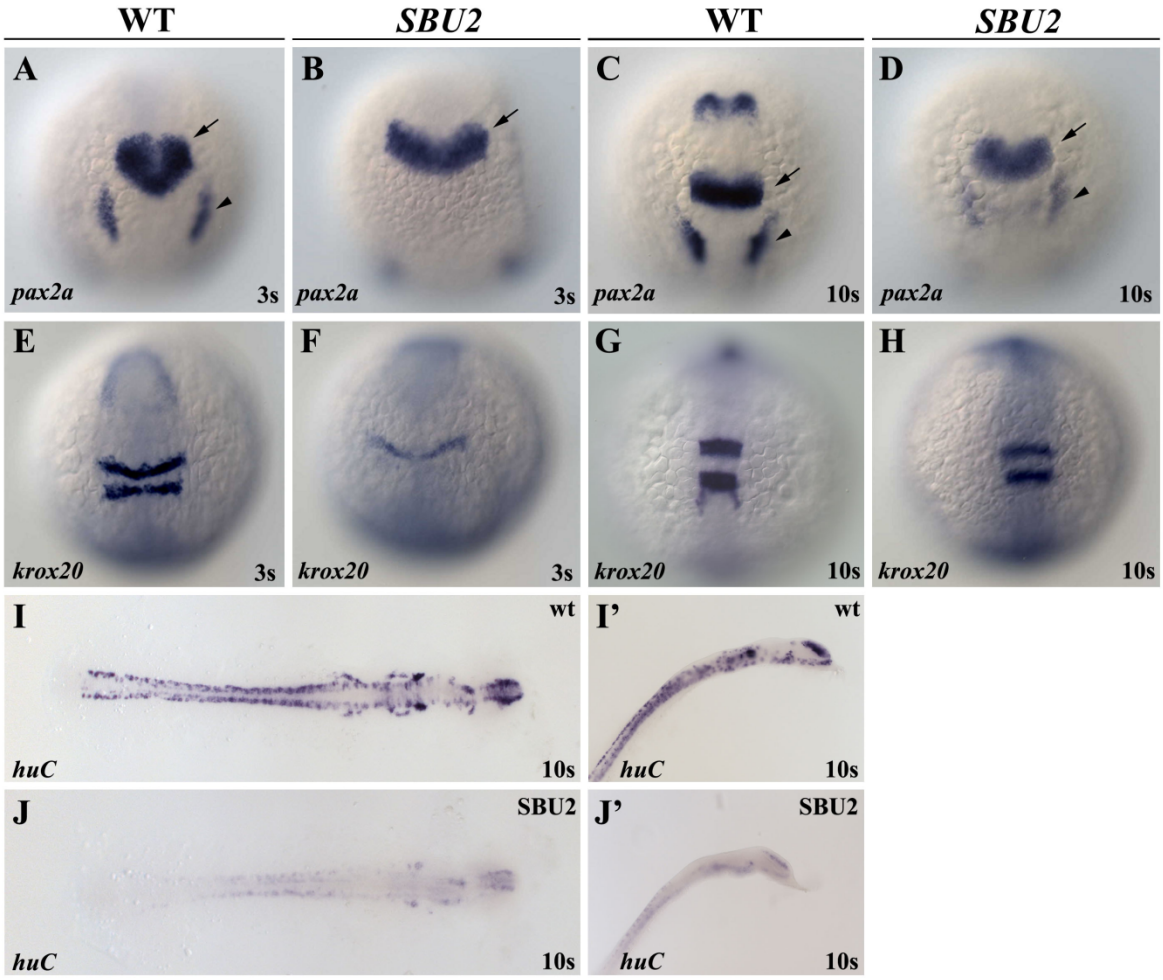

Figure 2.4: Neural *SBU2* mutants are not neurogenic. Whole mount RNA in situ hybridization of neural markers in wild-type and *SBU2* mutants. (A-J) Dorsal views; (A-H) anterior to the top, (I, J) flat mounted, anterior to the right. I', J' are lateral views of I and J, anterior to the top right. Morphology of the MHB domain expressing *pax2a* at early somitogenesis (B) indicates a delay in development of MHB in *SBU2* mutants. Later, at 10 somite stage (D) *pax2a* expression resembles much earlier stage wild type expression domain (A). Likewise, although hindbrain marker *krox20* expression is also delayed and relatively reduced (E and F) later in the development, expression pattern appears similar to wild-type embryos (G and H). RNA *in situ* hybridization using *huC* probe revealed that *SBU2* embryos have reductions in early differentiating neurons (I, I' and J, J'). Arrows denote MHB and arrowheads denote otic placode.

To confirm that disruption of the *spt6* gene produces the *SBU2* phenotype, we assayed the ability of *spt6* mRNA to rescue the *SBU2* phenotype and determined whether microinjection of morpholinos directed against *spt6* phenocopy the SBU2 mutants. *spt6* mRNA was injected into embryos from a *SBU2* heterozygote intercross. Overexpression of *spt6* sense RNA in *SBU2* mutants rescues most of the somitogenesis and tail elongation defects (compare Fig. 2.5E and 2.5G). Overexpression of *spt6* mRNA doesn't produce an effect on wild type embryos (data not shown).

Next, we designed a morpholino antisense oligonucleotide to span the boundary between the 30th exon and 30th intron of *spt6*. *spt6* morpholino binding to the *spt6* pre-mRNA is predicted to create a missplicing event that deletes exon 30 and causes a frameshift mutation. The protein transcribed from that misspliced *spt6* RNA is predicted to closely mimic the Spt6 protein structure in SBU2 mutants. Injection of *spt6* morpholino into genotypically wild-type siblings of SBU2 mutants results in embryos that strongly resemble the *SBU2* phenotype (compare Fig. 2.5E and 2.5H). Based on linkage, sequence change, rescue and morpholino experiments; we conclude that disruption of *spt6* results in the *SBU2* phenotype.

An *spt6* mutation was previously shown to be the cause of the *pandora* phenotype [69]. *pandora* mutants exhibit defects in cardiac differentiation, pigmentation and ear formation. Stronger defects in these cell types are also observed in *SBU2* mutants (data not shown). A complementation test was performed to determine if the two mutations are allelic. Since the two mutations fail to complement, we designate our allele as pan^{SBU2}. pan^{m313}/pan^{SBU2} embryos resemble pan^{m313} mutants (data not shown). The genetic lesion in *pan* produces a truncated protein of 829 amino acids. We think that both mutations likely produce non-functional proteins. Because injection of the *spt6* morpholino into some wild-type stocks produces a phenotype (Fig. 2.5I) more similar to pan^{m313} (Fig. 5F) than pan^{SBU2} (Fig. 2.5E), we conclude that the phenotypic differences between pan^{m313} and pan^{SBU2} stem from genetic background differences.

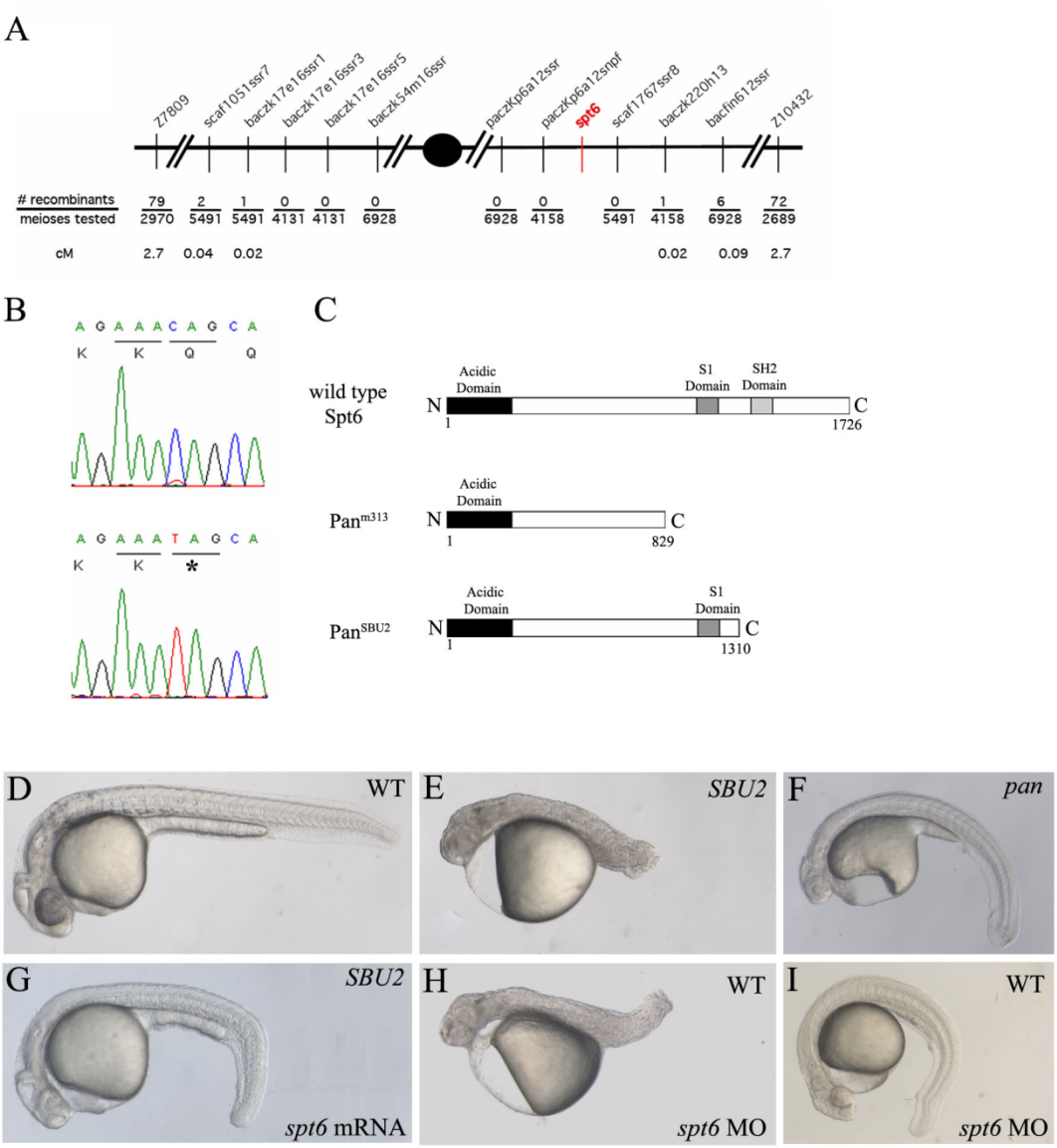

Figure 2.5: *SBU2* phenotype is the result of a non-sense mutation on *spt6* gene. *SBU2* maps to linkage group 21 between Z7809 and Z10432 (A). Sequencing analysis revealed a C to T transition at the 3931st nucleotide of the coding sequence of the *spt6* gene (B). Predicted Spt6 protein structure in wild type, *pan*^{m313} and *pan*^{SBU2} mutant embryos (C). The premature stop codon in *SBU2* is predicted to produce a truncated protein which lacks SH2 domain (C). The defects in *SBU2* mutants can be rescued by injection of *spt6* mRNA (G). Microinjection of *spt6* morpholino into the progeny from intercrosses of wild-type siblings of *SBU2* heterozygotes, phenocopies *SBU2* mutants (H). However, in some wild type stocks, the phenotype upon injection of *spt6* morpholino is much weaker (I) and resembles *pan* phenotype (F). (D, E, G, H) are 27-hour-old; (F and I) are 48-hour old embryos. Asterisk denotes stop codon in (B).

2.2.6 Morpholino knockdown of *spt6* suppresses notch signaling

Since the somite defects in *spt6* mutants resemble Notch pathway mutants, we sought to determine whether Spt6 is required for activation of the Notch pathway. We activated the Notch pathway by overexpressing the intracellular domain of the Notch protein (NICD) in embryos with compromised Spt6 function and measured transcript levels of notch target genes at the 18-somite stage (Fig. 2.6A-D). As expected, activation of Notch pathway by overexpression of NICD mRNA induced the transcription of Notch pathway target genes, *her1*, *her6*, *her7* and notch regulated ankyrin repeat protein (*nrarp*) (Fig. 2.6A-D, third bar). Conversely, injection of *spt6* morpholino to reduce functional Spt6 protein levels did not reduce the transcript levels of those genes (Fig. 2.6A-D, second bar). However, induction of target genes by the NICD mRNA was suppressed by knockdown of Spt6 (Fig. 2.6A-D, fourth bar). We did not observe differences in the levels of notch target gene expression in the Spt6 morphant embryos as we did in the RNA *in situ* hybridization analysis of SBU2 (fig 2.2). This disparity likely reflects associated with genetic background differences between the morphants and mutants as well as differences in the stages analyzed. Nevertheless, these results demonstrate that Spt6 is required for proper response to notch activation.

2.2.7 Spt6 physically interacts with Notch

Spt6 is a nuclear factor which interacts with histones to modulate chromatin structure during transcription elongation [70]. Moreover, a yeast two-hybrid screen revealed an interaction of Spt6 (EMB-5) with ankyrin repeats of LIN-12/GLP-1, notch family transmembrane receptors, in *C. elegans* [76]. To determine whether there is a physical interaction between zebrafish Spt6 and Notch protein, HEK293 cells were co-transfected with Flag-tagged zebrafish Spt6 and Myc-tagged intracellular domain of zebrafish Notch1a (NICD). As a positive control, Flag-tagged zebrafish Su(H) was co-transfected with NICD. Cell lysates were used in co-immunoprecipitation assay. Flag-tagged Spt6 or Su(H) was pulled from total cell lysate with anti-Flag antibody and associating proteins were studied with western blot analysis using an anti-myc antibody (Fig. 2.6E). This experiment showed that NICD is co-precipitated with either Spt6 or Su(H) demonstrating a direct or indirect interaction between Spt6 and intracellular

domain of Notch protein. This interaction likely mediates the regulation of transcription of Notch pathway associated genes.

2.3 Discussion:

We identified and characterized an embryonic lethal mutation, *SBU2,* which gives rise to somite abnormalities in zebrafish embryos. These defects are similar to, but more severe than Notch mutant embryos. *SBU2* mutants are characterized by severe posterior segmentation and differentiation defects, disruption of gene expression in paraxial and lateral plate mesoderm, but do not affect intermediate mesoderm. Moreover, although the patterns of many early regional neural markers in the mutant embryos are not severely altered, later, neural differentiation is highly disrupted. We utilized mRNA rescue and morpholino knock-down experiments to demonstrate that the phenotype observed in *SBU2* mutant embryos is due to disruption of the *spt6* locus. Altogether, our studies indicated that Spt6 has important functions during early patterning and somitogenesis of the zebrafish embryo.

2.3.1 Relationship of *SBU2* and *pandora*

A mutation that disrupts splicing of *spt6* and is predicted to give rise to a truncated protein was shown to give rise to *pan* phenotype [69]. Complementation studies between *SBU2* and *pan* confirmed that the two mutations are allelic. In pan^{m313} mutants, however, the truncated Spt6 protein is predicted to be much shorter than the protein produced in *SBU2* mutants. The Pan^{m313} protein lacks S1 RNA binding domain in addition to SH2 domain. Given the function of Spt6 as a modulator of chromatin structure, absence of the S1 nucleic acid binding domain in *pan* is consistent with the loss of function of the Spt6 protein. On the other hand, Spt6 protein produced by pan^{SBU2} which lack only SH2 domain might also fail to interact with other proteins in the transcription elongation machinery. Although both of the *spt6* alleles likely encode non-functional proteins, the phenotypic differences caused by those mutations are very striking. *SBU2* mutants reveal a much earlier and stronger phenotype than *pan* mutants

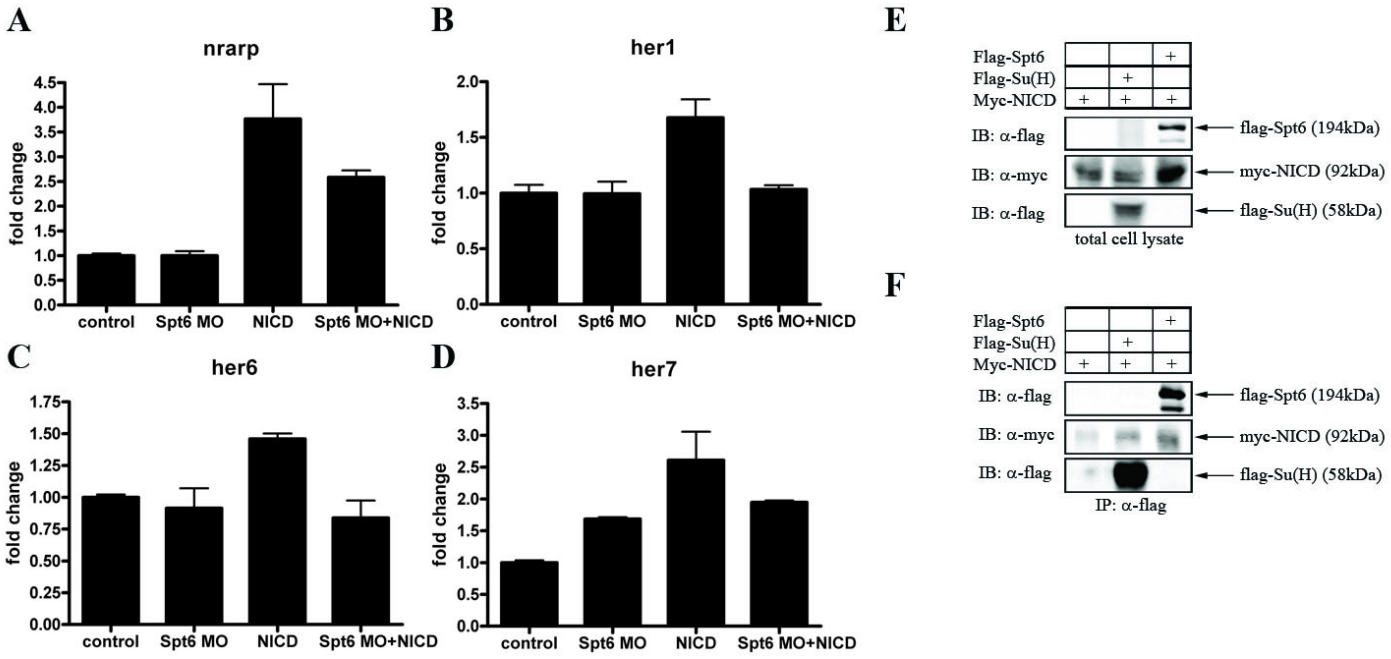

Figure 2.6: Spt6 genetically and physically interacts with Notch1a. (A-D) Activation of Notch pathway was monitored by the relative quantification of transcripts of Notch pathway target genes. Spt6 morpholino and/or the intracellular domain of Notch1a (NICD) was injected to 1-4 cell stage embryos; total RNA pools from 18 somite embryos were used for real time PCR. Each set of data is normalized to transcript level from the dye injected (control) embryos. Bars represent means of measurements from two different mRNA pools. Standard error of the mean is also shown. The data is representative of three independent experiments that showed similar trends. Levels of *nrarp*, *her1*, *her6* and *her7* transcripts are increased when Notch pathway is activated via NICD injection (third bar in A, B, C, and D). Microinjection of *spt6* morpholino does not significantly reduce the transcription of Notch pathway target genes (second bar in A, B, C, and D). However, *spt6* splice morpholino impedes activation of Notch pathway upon NICD injection; *nrarp*, *her1*, *her6* and *her7* transcript levels stay relatively constant with respect to either uninjected or *spt6* splice morpholino transcripts (fourth bar in A, B, C, D) when functional Spt6 protein is knocked down from NICD injected embryos. (E, F) Co-IP analysis of HEK293 cells transfected with flag-Spt6, flag-Su(H) and myc-NICD. (E) Western analysis of total cell lysates with anti-flag and anti-myc antibody; (F) western analysis of Co-IP assay using cell lysates from (E). Su(H) is used as positive control for co-immunoprecipitation assay (second lane, F). NICD is co-immunoprecipitated with Spt6 (third lane, F) indicating that Spt6 directly or indirectly interacts with NICD in HEK293 cells. A low level (background) interaction is detected between the myc-NICD and anti-flag antibody/bead in the absence of flag-tagged protein (First lane, F), however the intensity of this band is considerably less then flag-Su(H) or flag-Spt6 precipitated proteins (Lanes 2 and 3, F).

and die around 2 dpf while *pan* embryos display defects much later and usually survive more than 7 days. Moreover, microinjection of *spt6* morpholino can phenocopy pan^{SBU2} or pan^{m313} depending on the background of the injected embryos (Fig 2.5). These observations suggest that severity of the defects in *spt6* mutants is highly genetic background dependent and variations in levels of maternal Spt6 protein to some degree may impact the extent of the defects observed. Similarly, yeast are sensitive to SPT6 copy number [90].

2.3.2 Spt6 functions in the Notch pathway

Spt6 protein has been studied in human, mouse, zebrafish, Drosophila, *C. elegans* and yeast. It has been shown to interact with many components of the transcriptional machinery. In yeast, Spt6 protein has ATP-independent nucleosome assembly function, controlling transcription of various set of genes by modulating the assembly state of the nucleosomes during active transcription [70]. In addition *spt6* mutations can suppress the effects of the mutations affecting the Snf/Swi chromatin remodeling complex in yeast [91]. Similarly, in Drosophila, it was shown that Spt6 protein is associated only with the active form of RNA pol II and has a role in regulation of transcription [92]. Moreover, human SPT6 antagonistically interacts with histones as well as the transactivator domain of human cytomegalovirus pUL69 to modulate transcription [93]. Overall, Spt6 is a part of transcription elongation machinery and regulates the transcription of corresponding genes by modulating the chromatin structure in the cell in wide range of organisms. However, in *C.elegans*, EMB-5, a homolog of yeast Spt6, was characterized as a regulator of timing of the gut processor division during gastrulation and controller of oogenesis and required for specific synchronous cell division timing of E cells [94].

Many of the Notch pathway components found in invertebrates are conserved in vertebrates as well (reviewed in [33]). Our work provides further evidence that Spt6 function is also conserved in a vertebrate model and it interacts with complexes containing the Notch ICD. An interaction between the *C. elegans* homolog of Spt6, EMB-5 and ankyrin repeats of the LIN-12 and GLP-1, notch family transmembrane receptors [76] was identified through yeast 2-hybrid assay. Moreover, when *emb-5* function is eliminated from the *lin-12* mutant embryos, the penetrance of the *lin-12*

phenotype is enhanced whereas penetrance of the constitutively active *lin-12* phenotype is reduced. In addition, *emb-5* is required for the proper germline development regulated by *glp-1* [76]. Ectopic activation of *glp-1* cannot rescue the phenotype caused by *emb-5* mutation [76] indicating that *emb-5* is epistatic to *glp-1*. These observations also suggest that there is a direct functional interaction between e*mb-5* and *lin-12/glp1*.

A recent study also supports the functional interaction between Spt6 and Notch pathway in Drosophila [95]. Rad-6/Bre1 histone modification activity is essential for transcription of notch target genes [96]. Paf-1 complex is required for this activity [97]. Knocking-down Rtf-1, a component of the Paf-1 transcription elongation complex, in N^{nd-1} notch mutant background enhances the phenotype of the notch mutation. Furthermore, the zebrafish homolog of the yeast Rtf-1 protein was recently shown to be disrupted in a novel zebrafish mutant, *white zebra (wze)* (T. Akanuma and S. Takada, personal communications). *wze* also exhibits segmentation defects similar to Notch pathway mutants and pan^{SBU2}. Since genetic studies indicate that Spt6 interacts with Rtf-1 [98], there is a strong possibility that Spt6 also functions in notch signaling along with Paf-1/Bre1 transcription elongation complex. Other studies (reviewed in [99]) support the requirement for appropriate chromatin modifying and remodeling functions for proper transcription of particular genes.

In this study, we demonstrated a biochemical interaction between Spt6 and Notch protein in a co-immunoprecipitation study using HEK293 cells. Spt6 may directly bind the Notch ICD or be a part of a larger transcriptional complex. Since EMB-5 was shown to interact with the Ank repeats of both LIN-12 and GLP-1 in a yeast two-hybrid studies [76], we favor the direct interaction model. The functional interaction was also demonstrated by studying the Notch pathway response capabilities of Spt6 knockdown embryos. These observations indicate that a robust response to ectopic Notch activation requires Spt6 function.

In addition to playing a role in notch signaling, other cellular processes are affected by *spt6* mutation since the overall pan^{SBU2} phenotype is much more severe and complex than Notch pathway mutants. Most of the Notch pathway mutants can be raised to adulthood indicating that the somitogenesis defects observed in those embryos

improve later in development however in *pan*^{SBU2} mutants, defects become much worse; even the previously formed structures cannot be maintained, and embryos eventually deteriorate and die. Although *spt6* is required for notch-mediated segmentation of the zebrafish embryo, it is also required for many other basic cellular functions. While chromatin remodeling factors like Spt6 have broad cellular roles, they also may be required for specific signal transduction pathways and regulate specific developmental proccesses.

2.4 Materials and methods:

2.4.1 Fish husbandry and mutagenesis

Adult zebrafish strains and embryos obtained from natural crossings were maintained at 28.5°C. Developmental stages of the embryos were determined according to Kimmel *et. al*. [5]. For mutagensis adult fish were placed in 3.0 mm ENU for 1 hour, once a week for three weeks.

2.4.2 Positional mapping of SBU2

Genomic DNA extractions and PCR conditions were performed as described in [100]. SSLP primers were designed using the zebrafish SSR program (http://danio.mgh.harvard.edu). PCR products were electrophoresed on 3% MetaPhore (Cambrex, Rockland, ME) agarose gels. New polymorphic marker sequences were:

scaf1051ssr7	F: GCCAGTAAATTTTGGCCTTG
	R: GACGTGTGAAGCTGCAGAAA
baczk17e16ssr1	F: ACTGTGCTCTGATGCCTCCT
	R: TGCAAAAATAAGCAAATAAACAAA

baczk17e16ssr3	F: CATTCCGAAATGACCCAGTT
	R: GCCTTTGATTATGTCTGTAAAAGC
baczk17e16ssr5	F: CACAACAACCAACCGCTCTA
	R: CGCAGTACTGAAGACGCAAA
baczk54m16ssr	F: GCCTCGTCCCTACAAACAAA
	R: AACCGCTTGGTATGCTGAAC
paczkp6a12ssr	F: CAAACAACAACTGGGCACTTT
	R: AGATCCAGATCCGGCTTGA
paczkp6a12snpf	F: CACAAAGGAGATGTCATGCTG
	R: GCAAGACTTTAACACTGCTACCAGAC
scaf1767ssr8	F: GTGCAGGCCTTGGTGTGTAT
	R: AAGGTTACCATAAGCCATTAACAA
baczk220h13	F: CAGGTATTTTCCTACACTAACAACAC
	R: AATTGCCAGATGAAACATGC
bacfin612ssr	F: ACATCCACACAGCCACTCAT
	R: GGGGTGTAATGGTACACTGGA

2.4.3 Expression constructs, mRNA synthesis and morpholinos:

spt6 and myc-*NICD* expression constructs were kindly provided by Deborah Yelon and Scott Holley and generation of these constructs is previously described [69, 101]. 3XFlag tag was inserted into to N-terminal *spt6* construct at BamHI site of $pCS2^{+}$ vector. *su(H)* ORF was amplified from 10 somite stage wild type total first strand cDNA using
GATGACAAGCTTAAGATGGCGCCTGTTGTGA/TACCCGGGATCCAGGTTAGGA

GACGGACATGG primer pair. Amplified fragment is then cloned to p3XFlag CMV 7.1 vector (Sigma) at HindIII and BamHI sites.

Capped sense mRNA was synthesized using mMESSAGE mMACHINE Kit (Ambion, Austin, TX). Splice morpholino that target 30th exon-intron boundary of the *spt6* pre-mRNA blocking the proper nuclear processing is designed and synthesized by Gene Tools. The sequence of the morpholino used is 5'-GCCATAGGAACAGCTCACCTCAGTG-3'. Standard control oligo (Gene Tools, Philomath, OR) is used as control. mRNA and morpholino solutions were diluted to desired concentration with 0.2 M KCl supplemented with phenol red. Typically, 100 pg of *spt6* mRNA, 500 pg of *NICD* mRNA and 10 ng of *spt6* splice morpholino is injected to one- to two-cell stage embryos.

2.4.4 Whole mount in-situ hybridization and immunohistochemistry

In situ hybridizations were performed according to Thisse et. al. [102]. Digoxigenin labeled probes for *in situ* hybridization was synthesized using T7, T3 or Sp6 RNA polymerase (Roche, Indianapolis, IN). Hybridized probes were detected using NBT/BCIP system (Roche, Indianapolis, IN). Stained embryos were re-fixed in 4% PFA and either stored in 100% methanol or cleared in Benzyl benzoate/benzyl alcohol solution (2:1) and mounted in Canada balsam/methyl salicylate (2.5% v/v) or flat mounted in 70% glycerol. Embryos were viewed with Zeiss Axioplan microscope, digitally photographed with Zeiss Axiocam camera. Images were processed and assembled with Zeiss Axiovision and Adobe Photoshop.

β-catenin, Fak, and F59 staining were performed as previously described [80, 84, 103-106]. Embryos were fixed in 4% paraformaldehyde (PFA) for 4 hours at room temperature and incubated in block for 1 hour. Staining was conducted in PBDT (1% BSA, 1% DMSO, 1% Triton X-100 in PBS), embryos were rinsed for 2 hours, then secondary staining proceeded overnight. Antibodies used were: mouse monoclonal anti-slow-twitch myosin (F59) (Devoto, et al. 1996, generous gift of Frank Stockdale) 1:10, rabbit polyclonal anti-pY^{397}FAK (Biosource, Camarillo, CA) 1:50, and rabbit polyclonal anti-β-catenin (Abcam, Cambridge, UK) 1:500. Alexa-Fluor 488, 546, and 633

conjugated goat anti-mouse and goat anti-rabbit secondary antibodies (Invitrogen, Carlsbad, CA) 1:200. Images were acquired using a Leica SP2 confocal microscope and a Zeiss ApoTome running on a Zeiss Axio Imager Z1. For confocal images, embryos were mounted in 100% glycerol and visualized using a 40x oil immersion lens. Image quality was optimized using 2-16 line averaging. Images were processed in Adobe Photoshop and collated in Adobe Illustrator.

2.4.5 Genotyping SBU2

All *SBU2* embryos younger than 10 somites are genotyped either after they reach to desired stage and imaged or scored after in-situ hybridization. Genomic DNA is extracted from whole embryos using DNeasy tissue kit (Qiagen, Valencia, CA) or followed the protocol previously described [107]. PCR primers used to genotype *SBU2* embryos are:

Spt6 pvuII F AATGCTGACTGGTTCTCAGCT

Spt6 R2 GCCGCATAATGAAGATCGAC

Following PCR, products were digested with PvuII which cuts the wild-type allele.

2.4.6 Relative quantitation of gene expression by real-time PCR

Total RNA was extracted from pools of five 18s *spt6* MO and/or *NICD* injected embryos using the Trizol reagent (Invitrogen, Carlsbad, CA). SuperScript II Reverse Transcriptase (Invitrogen, Carlsbad, CA) was used to synthesize first strand cDNA from 0.5 ng of total RNA. Real time PCR was carried out using ABI Prism 7900HT Fast Real-Time PCR system (Applied Biosystems, Foster City, CA) in 15 μL of final volume using 2X FastStart SYBR Green Master (Roche, Indianapolis, IN). Primer pairs used to amplify desired transcripts were:

β-actin: GATTCGCTGGAGATGATG/GTCTTTCTGTCCCATACCAA

her1: AGGCGATTCTAGCAAGGACA/CGAGTTATGGGTTTGGATGG

her6: CCTTGGTAGACTCCGAGGAAA/CGCTGAACAAAGAAAACAAGTG

her7: CAACCAACCTAATCAGAGACGA/ TCTGACAGGCAGTCTGATGG

nrarp: ACTGCTGCAGAACATGACCA/GTTTCACGAGCTCCAGGTTC

Total RNA amount of each sample is normalized to relative amount of *β-actin* transcripts in each pool. In each experiment, 2 pools of control and experimental samples were run in duplicates; Ct values of each pool are averaged and relative amounts of gene expression were calculated using relative standard curve prepared for each primer set in each particular real time PCR run.

2.4.7 Co-Immunoprecipitation and western analysis:

HEK293 cells were grown in DMEM/F12 containing 10% CS. Cells were transfected with 1μg of total DNA using deacylated linear PEI (MW=22,000). 24 hours after transfection, cells were harvested in 5mM EDTA/PBS and resuspended in ice-cold freeze/thaw lysis buffer (10mM Tris HCl pH 7.4, 10mM KCl, protease inhibitor cocktail (1:100) (Sigma, St Louis, MO) and subjected to three freeze/thaw cycles. Lysates were centrifuged to remove cell debris at 13000 rpm for 15 minutes. 5% of the supernatant was mixed with 5X SDS-buffer and boiled. The remaining lysate was cleared with 20 μL of Protein A coupled agarose beads (Sigma, St Louis, MO) for 30 minutes. Cleared lysate is then mixed with 1μg of α-Flag monoclonal antibody (Sigma, St Louis, MO) at 4°C for 2 hours. 20μL of Protein A coupled agarose beads (Sigma, St Louis, MO) is added to lysate-Ab mixture and mixed for additional 4 hours. Beads were separated from the lysate, washed with cold lysis buffer five times thoroughly, resuspended in 1X SDS-buffer and boiled. Total cell lysates and immunoprecipitates were electrophoresed on 7.5% polyacrylamide gel, electroblotted to nitrocellulose membrane. Membrane was probed at room temperature for 1 hour with mouse monoclonal α-flag (1:2,000) (clone M2, Sigma) and rabbit polyclonal α-myc (1:5,000) (Immunology Consultants Laboratories, Inc., Newberg, OR), followed by incubation with IRdye 800 conjugated α-mouse (1:10,000) (Rockland Immunochemicals, Gilbertsville, PA) and Alexa Fluor 680 conjugated α-rabbit (1:10000) (Invitrogen, Carlsbad, CA) at room temperature for 1 hour.

The membranes were scanned using Odyssey Imaging System (Li-Cor Biosciences, Lincoln, NB).

Chapter 3: Churchill and Sip1a repress FGF signaling during zebrafish somitogenesis

(This chapter is previously published in Developmental Dynamics 239(2010) 548-558

3.1 Introduction:

Fibroblast growth factors (FGFs) play essential roles in cell growth and differentiation in many developmental contexts [108-116]. During vertebrate embryogenesis, FGFs are required for induction of both mesoderm and neural ectoderm, patterning of the midbrain, posteriorization of the neural plate and segmentation of the mesoderm. In vertebrates, the FGF family contains over 20 ligands that interact with four receptors. The mechanisms that account for the diverse responses evoked by FGFs have yet to be fully elucidated, but depend on cell type specific modulators of signaling.

One such FGF effector is the zinc finger protein Churchill (ChCh), which regulates FGF activity during gastrulation. ChCh is slowly induced in response to FGF and acts as a switch between mesoderm and neural inducing activities of FGF in chick, Xenopus and zebrafish [117-119]. ChCh inhibits expression of mesodermal markers including *brachyury*, *Tbx6L,* and *spt* and blocks mesendoderm induction, which requires FGF signaling in cooperation with Activin/Nodal activity [120, 121]. ChCh also regulates

cell movements during gastrulation. In the chick, Chch blocks ingression of presumptive ectoderm through the primitive streak at the end of gastrulation. Therefore, these cells adopt neural fates instead of ingressing through the streak and becoming paraxial mesoderm [117]. Similarly, when zebrafish blastomeres with compromised ChCh activity are transplanted to the animal pole of wild type hosts, they leave the epiblast, migrate to the germ ring and acquire mesodermal fates [122].

ChCh was initially thought to regulate transcription of target genes via a direct DNA interaction. However, subsequent biophysical characterization of ChCh has suggested that it may not be a DNA binding protein [123]. None-the-less, by direct or indirect mechanisms, ChCh induces *sip1* (Smad Interacting Protein 1) transcription [117-119], which is key to its activity. Sip1 is a multifunctional molecule that modulates TGF-β signaling by converting activated forms of both Smad1/5 and Smad2/3 to transcriptional repressors [124-127]. In addition, Sip1 regulates cell movements by directly repressing E-cadherin transcription [124, 128] and mesoderm induction by directly impeding Xbra transcription [124, 125].

In zebrafish, *chch* is expressed after gastrulation [118], but later roles for ChCh have not been studied. We now present data that ChCh and Sip1 are required for somitogenesis. Segmentation is an essential step in formation of the vertebrate body axis. Mesodermal segmentation is established by sequentially dividing the unsegmented presomitic mesoderm into the bilaterally segmented structures called somites. The "clock and wavefront" model describes the mechanisms of regulation of somitogenesis [4, 15, 17, 22, 24, 25, 129]. In zebrafish, the "clock and wavefront" model proposes that function of a molecular oscillator in the presomitic mesoderm (PSM) results in controlled expression of a set of genes associated with the Notch pathway [22, 55, 130, 131]. Simultaneously, the wavefront modulates the ability of the PSM to respond to the morphogenic signals and produce segments [7, 132, 133]. The pulses generated by the molecular clock are translated into very highly regulated spatial periodicity. Despite the similarities in somitogenesis between species, there are differences between amniotes and mammals in the segmentation program [133, 134]. For example, *lunatic fringe* and *delta* genes appear to function differently in mouse, chick and zebrafish [23, 135-138]. In

addition, the Wnt pathway is important for regulation of segmentation clock in mice [27, 139], but not zebrafish.

Previous studies revealed that FGF signaling at the PSM regulates the wavefront position during somitogenesis. FGF modulates somite size by impeding maturation of PSM [64, 65, 140, 141]. Blocking FGF signaling increases somite length, while activating signaling has the opposite effect [65]. In addition, activation of FGF signaling blocks convergence movements and expands somite width [114, 142]. It is important to define regulators of FGF signaling in the PSM in order to determine how precise positional cues within the PSM are generated.

Here, we demonstrate that ChCh and Sip1a modulate FGF signaling in the PSM during somitogenesis. Surprisingly, we find that ChCh and Sip1 repress FGF expression. During somitogenesis, knockdown of *chch* or *sip1a* results in somites that are less extended thru anterior-posterior (A/P) axis while they are over-extended thru mediolateral axis. We also found that inhibition of ChCh and Sip1a perturbs oscillating gene expression in the forming somites. In ChCh or Sip1 compromised embryos, *fgf8* expression in the paraxial mesoderm is expanded rostrally leading to altered somite size. Manipulations that reduced FGF8 signaling in ChCh compromised embryos restored somite size. This demonstrated that ChCh and Sip1a regulate somite morphogenesis by limiting FGF signaling. Together, these findings establish a novel role for ChCh as a repressor of FGF signaling.

3.2 Results:

3.2.1 Role of ChCh and Sip1 in somitogenesis:

In a previous study, we observed that ChCh is required for proper somite formation [122]. However, the mechanism of action of ChCh in somitogenesis is unknown. To investigate the function of ChCh in zebrafish somitogenesis, we inhibited ChCh activity using two translation blocking morpholinos (*chch* ATG MO and MO2) [122]. Microinjection of the *chch* ATG MO presents a similar, but stronger somite

phenotype than that produced by *chch* ATG MO2 microinjection. *chch* morpholino injected embryos are morphologically indistinguishable from control morpholino injected siblings until 75-95% epiboly stage (Fig 3.1B, C). Dorsal views of the 12-somite stage *chch* morphants reveals that somites are less extended thru anterior-posterior axis while they are over-extended thru mediolateral axis (Fig. 3.1K-M, 52%, n= 128). Moreover, these embryos have a shorter and wider body axis (Fig. 3.1G, L; H, M). At 24 hours post fertilization, somites in ChCh compromised embryos are enlarged and lack their characteristic chevron shape (Fig. 3.1Q). Furthermore, although roughly 30 pairs of somites are formed in wild type siblings, *chch* morphants only form 22-26 somites (Fig. 3.1Q and data not shown). Taken together, these results demonstrate that ChCh is required during somitogenesis.

Because ChCh activity is mediated by Sip1 during gastrulation [117] and homozygous *Sip1* knockout mice have a somite phenotype similar to *chch* morphants [143], we asked whether Sip1 inhibition produced similar somite defects in zebrafish. Zebrafish have two *sip1* genes (*sip1a* and *sip1b*) [144]. To investigate the function of Sip1 in zebrafish somitogenesis, we inhibited Sip1 activity using previously characterized *sip1a* and *sip1b* morpholinos [144]. The *sip1a* ATG MO injected embryos have a somite phenotype similar to c*hch* MO injected embryos, but the overall phenotype is more severe (Fig. 3.1I, N (89%, n=112) and data not shown). As in *chch* morphants, the somites are shorter thru anterior-posterior axis and over-extended thru mediolateral axis (Fig. 3.1N). Microinjection of *sip1a* splice morpholino also produced embryos were also short in anterior-posterior axis and elongated in the mediolateral axis (Fig. 3.1J, O). Similar to *chch* morphants, somites are enlarged and lost their characteristic chevron shape at 24 hpf (Fig. 3.1R, S). Because this morpholino alters mRNA structure, we were able to monitor the effectiveness of the knockdown on eliminating wild-type mRNA (Fig 3.2). Until dome stage, only wild-type mRNA is detected, which is presumably maternal message that is unaltered by the splice morpholino. Beginning at dome stage (4.3 hpf), the smaller misspliced product is detected. By 75% epiboly (8 hpf), no wild-type mRNA is detected.

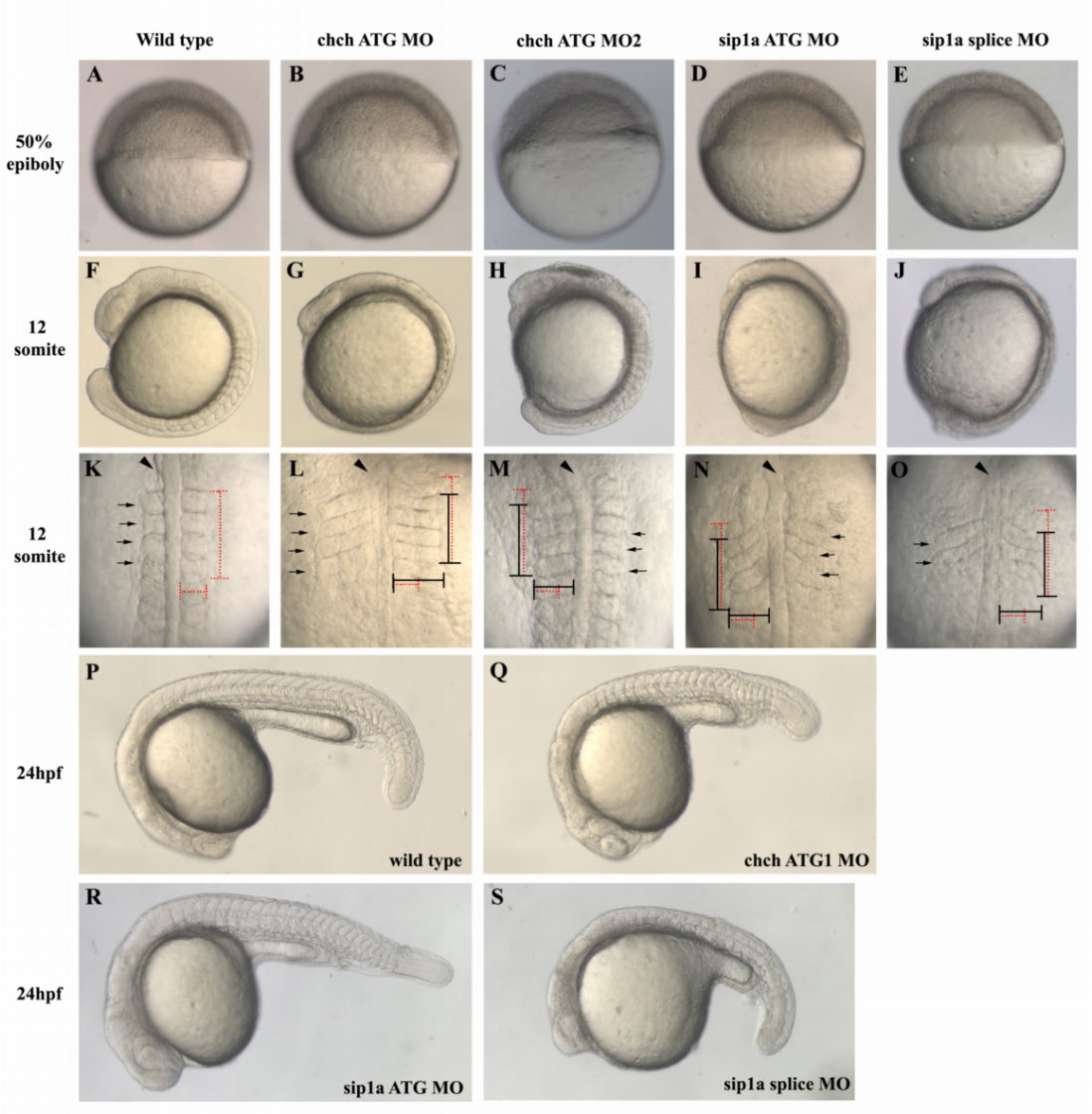

Figure 3.1: ChCh and Sip1a are required for somitogenesis. Living wild-type, ChCh and Sip1a-compromised embryos. Early epiboly movements appear normal in *chch* or *sip1a* morphants (A-E). By 12s misshapen somites are apparent in both *chch* and *sip1* morpholino treated embryos (F-J). In these embryos, somites are less extended thru anterior-posterior axis and over-extended thru mediolateral axis (K-O). Horizontal and vertical red dotted lines span the width and length of the first four wild type somites for comparison to the first four somites of morphant embryos, which are marked with a black line (K-O). At 24hpf, somites are enlarged and misshapen in both ChCh and Sip1a compromised embryos (P-S). Arrowheads denote notochord and black arrows denote somites. (A-J, P-S) are lateral views; (K-O), dorsal views.

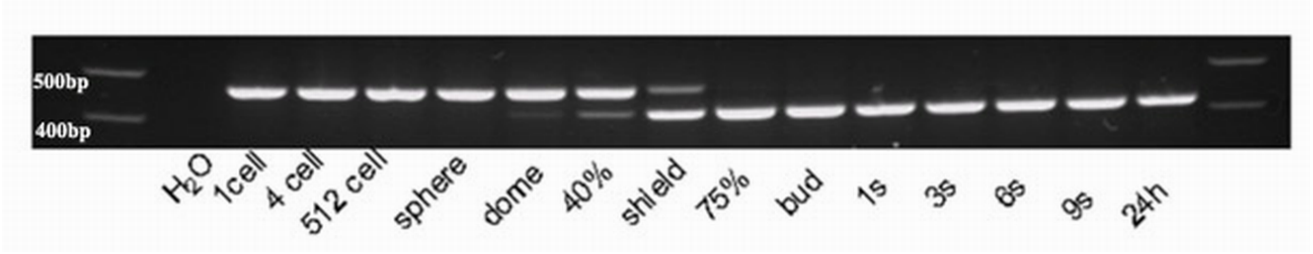

Figure 3.2: *sip1a* splice morpholino is effective in eliminating wild-type *sip1a* mRNA. RT-PCR of mRNA from staged *sip1a* splice MO injected embryos with *sip1a* specific primers reveals that the smaller misspliced product is detected by dome stage (4.3 hpf). By 75% epiboly (8 hpf), no wild-type mRNA is detected.

An alternatively spliced form of *sip1a* that lacks a portion of exon 8 has been described [144]. The alternative splice lacks one zinc finger that is present in the longer form (Fig 3.3, blue bar, Supp Fig. 3A, dark blue box). We identified a similar alternatively spliced form of Sip1b that contains a deletion of 66 bp of exon 8 (Fig. 3.3). Since both *sip1a* and *sip1b* contained forms that lack the same region, we sought to determine whether either form of *sip1a* was required for somite formation. Both *sip1a* forms were detected by RT-PCR during a series of stages spanning the first 24 hpf (data not shown). We designed morpholinos to target the exon 8/intron 8 boundary (*sip1a* splice MO2, Fig 3.4A, pink bar) to drive production of the shorter form and a morpholino (*sip1a* splice MO3, Fig 3.4A, orange bar) that targets the alternative splice site in exon 8 and blocks production of the shorter form (leaving only the long form). Analysis of cDNA from embryo injected with each morpholino revealed that *sip1a* splice MO2 efficiently altered splicing so that only the shorter form was produced while *sip1a* splice MO3 eliminated the shorter form (Fig 3.4B, C). Somitogenesis was not altered by microinjection of either morpholino (data not shown). Due to toxic effects of co-injecting high doses of the two morpholinos (10 ng each), we were unable to analyze the effects of blocking production of both the long and short Sip1a forms in the same embryos. However, these experiments suggest that each Sip1a form is likely sufficient for normal somite development.

In a previous report, *sip1b* morphants were reported to have severe defects and produce only a few somites [144]. We observed a more severe phenotype than Delalande

et. al. when we microinjected low doses of *sip1b* MO (data not shown). Therefore, we were unable to address the role of *sip1b* in somite formation using morpholino approaches.

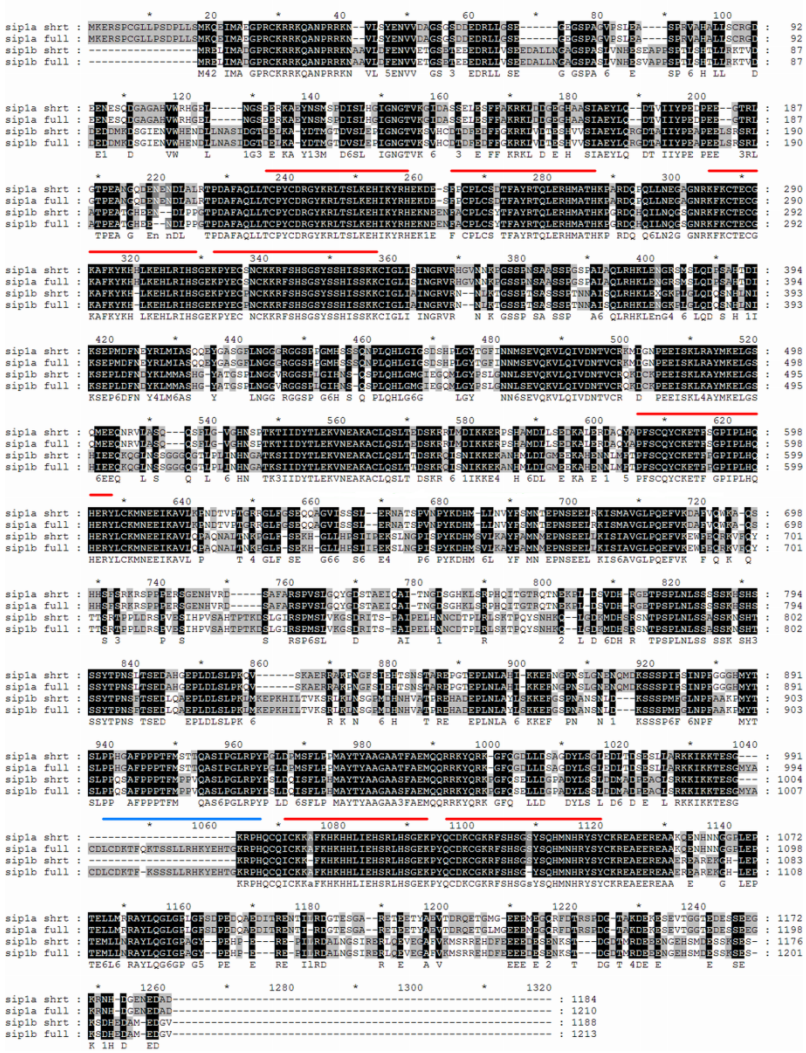

Figure 3.3: Comparison of zebrafish Sip1a and Sip1b proteins. Genedoc software is used to align the predicted protein sequences. Predicted domains of Sip1a and Sip1b is lined with colored bars: C2H2 type zinc fingers present in both Sip1a and Sip1b (red), C2H2 type zinc finger region that is absent from Sip1a and Sip1b short forms (blue). Identical and similar amino acids conserved among all proteins are shown in black and dark gray boxes, respectively. Lighter shades of gray or no shading represent low levels of amino acid conservation and the lack of conservation, respectively.

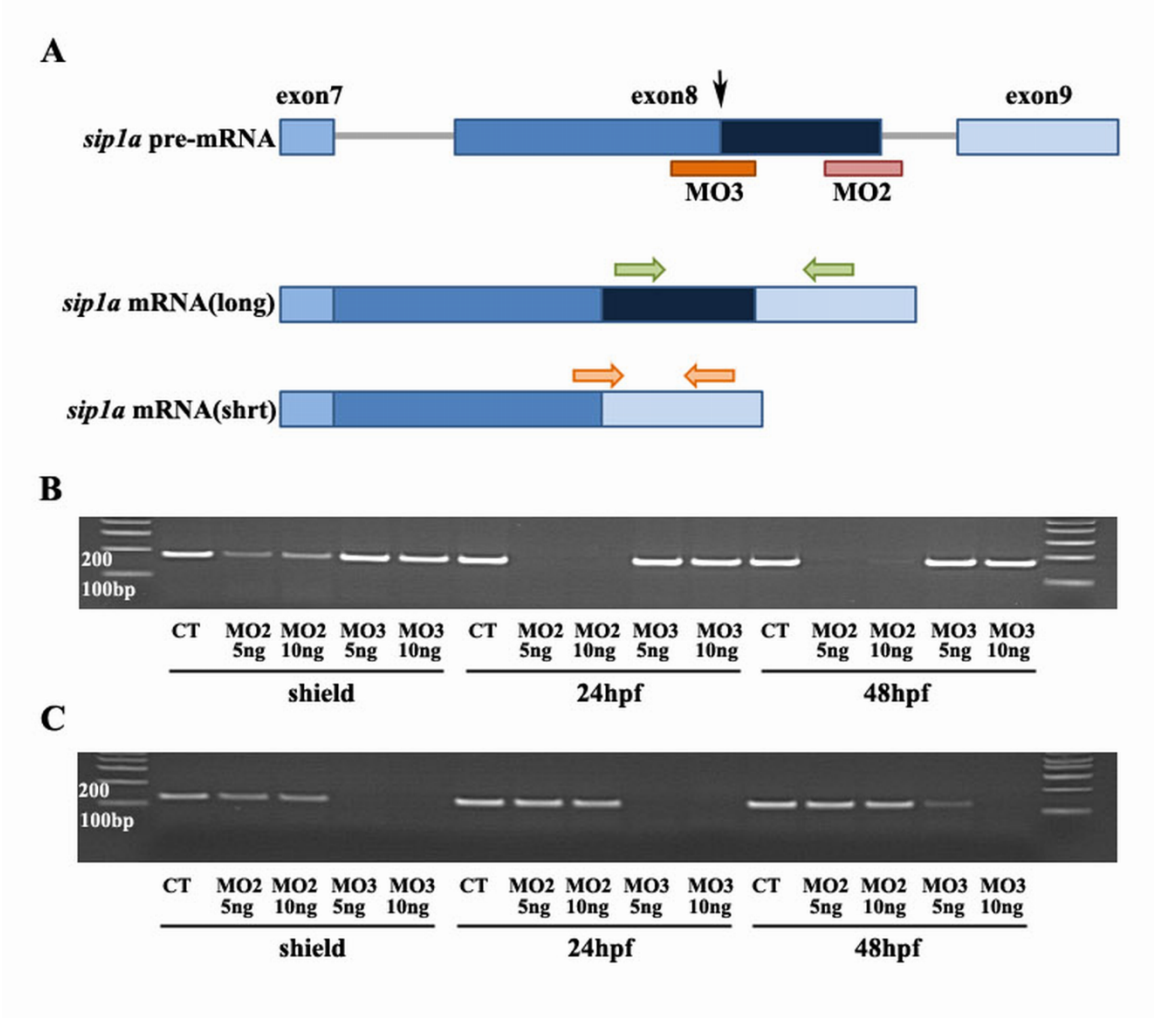

Figure 3.4: *sip1a* splice variant targeting morpholinos efficiently eliminate short and long forms. Diagram of the alternative splicing within the 3' region of the *sip1a* pre-mRNA (A). Alternative splicing of exon 8 eliminates one zinc finger (dark blue box) which is present in the longer form. Sip1a MO3 (orange bar) targeted to alternative splice site in exon 8 (denoted by black arrow) blocks the alternating splicing event and eliminates production of the short form. Sip1a MO2 (pink bar) blocks the pre-mRNA splicing event needed to generate the long form by targeting the splice site at the 3' end of exon 8. (B) RT-PCR of mRNA from staged sip1a splice MO2 and MO3 injected embryos with *sip1a* full length specific primers (B, green arrows in A) and *sip1a* short form specific primers (C, orange arrows in A). *sip1* splice MO2 efficiently altered splicing so that the full length message is eliminated and only the shorter form was produced (B) while *sip1* splice MO3 blocked production of the shorter form (C).

3.2.2 ChCh and Sip1a are required for pattering of presomitic mesoderm

During somitogenesis, a series of highly regulated morphogenetic processes produce periodic and symmetrically formed somite boundaries. To characterize the origin of problem underlying severe somite defects in ChCh and Sip1a-compromised embryos, we performed a series of RNA *in situ* hybridizations with 14 somite stage *chch* and *sip1a* MO injected embryos. Since somites are derived from paraxial mesoderm cells, we analyzed the state of the presomitic mesoderm cells in ChCh and Sip1a compromised embryos. *papC* encodes a structural transmembrane protein and regulates the mesodermal segmentation during zebrafish development. In wild-type control embryos, four *papC* expression stripes corresponds to the (prospective) somites at the segmentation plate [145], Fig. 3.5A). However, in *chch* and *sip1a* morphants, the number of stripes ranges from 5-8 (Fig. 3.5B, C). Moreover, tail bud expression domain of *papC* in ChCh and Sip1a compromised embryos is much broader mediolaterally than in wild type siblings (Fig. 3.5A-C).

Rostrocaudal polarity of the somites is also disrupted in ChCh and Sip1a compromised embryos. The segmental expression of myogenic regulatory factor *myoD* in the posterior half of the somites [146] are extended in the mediolateral axis (Fig. 3.5D-F). On the other hand, expression of *ephB2* [147] (Fig. 2G-I), *dld* [20, 22] (Fig. 3.5J-L) and *fgf8* (Fig. 3.6G-I) in the anterior half of the somites is reduced and expression domains are no longer restricted to anterior region of the somites in both *chch* and *sip1a* morphants. Therefore, we conclude that rostrocaudal somite polarity requires ChCh and Sip1.

3.2.3 Inhibition of ChCh and Sip1a alters periodic gene expression

The “clock and wavefront” model describes the timing and positioning of somite boundaries during segmentation of the mesoderm [15, 17, 22, 24, 25, 129]. In this model, somite size is the synchronous function of frequency of “molecular clock” oscillations and of the pace of “wavefront” progression. In *chch* and *sip1a* morphants, formed somites are smaller thru anterior-posterior axis. Either a faster ticking “molecular clock” or slowed down “wavefront” progression during somitogenesis can trigger reduction in somite size.

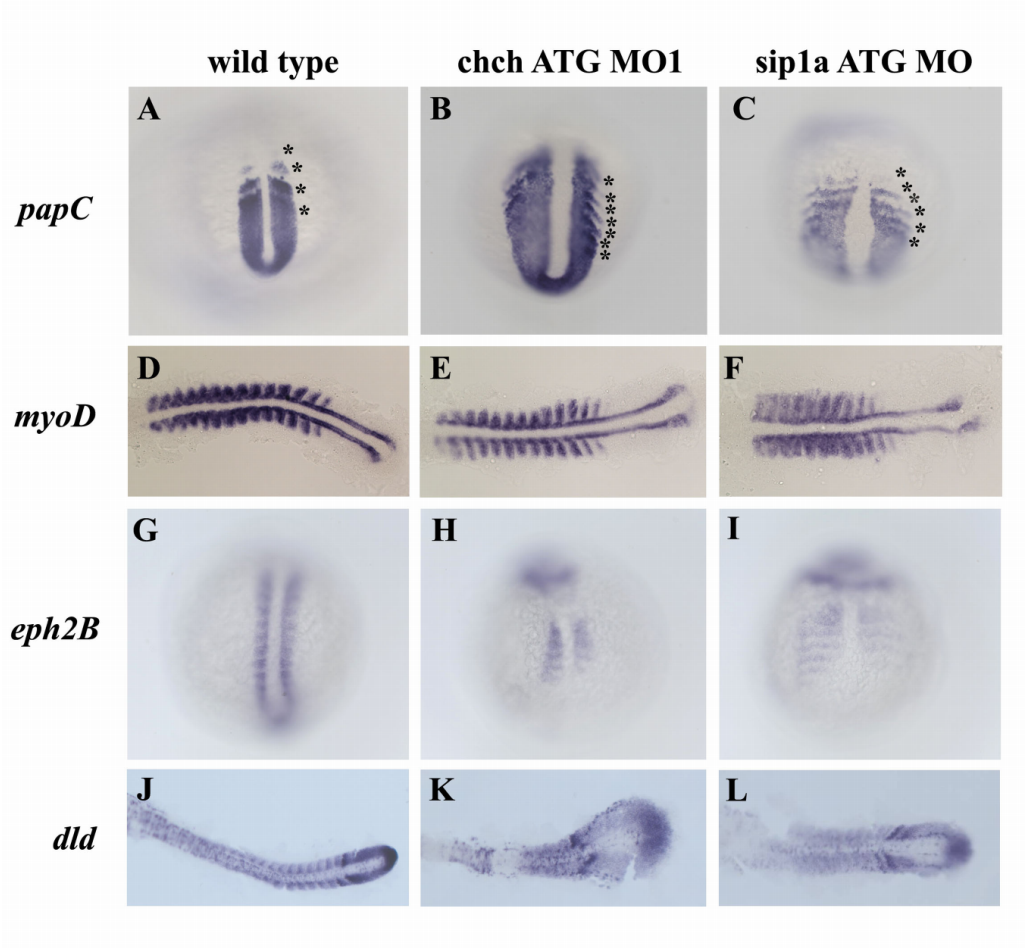

Figure 3.5: Patterning of the presomitic and somitic mesoderm is disrupted in ChCh and Sip1a compromised embryos. Whole mount (A-C, G-I) and flat mount (D-F, J-L) RNA *in situ* hybridization of somite markers in wild type, ChCh and Sip1a compromised embryos. All views are dorsal; anterior to the top (A-C, G-I) and anterior to the left (D-F, J-L)). The expression domains of the PSM marker, *papC* is broader mediolaterally in ChCh and Sip1a compromised embryos than the wild type siblings (A-C). The number of the *papC* expression stripes corresponding to the prospective and formed somites at the segmentation plate in c*hch* and *sip1a* MO is higher than in wild type siblings (A-C, compare asterisks number). The myogenic regulatory factor, *myoD,* is expressed in the posterior somite compartment in *chch* and *sip1a* MO injected embryos as in wild-type embryos (D-F). *ephB2* and *dld* expression at the anterior half of the somites (G-L) is reduced and diffuse. Asterisks denote (prospective) somites.

To test whether cyclic gene expression is altered in ChCh and Sip1a compromised embryos, we assayed *her1* and *her7* expression by RNA *in-situ* hybridization. *her1* and *her7* are both the output of the "molecular clock" and have characteristic 1 to 2 stripe expression domain in the PSM at 10 somite stage (Fig. 3.6A,D) [21]. However, the number of stripes observed in the ChCh and Sip1a compromised embryos ranged from 3 to 5 (Fig. 3.6A-C; D-F, marked with asterisks) indicating that impeding ChCh or Sip1a averts the proper termination of cyclic *her1* and *her7* expression in the anterior PSM.

However, the performance and pace of the "molecular clock" is not substantially altered because despite the size difference, duration of somite formation in ChCh and Sip1a compromised embryos is comparable to control morpholino injected siblings (Fig 3.7 and data not shown).

Failure to properly terminate *her1* and *her7* cyclic expression in the anterior PSM can be the result of slowed wavefront progression because the "wavefront" facilitates the transition of the PSM cells from the immature state to mature state by arresting the oscillating *her1* and *her7* wave. If the pace of the wavefront progression is slower, the overall rate of maturation of the PSM and therefore arresting the expression of cyclic *her1* and *her7* expression would also be slowed.

FGF signaling at the PSM is required for the regulation of the position of the wavefront during somitogenesis [64, 65, 140, 141]. A threshold level of FGF signaling facilitates the transition of the PSM cells from the immature state to mature state [64, 65]. Ectopic activation of the FGF signaling in zebrafish by surgically inserting FGF8 soaked beads in one side of the PSM gives rise to narrower somites in the region anterior to the FGF bead , while blocking FGF signaling has the opposite effect. On the FGF8 soaked bead implanted side, *her1* expression domain also extends more anteriorly than the control side [65].

To determine whether the somite alterations in *chch* or *sip1* morphants are associated with altered *fgf8* gene expression, we assayed *fgf8* expression in these embryos by *RNA in-situ hybridization.* In both *chch* and *sip1a* ATG morpholino injected embryos, *fgf8* expression domain is expanded rostrally and extends into the midline and sometimes

the (putative) somitic mesoderm (Fig. 3.6G-I). This suggests that the progression of the wavefront is much slower in ChCh and Sip1a compromised embryos. Slowing the wavefront is predicted to result in a broader zone of immature PSM. A similar phenomenon was also observed in *Sip1a* knockout mice [143]

Rostral expansion of *fgf8* expression domain at tailbud can be explained by local changes in cell number in the PSM. We tested whether rate of cell proliferation is also altered in ChCh and Sip1a compromised embryos using cell proliferation marker anti-phosphorylated histone H3 antibody. There is no significant difference between ChCh or Sip1a compromised embryos and their wild type siblings (n= 29, 31 and 19 respectively, data not shown). This indicates that rostral expansion of *fgf8* expression domain is not due to altered cell proliferation.

3.2.4 The effects of *chch* knockdown on somite morphology are due to expanded FGF8 activity

In ChCh or Sip1a compromised embryos, *fgf8* expression in the paraxial mesoderm is expanded rostrally and somites are narrower at the A/P axis and wider in the mediolateral axis. We hypothesized that the expansion in FGF8 expression in these embryos caused alterations in somite morphology. To test that hypothesis, we determined the effects of *chch* and *sip1a* knockdown on embryos with compromised FGF signaling. If rostral expansion of *fgf8* is the cause of the somite phenotype observed in ChCh or Sip1a compromised embryos, then reduction of FGF8 activity will restore wild-type somite morphology. We employed two means to attenuate FGF activity, microinjection *sprouty4 (spry4)* mRNA and *acerebellar (fgf8/ace)* mutant embryos.

spry4 is a feedback induced antagonist of FGF signaling. FGF8 induces *spry4* expression which in turn inhibits FGF activity [148]. Microinjection of *spry4* sense RNA weakly impedes FGF8 signaling in zebrafish [148]. Injection of *spry4* sense RNA into *chch* ATG morphants reduced the number of embryos with narrowed somites from 58% (*ChCh* ATG MO+*lacZ*) to 45% (*ChCh* ATG MO+*spry4* RNA)) ($p = 0.0063$) (Fig 3.8).

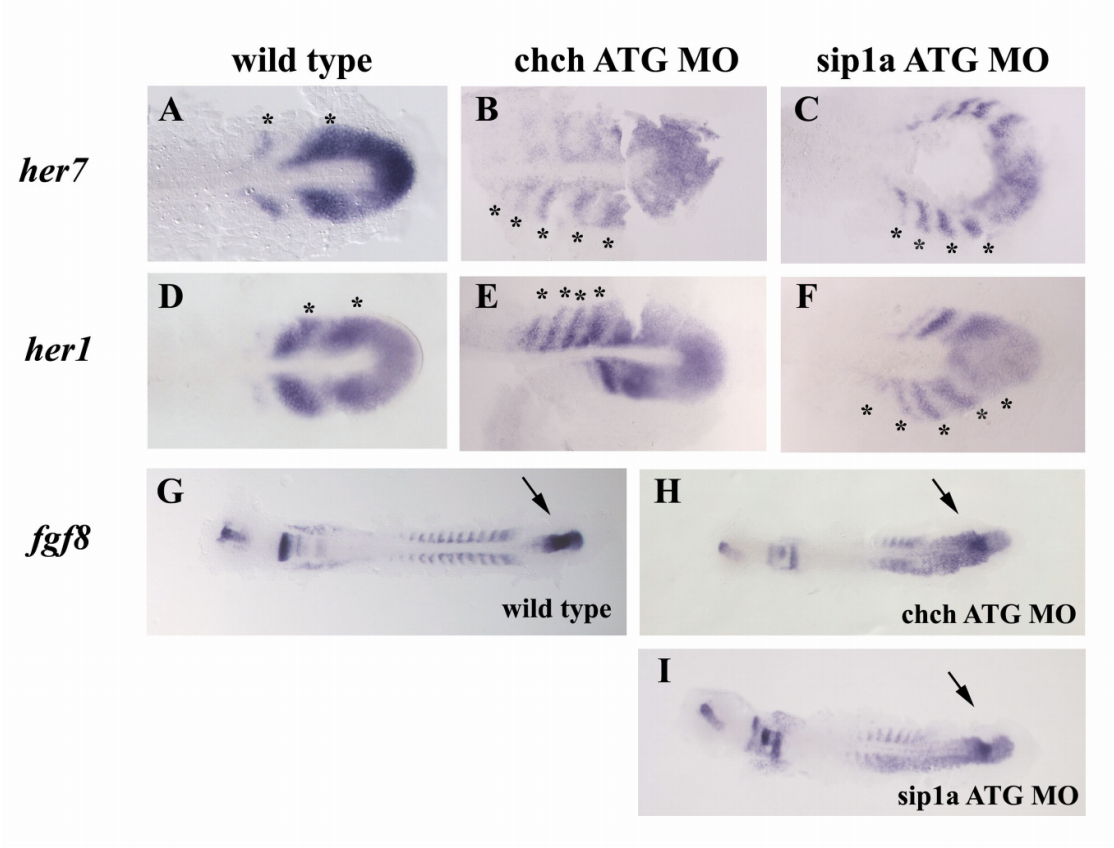

Figure 3.6: Inhibition of ChCh and Sip1a affects the components of the "clock and wavefront model". Flat mount RNA *in situ* hybridization of 10 somite stage wild type, ChCh and Sip1a compromised embryos(A-I). All views are dorsal; anterior to the left. In wildtype embryos, periodic activation of Notch signaling provides cycling gene expression of Notch pathway genes such as *her1* and *her7* (A-F). The number of the *her7* expressing stripes in *chch* and *sip1a* ATG MO injected embryos ranges from 4 to 5 (B,C; E,F). *fgf8* expression domain at tailbud is expanded anteriorly in ChCh and Sip1a compromised embryos (G-I). Asterisks denote each *her1* or *her7* expressing premesoderm stripe (A-F). Arrows denotes *fgf8* tailbud expression domain (G-I).

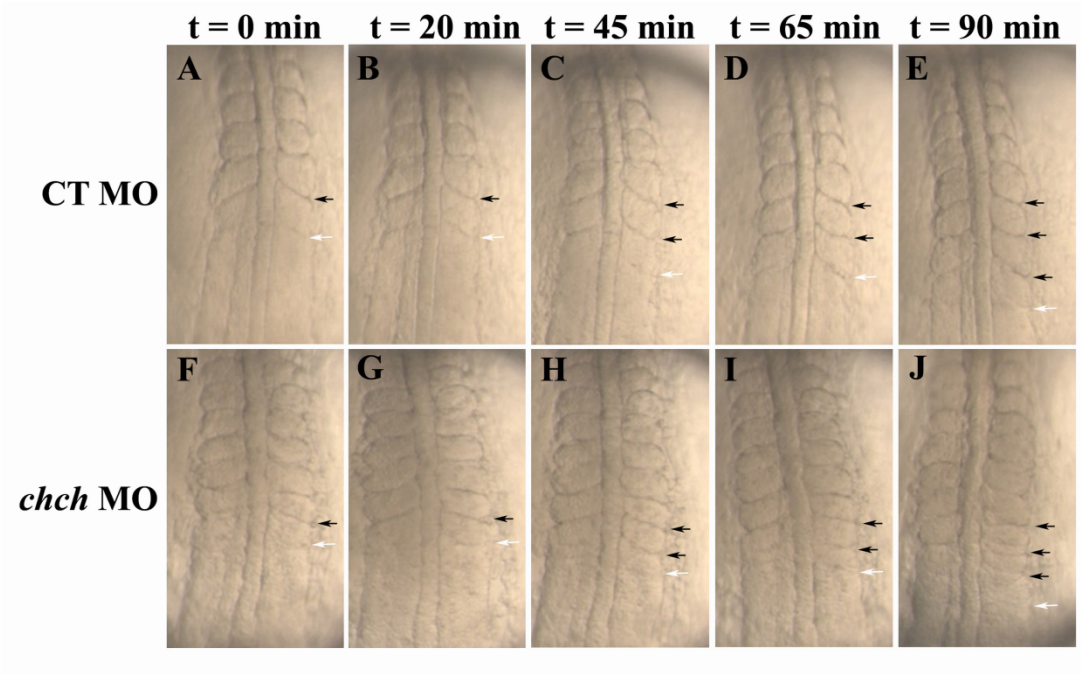

Figure 3.7: Pace of the "molecular clock" is not significantly altered in ChCh-compromised embryos. Living wild type and ChCh-compromised embryos beginning at the 7 somite stage. Duration of somite formation in both control (A-E) and ChCh-compromised embryos (F-J) is approximately 45 mins at 23°C. Black arrows denote already formed somite boundaries and white arrows denote newly forming segmentation furrow. All views are dorsal, anterior to the top (A-J).

Similarly, injection of *spry4* sense RNA into *sip1a* ATG morphants reduced the number of embryos with narrowed somites from 93% (*sip1a* ATG MO+*lacZ*) to 66% (*sip1a* ATG MO+*spry4* RNA)) ($p = 0.0044$) (Fig 3.8). The ability of *spry4* to restore somite morphology in only a subset of embryos likely reflect the poor stability of the injected RNA [148].

To circumvent this difficulty, we assayed the effects of blocking ChCh and Sip1a in *ace/FGF8* mutants [63, 149]. *ace* mutants show a loss of the isthmus and cerebellum, but do not have overt somite defects due to redundant FGF activity [63, 65]. Injection of

chch ATG MO into *ace* homozygous embryos (somite length = 47.4 μm±2.4, n=15,) did not produce the alterations in somite morphology in control morpholino injected embryos (somite length = 48.1 μm±1.4, n= 20). In the same experiments, *chch* morpholino injection decreased somite length in wild type (somite length= 41.5 μm±4.6, n=32) and *ace* heterozygous siblings (somite length= 40.4 μm±2.4, n=29) (Fig. 3.9A).

Injection of *sip1a* ATG MO into *ace* homozygous embryos resulted in a slight narrowing of somites in the A/P axis (somite length = 47.1 μm±2.4, n=9) compared to control-injected embryos (somite length = 49.0 μm±2.1, n= 22). In the same experiments, somite length was decreased in *sip1a* ATG MO injected wild type (somite length = 40.1 μm±2.7, n= 17) and *ace* heterozygous siblings (somite length = 41.3 μm±2.3 n= 16). These findings suggest that the consequences of *chch* knockdown on somite size are largely due to expansion of FGF signaling. However, in Sip1a compromised embryos, the overall phenotype is more severe than Chch compromised embryos and reduction of FGF

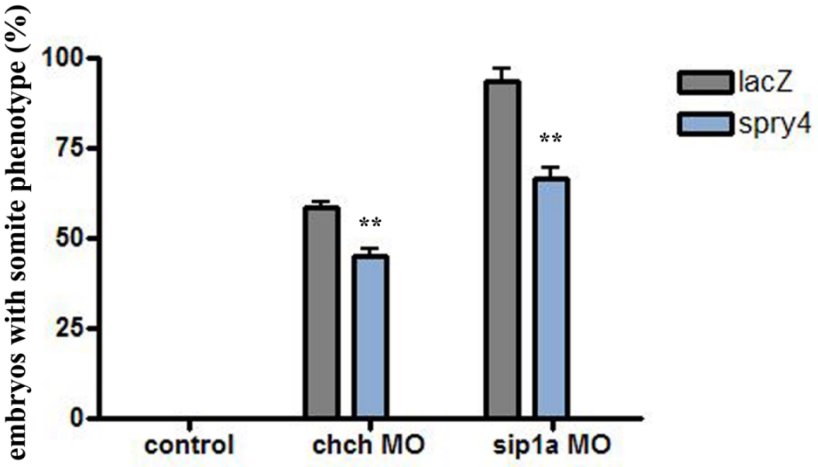

Figure 3.8: Somite malformation in ChCh and Sip1a compromised embryos can be partially rescued by FGF antagonist Spry4. Bar graph representation of *spry4* rescue assay in *chch* and *sip1a* ATG morphants. Injection of *spry4* sense RNA into *chch* and *sip1a* ATG morphants (blue bar) reduced the penetrance of the somite phenotype with respect to their *lacZ* injected siblings (gray bar).

signaling in these embryos is not sufficient to fully rescue the defects. Since Sip1 has wide range of functions that are distinct from known roles for ChCh including regulation of TGF-β and BMP pathways [124-127, 150, 151] and cell fate determination [124, 125] some of the somite phenotypes observed in *sip1a* morphants may be due to FGF independent activities of Sip1a.

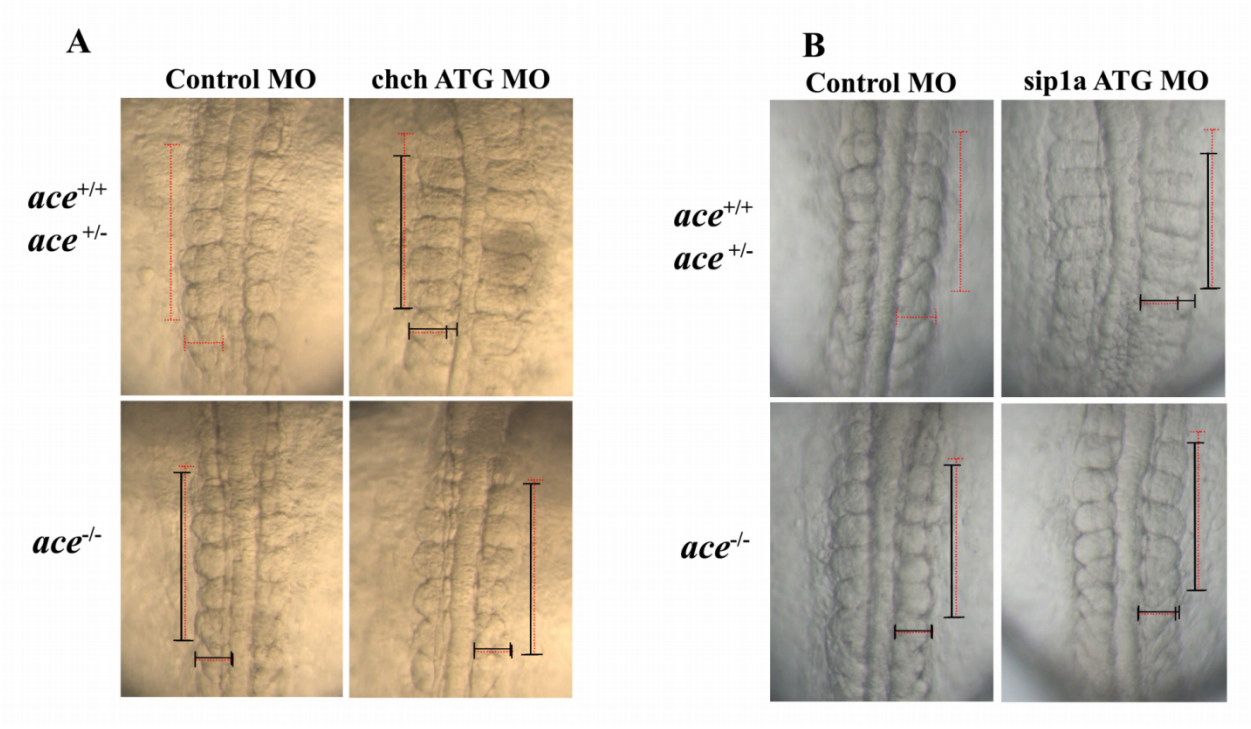

Figure 3.9: Somite malformation in ChCh compromised embryos can be rescued by reduction of FGF8. (A) Dorsal views of 10 somite stage and (B) 12 somite stage living embryos, anterior to the top. Somites are narrower at A/P axis, broader at mediolateral axis in wild type and *ace* heterozygous *chch* morphants, but not *ace* homozygous *chch* morphants (A). *ace* homozygous *sip1a* ATG morphants have still somite phenotype but the overall phenotype is much subtle (B). Horizontal and vertical red dotted line spans the first five somites of the control injected embryo width and length for comparison to the first five somite of morphant embryos which is indicated with a black line

3.2.5 Somite defects in ace mutants are unaltered by *chch* knockdown.

Previous studies have demonstrated the ChCh is an effector of FGF signaling. However, our results reveal that ChCh also represses *fgf8* expression. FGF signaling in the somites is required to induce *myoD* expression and terminal differentiation of subset of fast muscle cells. *ace* mutants have reduced somatic *myoD* expression [152]. If *fgf8* functions downstream of ChCh in somitogenesis, somite defects present in *ace* mutants will not be altered by *chch* knockdown. Therefore, we performed RNA *in-situ* hybridization with *myoD* probe on ChCh compromised *ace* mutant embryos. As expected, we observed that lateral *myoD* expression in the somites is lost in *ace* mutant embryos, but adaxial cell expression was unaffected [152] (Fig. 3.10C). We epistatically observed similar reduction of *myoD* expression in ChCh compromised $ace^{-/-}$ embryos as in control MO injected $ace^{-/-}$ embryos (Fig. 3.10D). This observation is consistent with the model that FGF8 acts downstream of ChCh during somite formation.

To determine whether ChCh and Sip1a modulate FGF signaling in other tissues, we examined the consequence of knockdown of ChCh and Sip1a in the isthmus, which is a well-characterized site of FGF activity. We also observed that the expression of the FGF target gene *pax2a* is expanded anteriorly in the isthmus in *chch* morphants, but not in *sip1a* morphants (Fig. 3.11A-C). While the hindbrain is wider in ChCh and Sip1a compromised embryos (probably due to convergence defects), a similar alteration was not observed in *krox20* expression (Fig. 3.11D-F). These results suggest that negative regulation of FGF8 by ChCh is not limited to the mesoderm, but that the ChCh has a broader function in modulating FGF signaling.

3.3 Discussion:

ChCh and Sip1 modulate FGF-dependent processes and act as a switch between mesodermal and neural inducing activities of FGF in chick, Xenopus and zebrafish [117, 122]. Although their regulatory properties and function during gastrulation have been

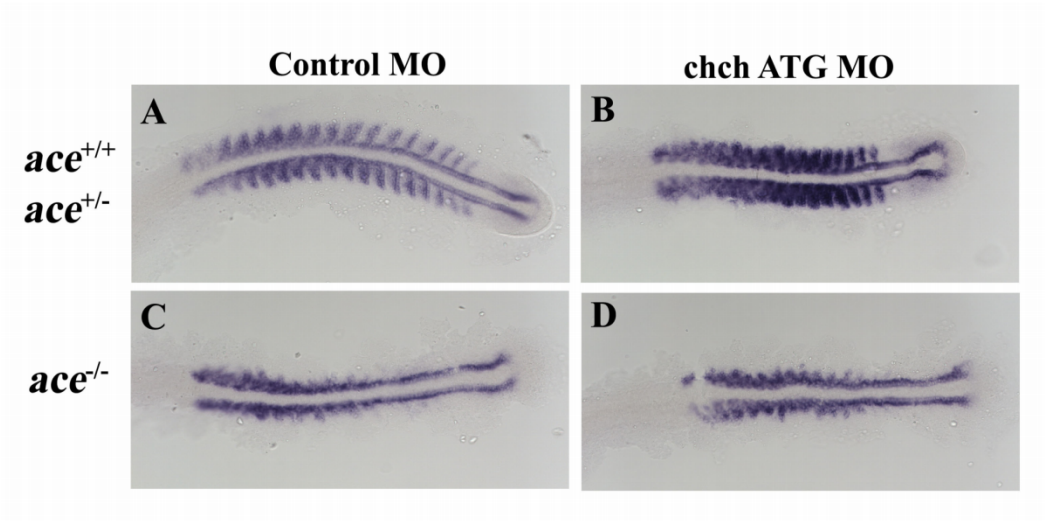

Figure 3.10: Somite defects in ace mutants are unaltered by ChCh knockdown. Flat mount RNA in situ hybridization of *myoD* in 17 somite stage ChCh compromised wild type, *ace*$^{+/-}$ and *ace*$^{-/-}$ embryos(A-D). All views are dorsal; anterior to the left. Lateral *myoD* expression in the somites is lost in *ace* mutant embryos. *myoD* expression pattern in ChCh compromised *ace*$^{-/-}$ embryos is similar to control MO injected siblings.

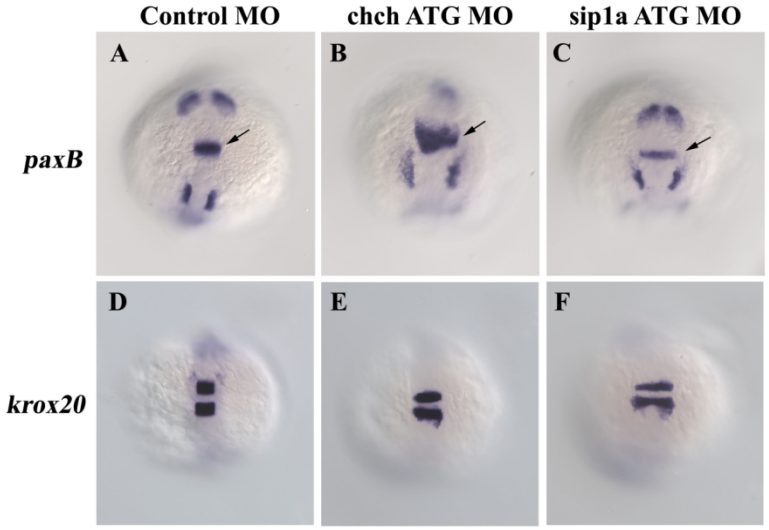

Figure 3.11: Repression of FGF8 by ChCh is not limited to the mesoderm. Whole mount RNA *in situ* hybridization of *pax2a and krox20* in 10-somite stage ChCh and Sip1a compromised embryos (A-C). All views are dorsal; anterior to the top. FGF target gene *pax2a* is expanded anteriorly in the isthmus in *chch* morphants, but not in *sip1a* morphants (A-C). The anterior extent of *krox20* expression is not altered by *chch* or s*ip1a* knockdown (D-F). Arrows denote isthmus.

studied extensively, very little is known about the requirements for ChCh and Sip1a at other stages. In zebrafish, both genes are expressed in the developing mesoderm [118,

144]. Previous studies using SIP1 knockout mice and *sip1* morphant zebrafish embryos did not clearly identify the function of Sip1 in somitogenesis [143, 144].

In the present study, we characterized the function of ChCh and Sip1a in zebrafish somitogenesis. Our data revealed that *chch* and *sip1a* knockdown resulted in embryos with somites that are less extended thru A/P axis while over-extended in the mediolateral axis. In addition, cyclic expression of *her1* and *her7* is maintained in formed somites in these embryos. We observed that these defects correlated with an anterior expansion of FGF8 expression in the tailbud. In ChCh morphants, the defects in somite morphology could almost entirely suppressed by blocking FGF8, while the same treatment only partially restored the defects in *sip1a* morphants. Taken together, these findings demonstrate that ChCh and Sip1a regulate somitogenesis by mediating the position of the FGF8 mediated wavefront in the zebrafish PSM.

Expanded FGF8 expression in PSM would be predicted to alter the FGF gradient that regulates somite length [65]. However, our finding that somite width was also altered by the enhanced FGF8 expression was surprising. Because expression of dominant-negative ChCh blocks FGF mediated mesoderm induction in animal cap assays [117], ChCh is generally thought of as a positive effector of FGF signaling. ChCh is induced in response to FGF in chick, xenopus and zebrafish [117, 118] and our results demonstrate that ChCh represses expression of FGF8, implying that it functions in a negative feedback loop to repress FGF signaling. In a broad context, this relationship is consistent with functions of ChCh in cell movement. Previous studies have shown that ChCh impedes cell movement [117, 122]. While FGFs have complex roles in cell migration, in many tissues FGF promotes cell migration [153-155]. Therefore it is conceivable that in the effects of ChCh on cell movement are due to blocking, rather then promoting FGF signaling. Further studies are needed to elucidate the precise mechanisms by which ChCh modulates FGF signal transduction.

The somite phenotype observed in *sip1a* ATG morphants is stronger than *chch* ATG morphants and cannot be fully restored by blocking FGF activity. Thus far, Sip1 is the only described transcriptional target of ChCh. In several situations, overexpression of *sip1* is sufficient to compensate for ChCh deficits [117, 119]. However, Sip1 has a wide

range of activities that are likely to be ChCh independent. These include regulation of TGFβ pathways [124-127], expression of BMP4 [150, 151], mesodermal gene expression [124, 125] and E-cadherin transcription [124, 128].

The functional differences between the alternatively spliced forms of zebrafish Sip1a remains unclear. The previously described alternatively spliced form of *sip1a* lacks a zinc finger [144]. Because we identified a structurally similar form of Sip1b (Fig. 3.3), we reasoned that the two forms have unique functions. To test for distinct activities during somitogenesis, we used splice morpholinos to block production of each form while leaving the other intact. Our approach demonstrated the effectiveness of morpholinos to specifically eliminate alternative spliced message. However, we were unable to detect somite defects or any other patterning defects in the respective Sip1a form-specific morphants. This suggests that each form can compensate for loss of the other during somitogenesis or that protein derived from maternal mRNA is sufficient to compensate for the loss of wild-type zygotic mRNA.

In conclusion, we studied the functions of ChCh and Sip1a during zebrafish somitogenesis and found that ChCh and Sip1a modulate somite morphogenesis by repressing FGF8 expression at the PSM. Significantly, we determined that *fgf8* is downstream of *ChCh,* suggesting a negative feedback loop between *chch*/*sip1a* and *fgf8*. Our data also demonstrates that regulation of FGF signaling by ChCh is not limited to the PSM. FGF signaling has diverse functions in a many biological processes and investigation of the vertebrate EST databases reveals that *ChCh* transcripts are detected in low levels in a wide array of tissues (data not shown). It will therefore be important for future studies to determine the importance of modulation of FGF signaling by ChCh in these contexts.

3.4 Materials and Methods

3.4.1 Adult fish and embryo maintenance

Adult zebrafish strains and embryos obtained from natural crossings were maintained at 28.5°C. Developmental stages of the embryos were determined according to Kimmel *et. al*. [5].

3.4.2 Expression constructs, mRNA synthesis and morpholinos:

spry4 ORF was amplified from 10 somite stage wild type total first strand cDNA using GTTCTAGAGGCTCGAGGAAGGTCCTGCAAACCAT/TCTTTTTGCAGG ATCCTGAGGAACACGACCTACA primer pair. Amplified fragment is then cloned to pCS2+ at BamHI and XhoI sites. Capped sense mRNA was synthesized using mMESSAGE mMACHINE Kit (Ambion).

The sequence of the morpholinos used is

chch ATG MO 5'- CAGTATAGTCCAGATCAGAAGACGC -3',

chch ATG MO2 5'- GCTTCTGGACACAACCGGTACACAT -3'[122]. *sip1a* and *sip1b* ATG and splice morpholinos are kindly provided by Iain T. Shepherd [144].

sip1a splice variant targeting MO2 5'- GTCTAAATGTGATATACCTGTGC -3'

sip1a splice variant targeting MO3 5'- CGCGTACATACCACTTTCAGTCTTC -3'

Primers used to monitor the efficiency of the splice variant targeting MO are:

MO2: ATGTACGCGTGTGACTTGTG / CATTTGTCGCACTGGTAAGG

MO3: TTAAGAAGACTGAAAGTGGAAAGC / CATTTGTCGCACTGGTAAG

Standard control oligo (Gene Tools) is used as control. mRNA and morpholino solutions were diluted to desired concentration with 0.2M KCl supplemented with phenol red. Typically, 500 pg of *spry4* mRNA, 10-15ng of *ChCh* ATG morpholino1 and *ChCh* ATG morpholino2, 2-4ng of *sip1a* ATG, 10ng of *sip1a* splice morpholino, 5ng of *sip1b* ATG, 1ng of *sip1b* splice morpholino is injected to one- to two-cell stage embryos.

3.4.3 Whole mount in-situ hybridization and immunohistochemistry

In situ hybridizations were performed according to Thisse *et. al*. [102]. Digoxigenin labeled probes for *in situ* hybridization was synthesized using T7, T3 or Sp6 RNA polymerase (Roche). Hybridized probes were detected using NBT/BCIP system (Roche). Stained embryos were re-fixed in 4% PFA and either stored in 100% methanol or cleared

in Benzyl benzoate/benzyl alcohol solution (2:1) and mounted in Canada balsam/methyl salicylate (2.5% v/v) or flat mounted in 70% glycerol. Embryos were viewed with Zeiss Axioplan microscope, digitally photographed with Zeiss Axiocam camera. Images were processed and assembled with Zeiss Axiovision and Adobe Photoshop.

Chapter 4: Background and Significance

Neural development is a multistep process which generates and shapes the complex nervous system. Neurodevelopment is initiated by neural induction and neurogenesis during early embryogenesis. During neurogenesis, while embryonic stem cells differentiate into neural but not non-neural cell fates in the developing nervous system, cells outside the nervous system retain their non-neural identity. This critical decision is managed by specific progression of temporal and spatial cues in the developing embryo.

Distinctive cell fates can be characterized by their unique assortment of non-coding transcripts and proteins which are crucial for specific functions of that particular cell type. Therefore, proper regulation of cell type specific gene expression is essential to ensure the specificity and diversity of different cell types. Over the past decades, numerous cis- and trans-regulatory elements were characterized for their involvement in transcription regulation machinery during cell-type specific differentiation. Specifically, trans-acting chromatin modifying enzymes have a crucial role in epigenetically regulating gene expression. Recent reports demonstrated that Neuron-restrictive Silencing Factor (NRSF)/ Repressor Element 1- Silencing Transcription Factor (REST) interact with

multiple chromatin modifying enzymes at regulatory sequences to negatively modulate multiple protein-coding and non-coding genes.

4.1 Molecular Basis of Epigenetic Regulation

The DNA in eukaryotic cells is tightly wrapped around strongly basic proteins called histones, which packs the DNA into more compact units. The N-terminal tails of histones are highly conserved and undergo post-translational modifications according to the genetic profile of the cell. These modifications reversibly change the local chromatin structures to modulate the DNA accessibility and regulate transcription. Acetylation and methylation of the histones are well studied and their implications on different biological processes are well established. Other modifications such as phosphorylation, ubiquitination, SUMOylation, citrullination and ADP-ribosylation also regulate transcription [156-163]. Modifications on different positions of the histone tails can regulate transcription differently. For example, hypermethylation on K9 position of histone H3 silences the gene while di-/tri-methylation on K4 position of histone H3 cause de-repression. However, again, these meanings also depend on the local chromatin structure and other modifications as well (Fig 4.1 and Table 4.1).

Another type of modification which alters the epigenetic code of the cell is DNA methylation. DNA methylation is a post-replication modification which is largely found on cytosines followed by a guanosine in the dinucleotide sequence CpG. Methylated cytosine, 5-Methylcytosine, establishes the silent chromatin state by attracting or repulsing DNA binding proteins however how the entire silencing machinery works is not fully understood [164, 165]. DNA methylation is one of the major mechanisms for transcription regulation uniquely in vertebrates; DNA of most invertebrates including *Drosophila* is not methylated.

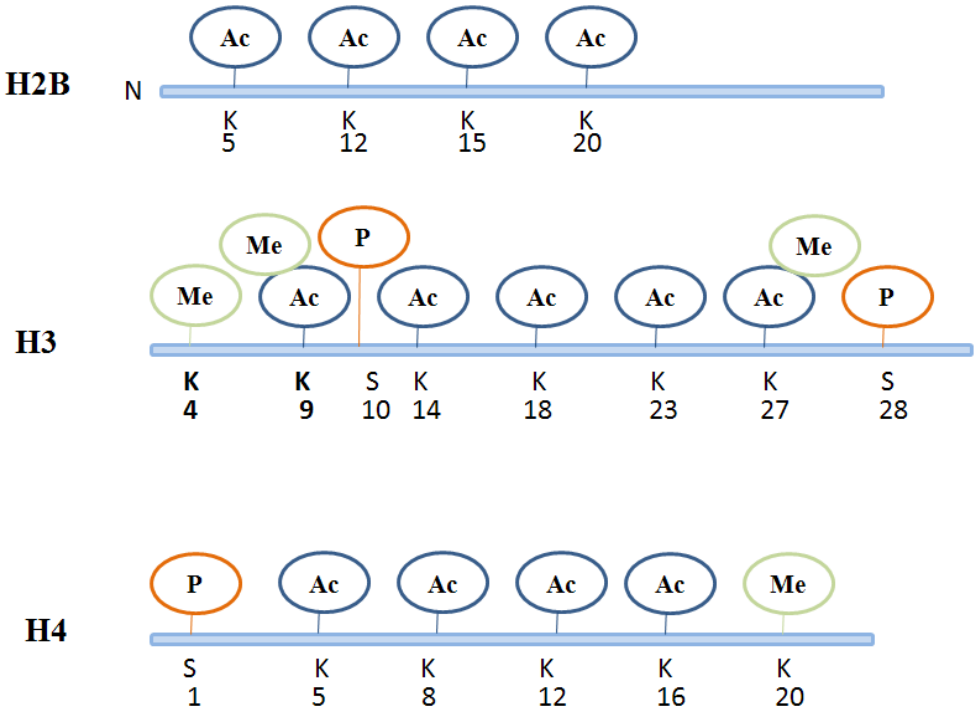

Figure 4.1: Covalent modification of core histone tails. Known modifications of three histone tails are indicated. Some positions can be modified in different ways such as H3K9. Histone H3K4 and histone H3K9 are modified by Rest associated CoRest complex (see section 4.2.1). Me: methyl group; Ac: Acetyl group; P: phosphate group.

Type of modification	Histone				
	H3K4	H3K9	H3K14	H3K27	H4K20
Mono-Me	activation	activation		activation	activation
Di-Me		repression		repression	
Tri-Me	activation	repression		repression	
acetylation		activation	activation		

Table 4.1: Histone modifications in transcription regulation. It should be noted that the effects of the modification of a particular position of the histone can depend on the local chromatin structure.

4.2 Neuron-restrictive Silencing Factor/ Repressor Element1 Silencing Transcription Factor (NRSF)/(REST)

Repressor Element-1 Silencing Transcription factor (REST, also known as Neuron-Restrictive Silencing Factor (NRSF) was discovered in 1995 as a transcription repressor which binds to a specific consensus ~21 bp Repressor Element 1 (RE1, also known as Neuron Restrictive Silencer Element (NRSE) present in the REST target genes and represses their transcription [166, 167]. It was originally thought that REST acts a master regulator of neural phenotype [168] because RE1 sites were only identified in several neuron specific genes [169-175]. However, many REST target genes which are essential for neural traits such as cytokines, ion channels, neurotransmitter receptors, synaptic vesicle proteins were identified thru computational and biochemical studies [176-178]. Besides high levels of non-neural expression, REST is also expressed in neural tissues, specifically in brain where transcription is repressed by REST [179-181]. Taken together, these observations suggested an additional function of REST during neural differentiation. Indeed, in a very elegant study, REST is shown to function as a key regulator of neural genes expression during neural differentiation [176]. REST transiently represses several neural genes in the progenitors while these genes were upregulated in terminally differentiated state, when REST is absent [176, 177, 182]. Hence, progression of neural differentiation and identity is partially controlled by REST as well.

4.2.1 Molecular mechanism of REST repression

REST binds to 21bp long canonical RE1 motif thru its eight Krüppel type zinc fingers [166, 167]. Computational and ChIPSAGE (SACO) analysis identified "expanded" RE1 site which contains insertions between 3-9 nt between 11^{th} and 12^{th} nucleotides whereas "compressed" RE1 site has one random nucleotide inserted between 9^{th} and 12^{th} nucleotides. ChIP and gel shift assays confirmed the binding ability of REST to these non-canonical RE1 sites [177]. Additional RE1 consensus sequences are identified by microarray analysis of the REST enriched ChIP samples (ChIP-chip) [178] and deep sequencing analysis of REST enriched ChIP samples (ChIPSeq) [183]. It is estimated that there are ~25,000 REST binding sites in human genome [178] while

~10,000 REST binding sites are estimated in mouse genome[177]. However, the exact numbers are still not definite. On the other hand computational analysis estimates ~810 RE1 sites regulating ~4200 genes in zebrafish [184], (Ian Wood, personal communication). However, further biochemical analysis is needed to test the functionality of these "predicted" sites.

REST binding sites are not restricted to promoter regions of the gene [177, 185, 186]; REST functions very effectively at a distance and independent of orientation of the target site[177], however it is also proposed that optimal distance of the RE1 is within 2-3 kb of the transcriptional start site [186].

REST functions as a transcriptional repressor by recruiting two separate corepressor complexes, mSin3 and CoREST [187-191] (fig 4.2). The mSin3 complex, which consists of histone deacetylases HDAC1, HDAC2, HDAC4 and HDAC5, is recruited by the amino terminal repressor domain of the protein [188-192]. Other mSin3 complex components, including SAP30, SAP180, SAP130, SAP45, SDS3, and retinoblastoma-associated proteins RBBP4 and RBBP7, are also characterized but their function in the REST/mSin3 complex is still unknown [193-197].

REST carboxyl terminal repressor domain recruits the CoREST complex, which consists of histone deacetylases HDAC1 and HDAC2 [187, 198], histone H3K4 demetylase LSD1 [199] and histone H3K9 methytransferases G9a and Suv39h1 [200-203]. Histone H3K9 methytransferase G9a, but not Suv39h1, further recruits Heterochromatin protein 1 (HP1) to RE1 site to further condense the chromatin [200, 202] and to facilitate long term silencing of REST. Additionally, chromatin remodeling enzyme BRG1, another component of CoREST complex, enables REST to form more stable interactions with RE1 site by changing the nucleosome position [204]. Therefore, this REST/CoREST/BRG1 interaction may allow long term silencing of target genes.

During neural differentiation, although the relative *REST* transcript level is stable, REST protein is downregulated posttranslationally by the ubiquitin-independent proteosomal pathway[205]. Although REST is absent from RE1 sites, repression of several target genes still persist [176]. This repression is REST independent and

modulated by Methyl CpG binding protein2 MeCP2, which is recruited to the RE1 sites by CoREST repressor complex.

In summary, markers of functional REST/mSin3/CoREST silencing machinery are histone deacetylation, H3K9 methylation, and H3K4 demetylation. However, extent of each modification in the cell is context dependent. For example, in non-neural cells, high levels of silencing marks are observed while chromatin is tightly packed, making the chromatin inaccessible to the transcriptional machinery. On the other hand, in stem cells and neural progenitors, chromatin is less compact so that neural specific gene expression levels can be fine-tuned during development. Thus target genes are repressed in these cells but not completely silenced [176].

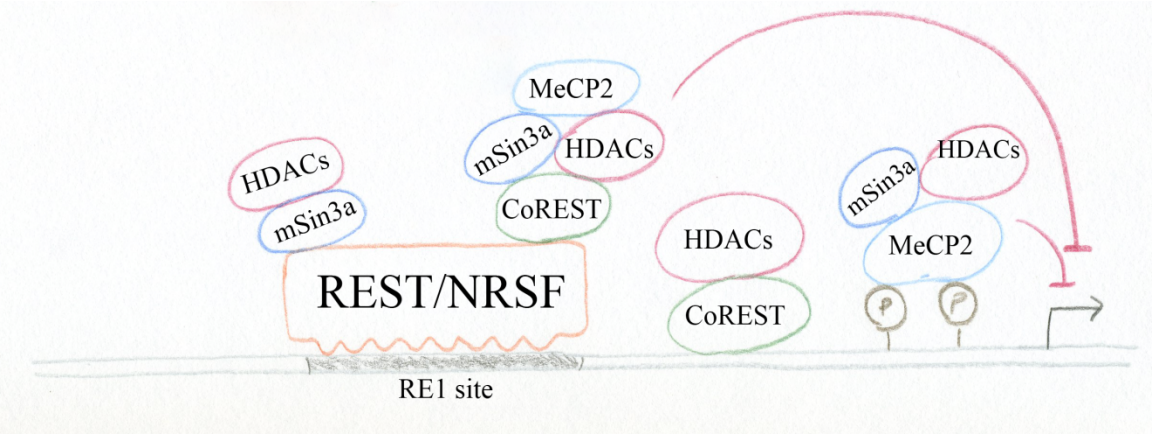

Figure 4.2: Mechanism of Rest mediated repression. Rest recruits co-repressors to target genes. N-terminus of Rest recruits mSin3 complex containing HDACs. C terminus of Rest recruits Corest repressor complex. This complex include HDACs, histone H3 K9 methyltransferases, HP1, histone H3K4 demetylase LSD1, methylated DNA binding protein MeCP2 to mediate gene silencing at the RE1 site. Rest independent long term repression is modulated by MeCP2 and CoRest complex.

4.2.2 REST function in development

REST is essential for mice, chick and Xenopus development [206-209]. Homozygous deletion of NRSF/REST in mice is embryonic lethal by E11.5. These embryos showed growth retardation, apoptosis and malformed telencephalic vesicles by E10.5. Moreover, a possible epithelial-mesencymal transition problem is also evident from abnormally patterned head mesenchyme and somites [206]. Moreover, in these embryos, loss of REST function led to derepression of only neuron specific βIII tubulin but not other neuronal genes [206] suggesting that redundant regulatory systems or lack of activators prevented the de-repression of these genes examined in this study. The in-vivo function of REST in mouse neurogenesis is still incomplete given the early embryonic lethality of *Rest*$^{-/-}$ homozygous mice. To study the consequences of loss of REST function in neurogenesis, generation of conditional *Rest* knockout mice is essential.

Similar to REST function in mice, overexpression of dominant negative form of REST caused derepression of Ng-CAM and SCG10 in addition to βIII tubulin not only in non-neural tissue but also in neural progenitors [206] in chick. On the other hand, overexpression of REST in developing spinal cord caused repression of several genes as well as axon guidance defects in chick spinal cord [209].

In Xenopus, loss of REST function by overexpression of dominant negative REST led to repression of several neural specific genes, including NaV1.2, N-tubulin and SCG10 in half of the injected embryos without overtly affecting neurogenesis [208]. This observation differs from what was seen in mice and chick and recent Xenopus loss-of-function studies. A likely explanation of this contradiction is the possible bifunctional role of REST in different cellular and developmental contexts. Inhibition of REST function in xenopus expands neural plate, interferes with ectoderm and neural crest patterning, and diminishes prospective epidermal markers [207]. Overall, these observations phenocopy decreased BMP signaling defects in the embryo [207], suggesting that REST modulates ectodermal patterning thru mechanisms parallel to BMP signaling.

In zebrafish, however, the precise function of Rest during development is not fully understood. Loss of Rest function by Rest morpholino microinjection caused changes in progenitor domains which give rise to distinct neural populations. These defects were implicated to defective Rest-Hedgehog (Hh) signaling interactions during development. When Hh signaling is elevated, loss of Rest function enhances the expression levels of the Hh target genes. On the other hand, when Hh signaling is repressed, expression levels of the Hh target genes are suppressed further upon loss of Rest function. Overall, these observations suggest that Rest and Hh signaling interactions are context dependent and Rest may act as a bi-functional component of the Hh signaling in distinct developmental processes [210].

The involvement of REST in maintenance of embryonic stem (ES) cell pluripotency is still controversial. REST is regulated by Oct4 and Nanog, transcription factors required to maintain the pluripotency of ES cells [211]. However, REST knockdown did not change the stemness and morphology of the ES cells [211]. On the other hand, Singh *et. al*., demonstrated that REST is required for self-renewal and pluripotency of the ES cells: When REST is knocked down in ES cells, pluripotency markers, including *Oct4* and *Nanog* are downregulated [212]. This observation is refuted in subsequent reports [213-217]. Further studies should be performed to resolve these contradictions.

REST function is also a key regulator of multiple fetal cardiac genes in heart development. Dominant negative REST expressing transgenic mice exhibits severe developmental defects including cardiomyopathy, which then lead to sudden death. A subset of fetal cardiac genes, including atrial natriuretic peptide, brain natriuretic peptide and alpha-skeletal actin were de-repressed when REST function is lost in post-natal hearts. Dynamic regulation of fetal cardiac genes is regulated by REST mediated repression. As well as heart development, REST also regulates pancreatic islet development. REST regulates *Pax4* [218], one of the key transcription factors involved in the formation of β-cells during pancreatic development and islet cell differentiation [219]. This function of REST may be important in β-cell differentiation.

4.2.3 REST function in disease states

Deregulation of REST has been implicated in molecular cause and progress of assorted diseases and disorders including different types of cancers, neurodegenerative diseases, and neurodevelopmental disorders such as Down syndrome and mental retardation [220-229].

REST functions as both tumor-supressor gene and oncogene depending on the cellular context. REST inactivation, overexpression and copy number variation (loss of heterogeneity) cause different types of cancers. Reduced or loss of REST function causes tumors in epithelial cells. For example, a mutation which results in truncated REST is associated with colorectal adenocarcinoma while shorter splice variants of REST are increased in small lung cell carcinomas [230]. Other truncated REST isoforms REST-FS, sNRSF and hREST-N62 are also associated with anchorage independent growth and metastasis [221], and neuroendocrine cancers [230, 231], respectively. On the other hand, some of medulloblastomas and neuroblastomas are linked to increased REST expression which functions as an oncogene leading to tumor formation [222, 232]. mSin3a, which interacts with N-terminus repressor domain of REST, regulates the cell proliferation inhibitor complex Mad/Max [233] and tumor suppressor protein, p53 [234]. Mutations in *Rest* gene can disrupt this regulation and cause tumorigenesis.

REST function has also been implicated in pathogenesis of Huntington's disease (HD). Huntington's disease is a neurodegenative disorder which is linked to selective neural loss in cerebral cortex and striatum [235]. Disease phenotype is associated with mutated Huntingtin gene and low levels of Brain-Derived Neurotrophic Factor (BDNF) in the striatal neurons which are mainly affected by HD. Moreover, deregulation of brain enriched RE1 containing microRNAs miR-9 and miR-9* is another proposed molecular pathology of HD [227]. The molecular basis of this repression is regulated by REST [224, 226, 235]. Wild type Huntingtin sequesters REST in the cytoplasm of the striatal neurons and limits its action. However, in the disease state, Huntingtin is mutated and can no longer keep REST in the cytoplasm, resulting in higher levels of REST in the nucleus and repression of its target genes, including BDNF and REST associated miRNAs [224, 226, 227].

Keeping the functional level of the REST at a precise state is important in many biological processes and physiological responses. For example, after global ischemic insult, both RNA and protein level of REST is upregulated in rat hippocampal and cortical neurons. Increased REST levels repressed the expression of *GluR2* leading to Ca^{2+} induced cell death [181]. However, in inhibitory neurons, REST functions as a neuroprotector by repressing mu-opioid receptor (MOR1) upon ischemic stress [236]. Therefore, precise control of REST mediated gene repression in different cell contexts is crucial for proper cellular response.

4.3 Targeted mutagenesis with zinc finger nucleases

Zebrafish is a great model organism due to its genetic and experimental advantages. However, reverse genetics techniques are fairly limited in zebrafish. Antisense morpholino oligomers (MO) are widely used to knock-down the target gene. Although it is a greatly practical and established method, it has some limitations. For example, with MO injections, gene of interest can only be knocked-down but not eliminated completely from the embryo. Effect of the MO injections is transient and repeated injection of MO is required for each experiment. Moreover, stability of the MO is not long enough to study juvenile or adult phenotypes. Another reverse genetics approach to eliminate gene function is Targeted Induced Local Lesions in Genomes (TILLING). Although this approach generates individuals with mutations in gene of interest, it is extremely time consuming and chances of getting null or hypomorphic alleles are very low.

Zinc finger nucleases (ZFNs) have been used to induce targeted mutation in plants, invertebrates and mammalian cell cultures [237-244]. Recently, two groups independently demonstrated that inducing targeted mutations in the zebrafish genome is also feasible with ZFNs [1, 2].

ZFNs are the artificial restriction enzymes generated by fusing a DNA recognition domain to the non-specific cleavage domain of type IIS restriction enzyme FokI. ZFNs work as dimers: Two ZFNs flanking target site heterodimerize to introduce site specific

double stranded breaks (DSB) in the genome (Fig 4.3). Endogenous DSB repair machinery can repair this break in two ways: If a matching template is present at the DSB site, break is repaired perfectly using homologous recombination dependent repair. However, if matching template is not present, the break is repaired by non-homologous end joining (NHEJ). NHEJ efficiently joins the ends of the DSB however small insertions or deletions are occasionally introduced at the site of the break. As a result of this imperfect repair, target gene is disrupted (Fig 4.3).

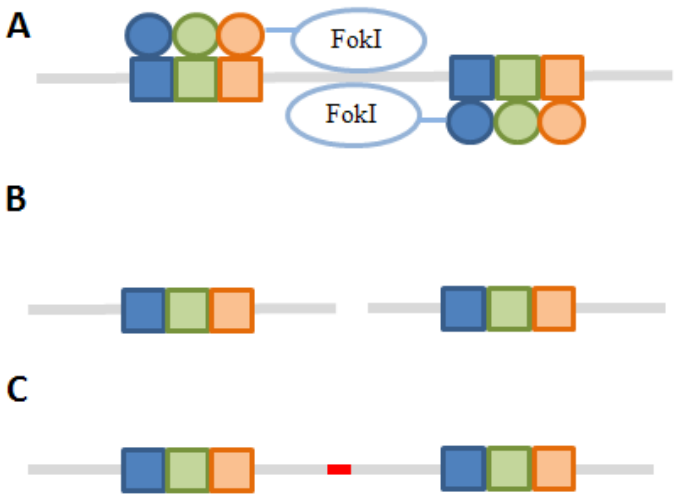

Figure 4.3: Mechanism of ZFN mediated gene targeting. ZFN consists of FokI nuclease domain and zinc finger arrays (A), which target specific triplets in the genome(A). Gray bar represents genomic DNA, circles represent ZFs, and squares represent triplet sequences on the genome. When two ZFNs heterodimerize at the target site, DSB is induced (B). Endogenous repair machinery may repair this break thru NHEJ introducing small insertions or deletions at the target site (red bar, C).

4.3.1 Engineering target specific zinc finger nucleases

The DNA recognition domain contains tandem array of 3-6 Cys_2His_2 type zinc fingers (ZF), each recognizing 3 base pairs. DNA recognition domain specificity is essential for successful application of ZFNs. Any "off-target" targeting of ZFN will generate "off-target" lesions in the genome. "Off target" mutations can complicate the analysis of "target" mutation phenotypes. Therefore, ZF arrays should be designed carefully to ensure high ZFN specificity. To provide improved specificity to the ZFNs,

longer recognition domains should be designed. For example, ZFN with four ZF arrays are always more specific than that containing three. However, finding a specific site which is recognized by 4 ZFs (12 base pairs) on both sides is more challenging.

There are different strategies to design ZFNs specific for the target gene. The simplest of all is the modular assembly. “Modules”, ZF domains which bind to specific triplets, are mixed and matched to fit whatever target sequence is desired [240-243, 245]. With this strategy, 3-4 ZF tandem arrays can be designed easily. However, this approach has limitations unless the target site contains GXX triplets [246]. Although individual zinc finger DNA recognition specificities are extensively studied, the behavior of the individual ZFs in tandem array cannot be predicted. In the tandem array, specificities of the ZFs may overlap or change in different contexts. Thus, new strategies are developed to engineer and validate the specificities of the ZFN DNA recognition domain. These strategies mostly rely on bacteria one- or two-hybrid and yeast two-hybrid assays [1-3]. Although these approaches are time consuming and require technical expertise, these approaches are becoming more widespread.

In this dissertation, we studied the function of REST in zebrafish neurogenesis. We targeted *rest* locus with ZFNs to generate embryos that lack functional Rest activity. A subset of Rest target genes are upregulated in *rest* mutants during early development and adult non-neural tissues. Phenotypes observed in embryos with diminished Rest function are similar to that of *rest* mutants. In *rest*, germ layer specification, early neural patterning and neurogenesis are not affected. However, the number of *olig2*+ migrating oligodendrocyte precursors (OPCs) is significantly reduced. This observation indicates that Rest subtly regulates development of neural subpopulations. Taken together, although Rest regulates neural genes *in-vivo*, it is not necessary for early neural development in zebrafish.

Chapter 5: Rest is essential for repression of multiple neural genes but not required for neurogenesis *in-vivo*

5.1 Introduction

Generation of distinctive cell types during development relies on differentially regulated gene expression patterns. Negative and positive transcriptional regulators function together to generate distinct combination of coding and non-coding transcripts that are crucial for differentiation and maintenance of specific neural subtypes [247-249]. Repressor Element-1 Silencing Transcription factor (REST, also known as Neuron-Restrictive Silencing Factor (NRSF) is a transcription repressor which regulates subset of neural specific gene expression [166, 167]. Rest functions as a hub which recruits co-repressors mSin3 and CoREST to 21 bp conserved Repressor Element 1 motif (RE1, also known as Neuron Restrictive Silencer Element (NRSE) [187-191]. These co-repressors consecutively employ additional silencing machinery including histone deacetylases [188-192], histone H3K4 demetylase LSD1 [199] and histone H3K9 methytransferases G9a and Suv39h1 [200-203] to regulate gene expression.

It was originally thought that REST silences only neural genes in non-neural cells and neural precursors [168] because RE1 sites were only identified in several neuron specific genes [169-175]. However, later, other RE1 sites which are not associated with

neural genes are also identified [168, 177, 178, 202]. NRSF/Rest mutant mouse embryos begin to degenerate at E9.5. Of the many neural markers examined, only neuron specific βIII tubulin is de-repressed in *Rest*$^{-/-}$ homozygous mice [206]. Similarly, overexpression of dominant negative form of REST in chick caused derepression of Ng-CAM, SCG10, and βIII tubulin in non-neural tissue and neural progenitors [206]. On the other hand, loss of REST function by overexpression of dominant negative REST led to repression of several neural specific genes, including NaV1.2, N-tubulin and SCG10 in Xenopus. Taken together, these observations suggest that REST mediated gene silencing is context dependent.

Rest mediated gene repression has been investigated extensively *in-vitro*. Although examination of effects of the Rest function in cell culture is useful, a more complete *in-vivo* study is necessary to study its function in more complex molecular and cellular context. *In-vivo* studies in mice and chick confirm the repressor function of the REST, however the early lethality of the knockout prevents a clear analysis of its role in central nervous system and neural differentiation [206]. On the other hand, overexpression of Rest caused axonal pathfinding errors in developing chick spinal cord suggesting that Rest regulated genes are essential for regulation of a subset of neural phenotype in the chick nervous system.

Here, we studied the function of REST in zebrafish neurogenesis. Zinc finger nuclease mediated gene targeting was used to generate embryos that lack functional Rest activity. When *rest* locus is disrupted, a subset of RE-1 containing Rest target genes, including *snap25b* and *bdnf* are upregulated during early development and adult non-neural tissues, indicating that REST acts as a repressor during early development and long term repression of Rest targets fails in non-neural adult tissue. In *rest* mutants, germ layer specification, early neural patterning and neurogenesis are not affected. On the other hand, development of specific neural subpopulations such as *olig2*+ oligodendrocyte precursors is controlled by Rest. Taken together, Rest is not necessary for early neural development but both short and long term Rest mediated repression activity is essential to regulate neural genes in developing embryos and non-neural adult tissues.

5.2 Results

5.2.1 Targeted *rest* gene disruption by zinc finger nucleases

We disrupted the zebrafish rest locus using zinc finger nuclease (ZFN) mediated gene targeting. A "modular assembly" approach was employed to generate specific ZFNs [1-3, 240-243, 245]. The ZiFiT software program (http://www.zincfingers.org/software-tools.htm) was used to identify 3 potential ZFN target sites close to the start codon of the *rest* gene (66th, 181st and 184th nt) comprised exclusively of GXX sequences. Two different zinc finger arrays were designed against for six "half"-target site (Table5.1). Conventional cloning strategies were employed to construct each array from clones in the Addgene Zinc Finger kit (www.addgene.com). Arrays were mixed-and-matched to generate 4 different ZFNs for each site.

Often, DNA-binding efficiencies of the zinc finger arrays are studied first, using *in-vitro* tests such as ELISA, mammalian, bacterial or yeast-cell based assays [1, 2, 242, 250-252] to limit the number of the ZFNs to be studied *in-vivo*. Because microinjection of zebrafish embryos is rapid, we reasoned that the efficacy of specific pairs could be efficiently tested in zebrafish to bypass cumbersome affinity selection assays. mRNA corresponding to each ZFN pair was microinjected into wild-type zebrafish embryos. DNA was prepared from the microinjected embryos and PCR-based genotyping assay was performed to determine the effects of the ZFN injections on the *rest* gene.

Because repair of double stranded breaks (DSB) induced by ZFNs results in insertion or deletion of short sequences of DNA at the target site, we expected to see an allele larger or smaller than the wild type allele (Fig 5.1) in ZFN-injected but not uninjected embryos. This analysis identified four "active" ZFN pairs against two sites of the *rest* gene (Fig 5.1, table 5.2, data not shown). We observed that 60% and 76% of the ZFN injected individuals had somatic mutations at 66th and 181st target sites, respectively (Table 5.2). Sequence analysis of the somatic mutations revealed 4 nt insertions or 5 nt deletions with the inserted/deleted sequence corresponding to the linker region (Fig5.1).

To establish whether "active" ZFNs can induce lesions in the germ line, embryos were raised to adulthood after injected with "active" ZFNs and progeny of these animals

genotyped by PCR. Several fish with germ line transmission of only 181st site lesions were recovered. Of 130 individuals analyzed, 9 founders carried ZFN induced *rest* mutations. The frequencies of transmission of the mutations ranged from 20% to 70%. Sequence analysis of the mutant alleles revealed four different sequence changes (+4nt, Δ6nt; Δ7nt; Δ39nt) in the linker region in progeny of microinjected fish (fig5.1). The differences in the alleles detected in somatic and germline mutations may reflect alterations in repair mechanisms in somatic and germ cells. We conclude that the modular design of zinc finger nucleases was effective in disrupting the zebrafish *rest* locus. ZFNs targeted against 181st nt induced germ line mutations. Overall, ~7% of the injected individuals carried ZFN induced *rest* gene in their germ line.

5.2.2 Phenotypic analysis of *rest* mutation

To evaluate the function of Rest in regulation of neurogenesis in zebrafish, we generated mutants lacking functional Rest activity. The majority of our studies utilized an allele that encoded a 7nt deletion in the first exon of *rest* (*rest*^{SBU29}) (Fig 5.1). Because the mutation produces a frameshift that eliminates the DNA binding domain, this mutation is predicted to be a null allele. Unexpectedly, *rest*^{SBU29} fish appear normal. This result contrasts with those observed in NRSF/REST deficient mouse embryos where significant abnormalities were observed at E9.5-E10 and deletion of NRSF/REST is lethal by E11.5 [206]. Furthermore, some mutants survived to adulthood and are viable. However, the numbers of mutants that survive to adulthood are lower than the expected Mendelian ratios. Out of the genotyped 96 adult fish, there were only 10 rest$^{-/-}$ fish while according mendelian ratios, expected number of rest$^{-/-}$ fish in the population was 24.

A

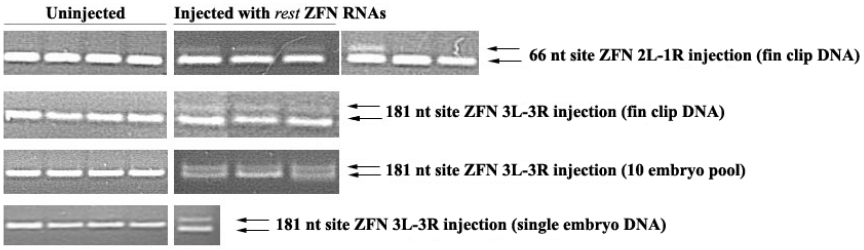

B

```
Somatic mutations (66th nt):
AGGTGTCTGCTCCTCAGC----TGGTGATGCTGGCGA(Wild type)
AGGTGTCTGCTCCTCAGCCAGCTGGTGATGCTGGCGA(+4)

Somatic mutations (66th nt):
AGGTGTCTGCTCCTCAGCTGGTGATGCTGGCGA(Wild type)
AGGTGTCTGCTC-----CTGGTGATGCTGGCGA(Δ5)

Germ line mutations (181st nt):
Wild type:CAGCAGCTACTCCGACAG----CGAAGAAGACGACG(wild type)
1636.54  :CAGCAGCTACTCCGACAGACAGCGAAGAAGACGACG(+4)
1634.21  :CAGCAGCTACTCCGACAGACAGCGAAGAAGACGACG(+4)
1634.40  :CAGCAGCTACTCCGACAGACAGCGAAGAAGACGACG(+4)
1633.4   :CAGCAGCTACTCCGACAGACAGCGAAGAAGACGACG(+4)

Germ line mutations(181st nt):
Wild type:TGGCCTGCAGCAGCTACTCCGACAGCGAAGAAGACGACGACGCCGTCGTGAGATAC(wild type)
1636.52  :TGGCCTGCAGCAGCTACTCC------GAAGAAGACGATGACGCCGTCGTGAGATAC(Δ6)
1596.13  :TGGCCTGCAGCAGCTACTC-------GAAGAAGACGATGACGCCGTCGTGAGATAC(Δ7)
1636.20  :TGGCCTGCAGCAGCTACTC-------GAAGAAGACGATGACGCCGTCGTGAGATAC(Δ7)
1636.49  :TGGCC-----------------------------------GTCGTGAGATAC(Δ39)
```

C

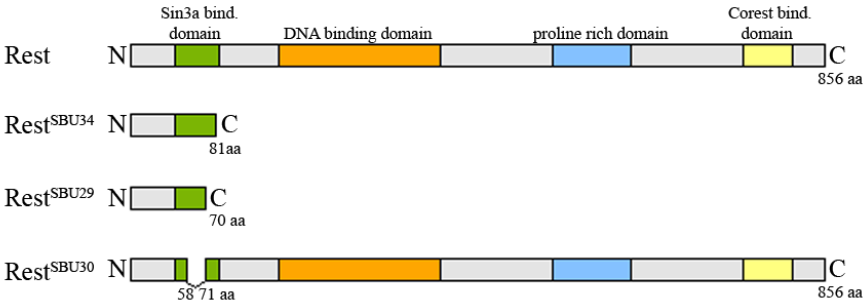

Figure 5.1: Targeted *rest* gene disruption by zinc finger nucleases. PCR based genotyping assay is performed to analyze the effects of the ZFN injections on the *rest* gene. In the injected embryos and adult somatic cells, the size of the PCR fragments amplified from target site is different from that of uninjected embryos (A). Lesions observed in adult fin-clips (somatic mutations) and progeny of the ZFN injected adult fish (B). Blue letters indicate the ZFN recognition site, black letters between blue letters is the target site, orange letters indicate insertions while orange dashed indicate deletions at the target site (B). Schematic representation of wild type and mutant Rest. ZFN mediated 7 nt deletion caused frameshift in *rest*^{SBU29} allele and generated a truncated protein which lacks DNA binding and C-terminal repressor domain (C).

ZFN name	"half" Target site	ZF array sequence
66th nt 1 Left*	GGA GCA GAC	PGEKPYKCPECGKSFSDPGNLVRHQRTH/ PGEKPYKCPECGKSFSQSGDLRRHQRTH/ PGEKPYKCPECGKSFSQRAHLERHQRTH
66th nt 2 Left*		PGEKPHICHIQGCGKVYGDRSNLTRHLRWH/ PGERPFMCTWSYCGKRFTQSGDLTRHKRTH/ PGEKKFACPECPKRFMQSGHLQRHIKTH
66th nt 1 Right*	GGT GAT GCT	PGEKPYKCPECGKSFSTSGELVRHQRTH/ PGEKPYKCPECGKSFSTSGNLVRHQRTH/ PGEKPYKCPECGKSFSTSGHLVRHQRTH
66th nt 2 Right		PGEKPHICHIQGCGKVYGQSSDLTRHLRWH/ PGERPFMCTWSYCGKRFTTSGNLVRHKRTH/ PGEKKFACPECPKRFMTSGHLVRHIKTH
181st nt 3 Left*	GGA GTA GCT	PGEKPYKCPECGKSFSTSGELVRHQRTH/ PGEKPYKCPECGKSFSQSSSLVRHQRTH/ PGEKPYKCPECGKSFSQRAHLERHQRTH
181st nt 4 Left*		PGEKPHICHIQGCGKVYGQSSDLTRHLRWH/ PGERPFMCTWSYCGKRFTQSGALARHKRTH/ PGEKKFACPECPKRFMQSGHLQRHIKTH
181st nt 3 Right*	GAA GAA GAC	PGEKPYKCPECGKSFSDPGNLVRHQRTH/ PGEKPYKCPECGKSFSQSSNLVRHQRTH/ PGEKPYKCPECGKSFSQSSNLVRHQRTH
181st nt 4 Right		PGEKPHICHIQGCGKVYGDRSNLTRHLRWH/ PGERPFMCTWSYCGKRFTQSGNLARHKRTH/ PGEKKFACPECPKRFMQSGNLARHIKTH
184th nt 5 Left	GTC GGA GTA	PGEKPYKCPECGKSFSQSSSLVRHQRTH/ PGEKPYKCPECGKSFSQRAHLERHQRTH/ PGEKPYKCPECGKSFSDPGALVRHQRTH
184th nt 6 Left		PGEKPHICHIQGCGKVYGQSGALTRHLRWH/ PGERPFMCTWSYCGKRFTQSGHLQRHKRTH/ PGEKKFACPECPKRFMDRSALARHIKTH
184th nt 5 Right	GAA GAC GAC	PGEKPYKCPECGKSFSDPGNLVRHQRTH/ PGEKPYKCPECGKSFSDPGNLVRHQRTH/ PGEKPYKCPECGKSFSQSSNLVRHQRTH
184th nt 6 Right		PGEKPHICHIQGCGKVYGDRSNLTRHLRWH/ PGERPFMCTWSYCGKRFTDRSNLTRHKRTH/ PGEKKFACPECPKRFMQSGNLARHIKTH

Table 5.1: Engineered zinc finger arrays to target *rest* with ZFNs. Two different zinc finger arrays were designed against for six "half"-target site. Sequences of the target sites and the recognition motifs of ZF arrays is indicated. Active ZFNs are marked with asterisk.

ZFN pair	Somatic mutations	Type of mutation	Germ line mutations	% mutant germ line	Type of mutation
2L-1R (66th nt)	12/20 (%60)	+4 ; Δ5 (10/12)	0/34 (%0)	N/A	N/A
3L-3R (181st nt)	19/25 (%76)	+4 (4/19)	8/108 (%7)	%20; %60; %70	+4; Δ6; Δ7; Δ39 (6/8)
4L-3R (181st nt)	N/A	N/A	1/22 (%4.5)	N/A	+4 (1/1)

Table 5.2: Analysis of *rest* targeting ZFN efficiency. Four "active" ZFN pairs against two sites of the *rest* gene induced lesions; three of these are shown here. More than 50% ZFN injected individuals had somatic mutations at both sites. However, only 2 of the 4 ZFNs induce germ line mutations.

To determine whether wild-type rest mRNA was present in *rest* mutants, we performed RT-PCR analysis of homozygous embryos from heterozygous *rest*^{SBU29} intercross at various developmental stages using primers flanking the mutation site. This experiment revealed that both wild type and *rest*^{SBU29} messages are present at shield stage but not at later stages (Fig 5.2). Presence of wild type *rest* mRNA in *rest*^{SBU29} homozygous embryos early in development indicates that *rest* gene is maternally expressed which agrees with our previous in situ analysis [210].

Interestingly, PCR analysis of heterozygous embryos revealed an extra amplified fragment (Fig 5.3, lane 5, band 3) besides fragments amplified from wild type (Fig 5.3, lane 5, band 2) and homozygous (Fig 5.3, lane 5, band 1) allele. We hypothesized that mutant amplicon anneals to wild type amplicon forming a heteroduplex during PCR reaction. Mismatching causes the double helix to change its conformation and retard its mobility during electrophoresis. To test this hypothesis, separately amplified wild type and mutant DNA fragments are combined together in 1:1 stoichiometry at either 4°C or at 96°C for 10 mins and electrophoresed on 2.5 % agarose gel. Heteroduplexes are only formed in the mixture which went through one denaturation/renaturation cycle (Fig 5.3, lane 7) but not in mixture which was kept at 4°C (Fig 5.3, lane 7).

Lack of morphological defects in *rest*^{SBU29} homozygous embryos suggested that maternal *rest* transcript could compensate for the loss of zygotic *rest* message in *rest*^{SBU29} mutants to some extent and mask more severe phenotypes. To eliminate maternal Rest

activity, we generated MZ*rest*^{SBU29} embryos by crossing homozygous *rest*^{SBU29} females with homozygous *rest*^{SBU29} males. To our surprise, MZ*rest*^{SBU29} fish also lack overt defects and are viable suggesting that Rest is not required for normal embryonic development in zebrafish.

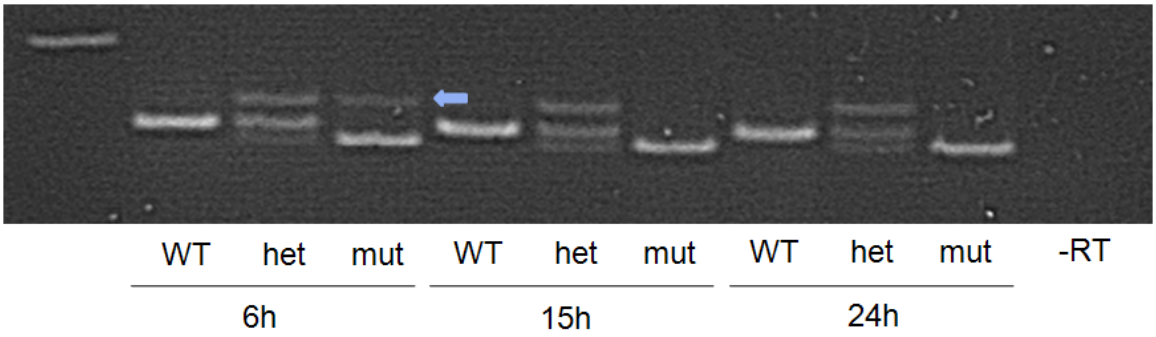

Figure 5.2: RT-PCR analysis of *rest* mutants. Embryos obtained from rest heterozygous intercross have both wild type (blue arrow) and *rest* messages at shield stage (6hpf, early gastrulation) but not at later stages.

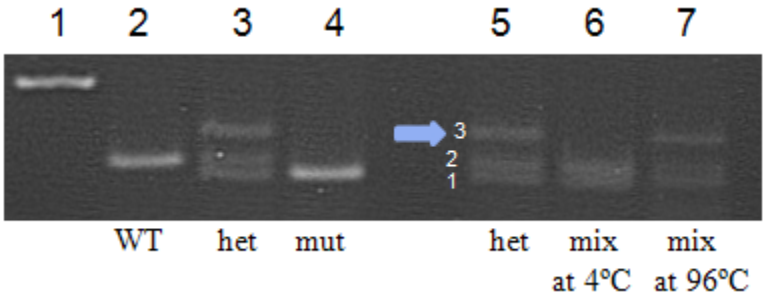

Figure 5.3: Heteroduplex analysis of *rest*$^{+/-}$ mutants. PCR analysis of heterozygous embryos revealed an extra amplified fragment (lane 5, band 3) as well as wild type (lane 5, band 2) and mutant (lane 5, band 1) amplicons. When wild type and mutant amplicons are combined together on ice, heteroduplex is not observed (lane6). However, heteroduplex is formed when the combined amplicons underwent one denaturation/annealing cycle (lane7). Blue arrow denotes the heteroduplex.

5.2.3 Transcript levels of RE-1 containing genes are differentially regulated by Rest

Zebrafish have about 1000 genes that contain RE1 sites and we sought to determine if these genes are misregulated in MZ *rest*^{SBU29} mutants. Stage matched MZ*rest*^{SBU29} and wild type embryos at a series of stages between sphere stage (late blastula) and 19 dpf embryos were used to analyze the expression levels of RE1 containing genes by quantitative RT-PCR. The overall expression profile of the Rest

mediated repression of the RE1 containing genes in *rest* mutants is considerably complex. The effects of loss of Rest function were most apparent prior to 24 hpf. De-repression of a subset of RE1 containing genes was observed at blastula and somite stages. At sphere stage, when blastomeres are still pluripotent, expression levels of most RE1 containing genes are either very low or absent in wild type embryos (Fig 5.4). Some of the genes expressed at that stage such as *snap25b, pcdh* and *bdnf* are upregulated 262, 2.5 and 2.6 fold, respectively in MZrest$^{-/-}$. Interestingly, a fraction of the genes' relative expression level, such as *grin1a,* is not changed in MZrest$^{-/-}$ at that stage. Similarly, during early neural differentiation, at 8 somite (8s) stage, loss of functional Rest in MZrest$^{-/-}$ embryos resulted in increased expression levels of *snap25a, snap25b,* and *grin1a* genes although other genes we investigated in this study such as *pcdh*, *bdnf* and *cacng2* were not upregulated in MZrest$^{-/-}$ embryos at this stage (Fig 5.4). This observation is also consistent with previous studies showing Rest function on regulation of RE1 containing genes is context dependent and not all Rest target genes are derepressed by loss of functional Rest [177, 202, 206, 253, 254]. At 24 hours post fertilization (hpf), none of the RE1 containing Rest target genes, including *snap25b,* are significantly regulated in MZrest$^{-/-}$ mutants (Fig 5.4). Rest function at pre-adult stages was also studied using perturbed whole 8-day-old and 19-day-old larvae. Similar to what was observed in 24-hour-old embryos, changes in expression levels of the Rest target genes we examined were not detected in MZrest$^{-/-}$ mutants (Fig 5.4). We also found a group of Rest target genes, such as *spop*, *bsx*, *gfap*, and n*euroD,* whose expression levels were not changed in MZrest$^{-/-}$ mutants at the stages we studied, from early sphere stage to late larval stage although these genes have the RE1 motif in their structure, suggesting redundant regulatory systems or lack of activators prevented the de-repression of these genes (Fig 5.4).

Several different studies provided evidence for the role of Rest in regulating neural genes in non-neural tissue [176, 206]. Utilizing whole embryos and larvae to study the function of Rest in tissue specific manner is not ideal since local regulation of gene expression levels could not be detected unless different tissue types were dissected carefully before qRT-PCR analysis. To study whether Rest is regulating neural genes in non-neural tissue in long term, we isolated different organs from adult wild type and

rest^{SBU29} adult fish and performed qRT-PCR analysis. Evidently, when Rest function is lost in adult non-neural tissue such as *rest*^{SBU29} pancreas, liver, ovaries, and muscle, repression mediated by Rest is released from the Rest target gene *snap25b* leading to increased transcript levels up to 1000 fold (Fig 5.5). However, changes in expression level of *snap25b* were not detected in mutant adult heart tissue suggesting presence of redundant regulatory systems in heart. Similarly, *snap25b* is not significantly regulated in neural brain tissue. Together, our data provide the first *in-vivo* evidence for a long term repression role of Rest. This observation is also compatible with the already established long term silencing function of Rest in non-neural cells and tissue *in-vitro* [168, 176, 202, 255-257].

5.2.4 Maternal Rest function is required for early gene regulation

To understand the role of maternal Rest in regulation of RE1 containing target genes in zebrafish embryos, we generated M*rest*^{SBU29} heterozygous embryos from *rest*^{SBU29} homozygous mutant mothers and wild type fathers. These embryos lack maternally deposited *rest* but zygotic message can be generated. qRT-PCR analysis demonstrated that loss of maternal *rest* function caused an increase in the Rest target gene expression levels of *snap25b* and *bdnf* at early stages (Fig 5.6, red bar). At later stages, the fold difference between wild type and M*rest*^{SBU29} is significantly reduced (Fig 5.6, red bar), suggesting that later in development, zygotic Rest compensates for the loss of maternal *rest* in these embryos.

In a reciprocal experiment, we generated *rest*^{SBU29} heterozygous embryos, in which maternal message is still present, by crossing wild type mothers and *rest*^{SBU29} homozygous mutant fathers. Expression levels of the RE1 containing target genes in these embryos are similar to wild type level (Fig 5.6, orange bar), indicating that presence of maternal Rest function is sufficient to regulate the early RE1 containing gene regulation. These results demonstrated that maternal Rest is required to repress expression of some RE1 containing genes during blastula stages. In a previous study [46], early (late blastula) loss of function of REST is shown to cause greater phenotype than that of later stages in xenopus. This is consistent with the necessity of the early Rest function during development.

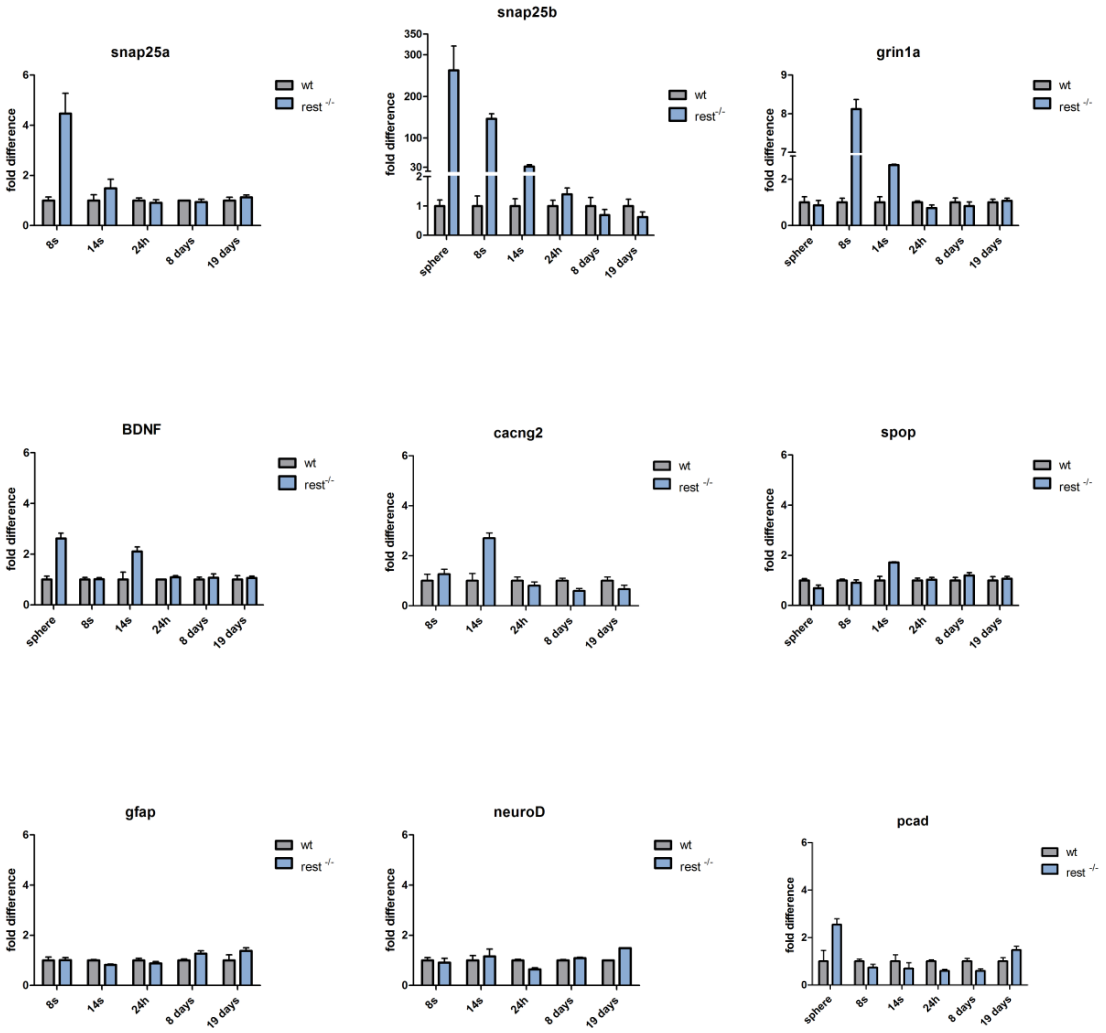

Figure 5.4: Transcript levels of RE-1 containing genes are differentially regulated by Rest. Quantitative RT-PCR analysis of the Rest target genes indicated that only a subset of genes was de-repressed in *rest* mutants. For example, *snap25b* is greatly mis-regulated in *rest* mutants at early stages but loss of Rest mediated repression did not affect the expression levels of *gfap* and *neuroD*. All fold differences are relative to wild type levels of the particular gene and expression levels of each gene is normalized against β-actin. Error bars represent the standard deviation from 3 different pools of embryos.

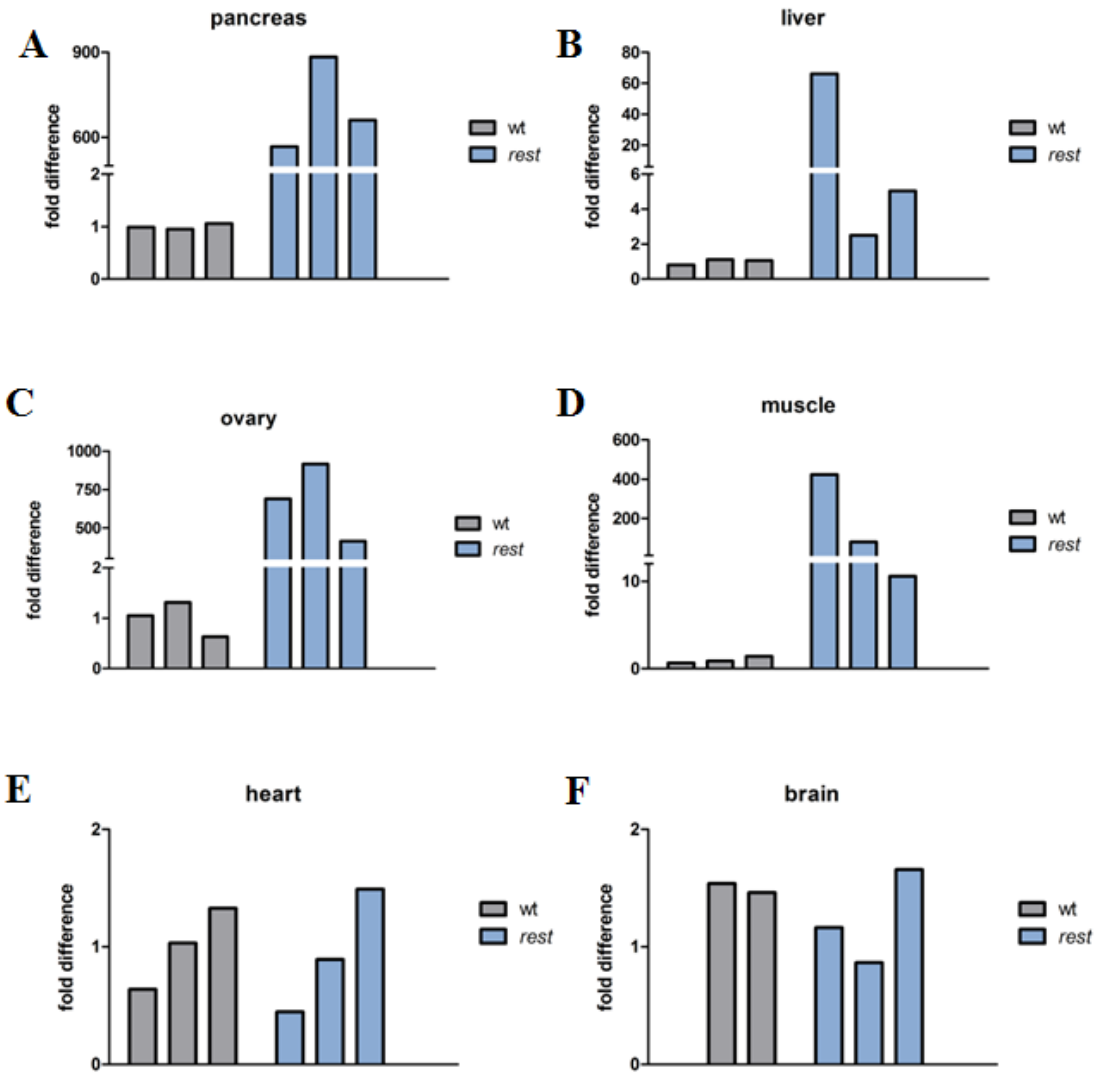

Figure 5.5: *snap25b* is differentially regulated in mutant adult non-neural tissues. Transcript level of the *snap25b* is upregulated in pancreas (A), liver (B), ovaries (C) and muscle (D) but not in heart (E) or brain (F) suggesting a role of Rest in long term repression of neural genes in non-neural adult tissues. Expression level of each gene is normalized against β-actin.

5.2.5 Phenotypes observed in DN-Rest and Rest-Morpholino injections are similar to that of *rest*^{SBU29}

We showed that Rest regulates the expression levels of RE1 containing genes by studying the expression levels of Rest target genes in *rest*^{SBU29} mutants. To confirm these observations are due to loss of Rest, we employed two independent approaches to decrease the function of Rest. Our first approach was to overexpress the dominant negative Rest (dnRest), which lacks N and C terminal repressor domains of the protein and compete with endogenous Rest for binding to RE1 sites [166, 253]. Loss of Rest function by injection of dnRest caused the upregulation of *snap25b* at the 8s stage but not earlier. In contrast, *bdnf* expression was increased at sphere stage, but not at the 8s stage (Fig 5.7B). This observation is consistent with the finding from the MZ*rest* mutants that *snap25b* and *bdnf* are derepressed by the loss of Rest activity, but differs in that *snap25b* was upregulated both early and later stage**s** in the mutants.

In a second approach, morpholinos were used to knock-down the *rest* gene. Both translation blocking ATG MO and splice blocking splice MO [210] were injected into one-cell stage embryos and expression levels of Rest target genes were studied by qRT-PCR at early and late stages. Similar to MZrest$^{-/-}$ mutant phenotype, *snap25b* and *bdnf* are upregulated upon decreased Rest function at sphere stage. Interestingly, *bdnf* expression levels are increased in *rest* MO injected embryos at 8s while in the *rest* mutants, *bdnf* levels were unaltered at the same developmental stage (Fig 5.7A).

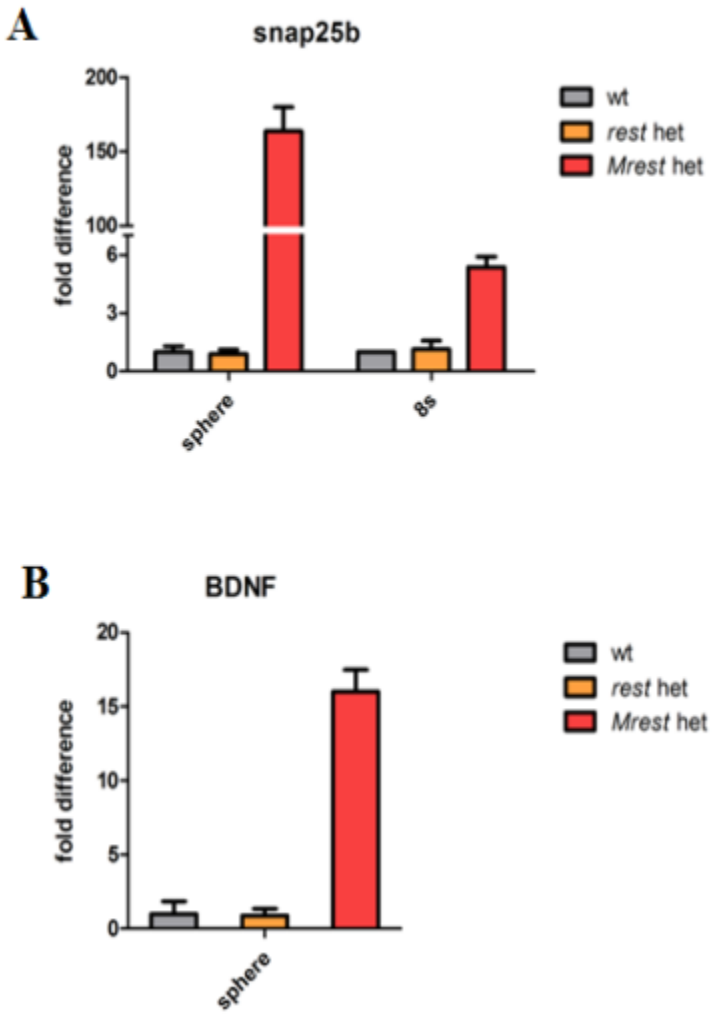

Figure 5.6: Maternal Rest function is required for early gene regulation. Expression levels of Rest target genes *snap25b* (A) and *bdnf* (B) were examined by qRT-PCR in rest heterozygous embryos, which has maternal *rest* message and Mrest heterozygous embryos, which lacks maternal *rest* message. Loss of maternal *rest* function caused an increase in the Rest target gene expression levels of *snap25b* and *bdnf* at early stages but not in embryos with functional maternal Rest. All fold differences are relative to wild type levels of the particular gene and expression levels of each gene are normalized against β-actin. Error bars represent the standard deviation from 3 different pools of embryos.

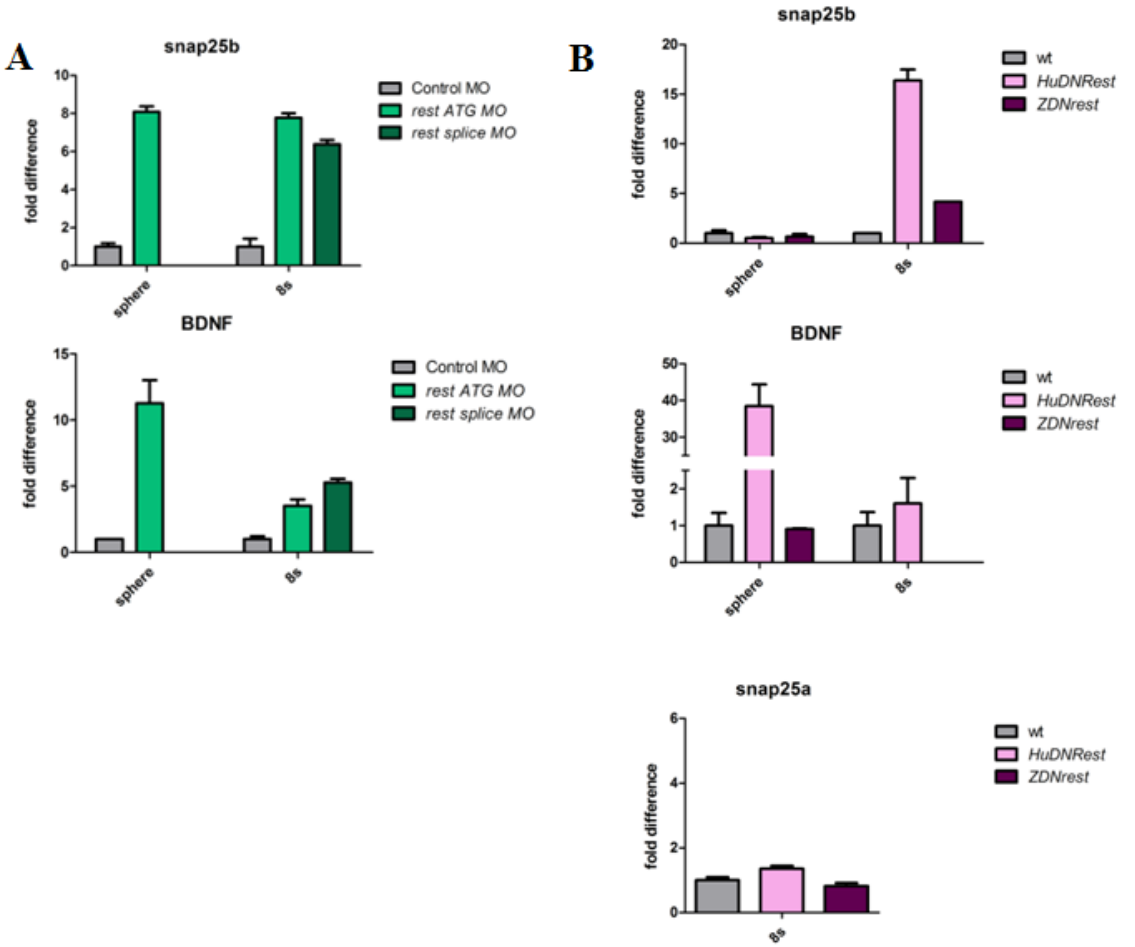

Figure 5.7: Phenotypes observed in DN-Rest and Rest-Morpholino injections are similar to that of *rest*^{SBU29}. Expression levels of Rest target genes *snap25a, snap25b* and *bdnf* were examined by qRT-PCR in *rest* morphants (A) and in embryos overexpressing dnRest(B). *snap25b* and *bdnf* expression levels are increased in *rest* morphants at both stages examined (A). *snap25b* is only induced at 8 somite stage in dnRest overexpressing embryos but not earlier. On the other hand, bdnf de-repression is only seen at early sphere stage. snap25a levels were not changed in dnRest overexpressing embryos. All fold differences are relative to wild type levels of the particular gene and expression levels of each gene is normalized against β-actin. Error bar represents the standard deviation from 3 different pools of embryos.

5.2.6 RE-1 containing genes are not derepressed by *rest*Δ39

To further characterize the domains of Rest function in zebrafish development, we studied *rest*^{SBU30} mutation (Δ39 nt) generated by ZFN injection. This mutation causes 13 amino acid deletion in Rest protein structure, but not a frameshift (Fig5.1). We hypothesize that this mutation is hypomorphic but not null since mutant protein still has DNA binding domain and repressor domains. To test this hypothesis, we generated MZ*rest*^{restSBU30} embryos and relative expression levels of Rest target genes are studied in these embryos by qRT PCR. Overall, we did not observe any change in transcript levels of the Rest target genes in MZ*rest*^{restSBU30} embryos (Fig 5.8) suggesting that the deleted 13 amino acids, residues 58-71, were not vital for the proper Rest repressor function to regulate the gene expression levels.

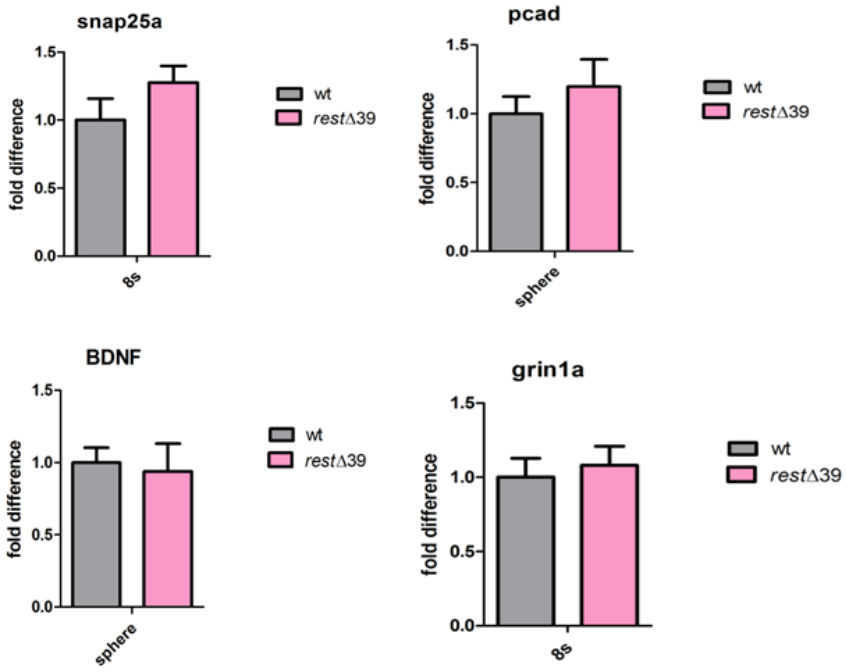

Figure 5.8: RE-1 containing genes are not derepressed by *rest*Δ39. Expression levels of Rest target genes *snap25a, pcad, grin1a* and *bdnf* were examined by qRT-PCR in *rest*Δ39 mutants. Expression levels of the studied genes were not changed in *rest*Δ39 mutants. All fold differences are relative to wild type levels of the particular gene and expression levels of each gene is normalized against β-actin. Error bars represent the standard deviation from 3 different pools of embryos.

5.2.7 Germ layer formation and early neural patterning are normal in *rest*^{SBU29} mutants

in-vivo studies established that Rest functions as a repressor of neural genes such as βIII tubulin, Ng-CAM and SCG10 in non-neural tissues [206]. In *Rest* knockout mice, cellular disorganization is observed in head mesenchyme of the midbrain, and mytomal cells in the somite. However, overall, germ layer formation and early patterning seem to be minimally affected in these embryos [206]. On the other hand, in Xenopus, upon injection of dnXRest, neural plate is expanded while epidermal and neural crest markers were decreased, showing early ectodermal patterning defects [207]. Moreover, in-vivo studies reported conflicting observations on the role of Rest in stem cell maintenance. Singh et. al. demonstrated that REST is required for self-renewal and pluripotency of the ES cells [212], while other reports strongly contested this observation [213-217].

To study whether Rest function is necessary for proper germ layer specification or early neural patterning in zebrafish, we analyzed the expression of early patterning genes by RNA *in-situ* hybridization in *rest*^{SBU29} mutants. Mesodermal markers *ntl* and *myoD*, and endodermal marker *axial* expression is not affected in *rest*^{SBU29} mutants (Fig 5.9). Furthermore, organizer marker *chd* and early dorsal neural plate and neural crest marker *pax3* are also similar to stage matched wild-type embryos (Fig 5.9). Overall, these results suggest that germ layer specification and early patterning is not affected in *rest*^{SBU29} embryos.

5.2.8 Loss of Rest function does not affect neurogenesis

We demonstrated that several neural genes are upregulated in *rest*^{SBU29} mutants by qRT-PCR. However, local regulation of these genes and their effects on fate specification could not be detected unless in-situ hybridization is employed to detect domain specific influences. To investigate the loss of Rest function on neural cell fate determination and differentiation, changes in expression domains of proneural and pan-neural markers were assayed in *rest*^{SBU29} mutants by RNA *in-situ* hybridization. Examination of pro-neural markers *zash1a* and *ngn* did not reveal any differences between stage matched wild type and *rest* mutants (Fig 5.10) Interestingly, the mouse homolog of *zash1a*, MASH1, is

shown to be upregulated in cortical progenitors when the presence of the REST is decreased dramatically on the MASH1 gene [176], suggesting the presence of redundant regulatory systems or the lack of activators in zebrafish proneural cells.

To study the effects of loss of Rest function in zebrafish neurogenesis, we examined the expression levels of pan-neural marker *huC* (*elavl3*) in *rest* mutants. Since Rest is shown to be the regulator of the neural gene expression, we predicted to observe ectopic neurogenesis in non-neural tissue in *rest* mutants which lack functional Rest. To our surprise, *rest*^{SBU29} mutants did not show any ectopic *huC* expression neither at early nor late stages of neurogenesis in non-neural tissue (Fig 5.11). This observation is consistent with the proposed function of Rest in mice and chick, in which NFSF is required for repression of neural genes in non-neural tissue but not cell-fate determination [206].

Effects of Rest loss of function on neurogenesis might be masked by redundant mechanisms that limit neurogenesis. To test this possibility, we removed the Rest function in neurogenic *mindbomb* (*mib*) mutants which lack Notch regulated lateral inhibition [258]. Thus, in *rest*; *mib* double mutants, two different neural regulatory mechanisms were eliminated and the effect of *rest* knock-out on the neurogenic phenotype of *mib* was examined. Pan-neural marker *huC* in-situ hybridization at early stages of neurogenesis revealed no difference between wild type and *rest*; *mib* double mutant siblings (Fig 5.12). This observation suggests that loss of Rest function does not enhance the neurogenic phenotype of *mib*.

5.2.9 Number of migrating *olig2*+ oligodendrocyte precursors are significantly reduced in *rest*^{SBU29}

Neural fate determination is grossly normal in *rest* mutants. To study the subtle differences in neural subpopulations which lack functional Rest, we generated Tg (*olig2*:GFP); MZ*rest*^{SBU29} double mutants and examined the behavior of *olig2*+ oligodendrocyte precursors (OPCs). These cells are originated from *olig2*+ primary motoneurons located in the ventral spinal cord [259]. While expression of both Olig2 and Ngn2 promotes motoneuron development, downregulation of Ngn2 in Olig2+ cells leads

to differentiation into OPCs [260-262], which then migrate more dorsal regions of the spinal cord. At 2 and 3 dpf, number of migrating *olig2*+ OPCs is significantly reduced in *rest*^{SBU29} mutants however not in the older larvae (Fig. 5.13). This phenotype can be the result of failed/delayed differentiation or dorsal migration of the OPCs or progressive cell death. Further analysis is required to discover the molecular mechanisms behind this observation.

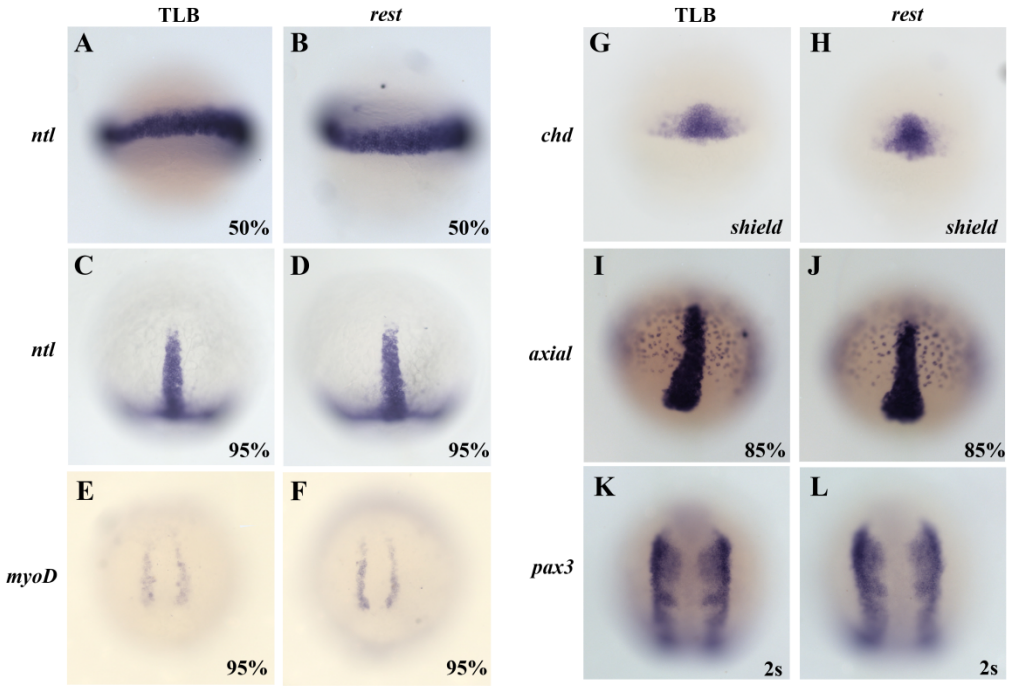

Figure 5.9: Germ layer formation and early neural patterning is normal in *rest*^{SBU29} mutants. Whole mount RNA in situ hybridization of germ layer and early neural patterning markers in wild-type and *rest* mutants. All views are dorsal, anterior to the top. Developmental stages of the embryos are indicated at lower right corner of each view. Expression domains of mesoderm markers ntl and myoD are not affected in *rest* mutants (A-F). Similarly, endoderm marker axial is also not altered in rest mutants (I, J). Moreover, organizer marker *chd* and early dorsal neural plate and neural crest marker *pax3* expression domains in *rest* mutants are also similar to stage matched wild-type embryos (G, H; K, L). Overall, rest embryos have no defect in germ layer specification and early neural patterning.

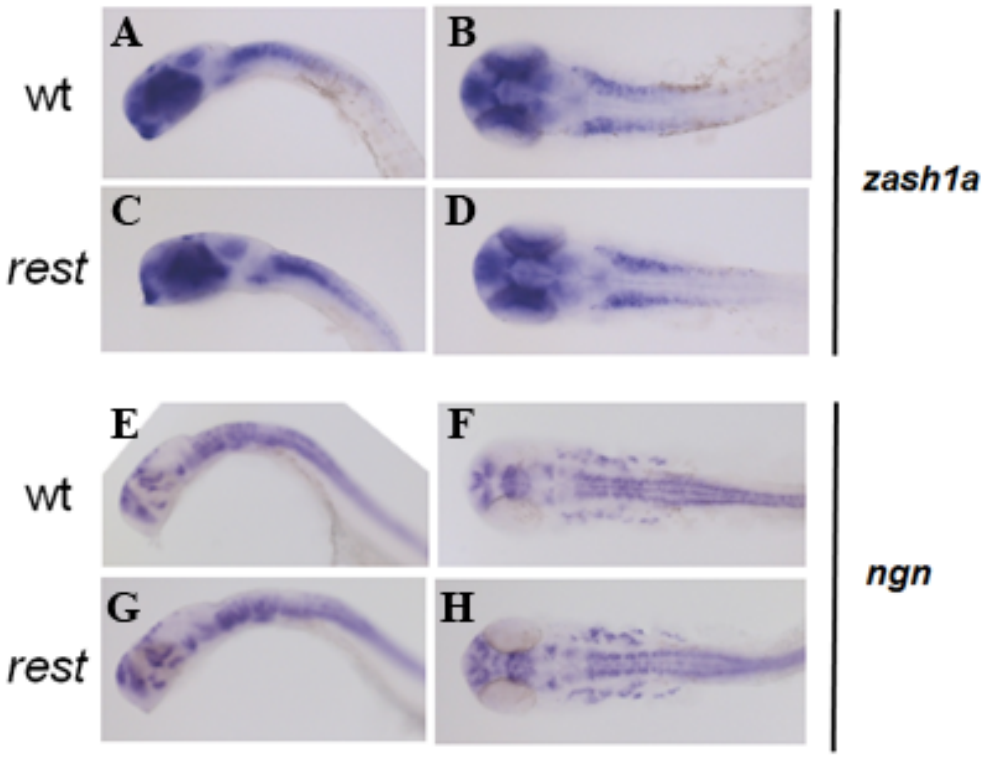

Figure 5.10: Number of progenitors is not affected in rest mutants. Flat mounted RNA in situ hybridization of proneural markers *zash1a* (A-D) and *ngn* (E-H) in 24-hour-old wild-type and *rest* mutants. A, C, E and G are lateral views; B, D, F, H are dorsal views, anterior to the left. Examination of pro-neural markers *zash1a* and *ngn* did not reveal any differences between stage matched wild type and *rest* mutants.

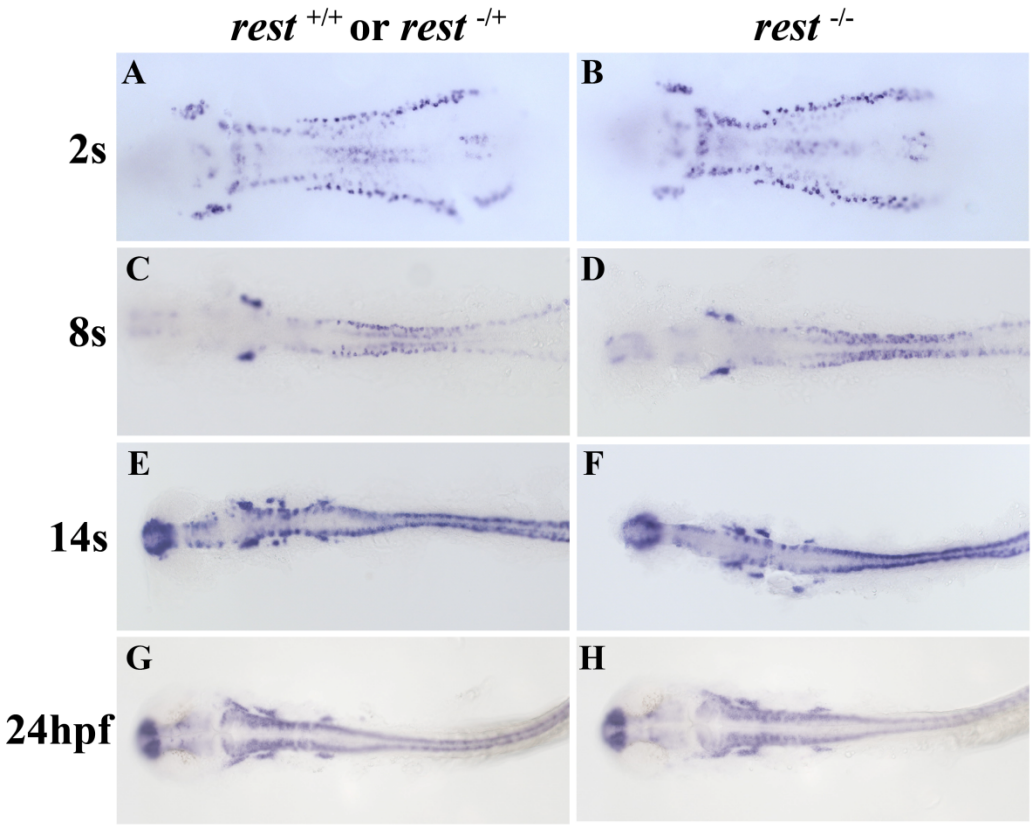

Figure 5.11: Neurogenesis is not overtly affected in *rest* mutants. Flat mounted RNA in situ hybridization of pan-neural marker *huC/elavl3* at stage matched 2 somite (A, B), 8 somite(C, D), 14 somite (E, F) and 24hpf (G, H) wild type and *rest* mutants. All views are dorsal, anterior to the left. *rest* mutants did not show any ectopic *huC/elavl3* expression neither at early nor late stages of neurogenesis in non-neural tissue.

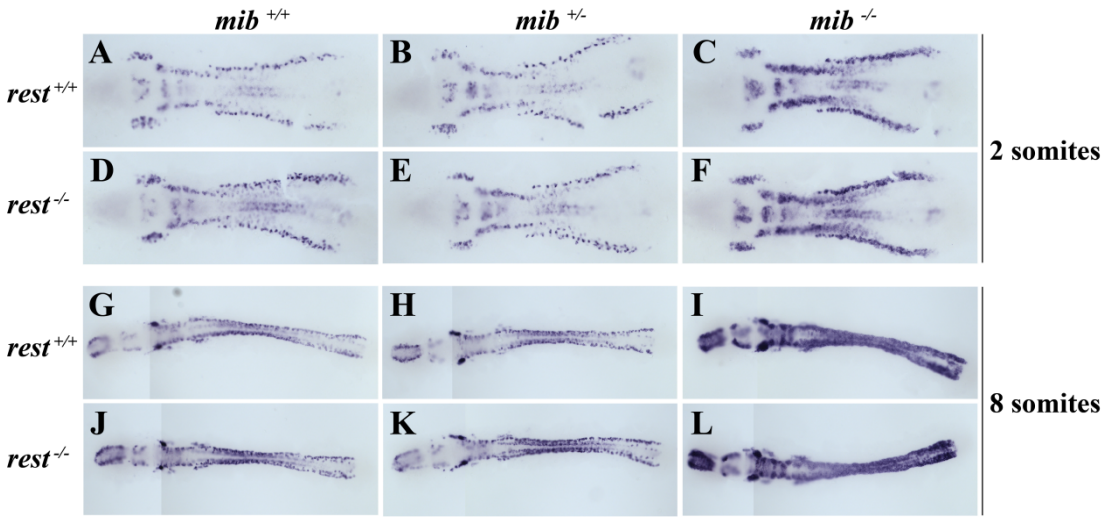

Figure 5.12: Rest function does not enhance the neurogenic phenotype of *mib*. Flat mounted RNA in situ hybridization of pan-neural marker *huC/elavl3* at stage matched 2 somite (A-F) and 8 somite (G-L) wild type and *rest; mib* double mutants. All views are dorsal, anterior to the left. Rest loss in $mib^{+/-}$ (E, K) and $mib^{-/-}$ (F, L) backgrounds did not enhance the neurogenic phenotype of the $mib^{+/-}$ (B, H) and $mib^{-/-}$ (C, I) with functional Rest.

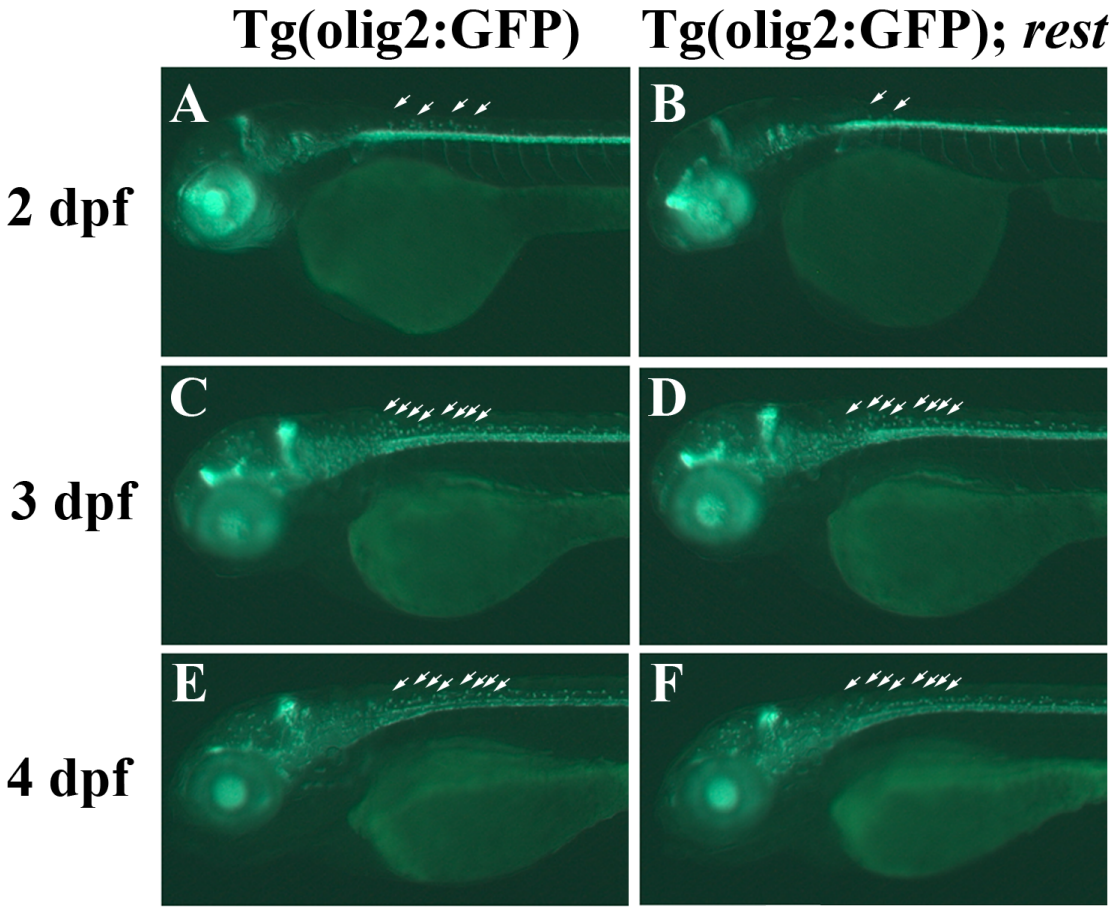

Figure 5.13: Rest function is critical for regulation of the migrating OPCs in the dorsal spinal cord. Lateral views of living 2-, 3-, and 4-day-old Tg (*olig2*:GFP) and Tg (*olig2*:GFP); MZ*rest*^{SBU29} mutants (A-F). Number of migrating *olig2*+ oligodendrocyte precursors are significantly reduced in *rest* mutants at 2 and 3 days post fertilization (B,D). Average number of migrating OPCs in Tg (*olig2*:GFP) at 2dpf is ~24 while Tg (*olig2*:GFP); MZ*rest*^{SBU29} mutants have only ~5 migrating OPCs. Similarly, at 3dpf, number of migrating OPCs in Tg (*olig2*:GFP); MZ*rest*^{SBU29} mutants is reduced to ~76 while Tg (*olig2*:GFP) fish have ~96 migrating OPCs. The number of the migrating OPCs in 4-day-old *rest* mutants is similar to that in embryos with functional Rest (94 vs 86). Arrows indicate migrating OPCs.

5.3 Discussion:

Here, we studied the function of REST in zebrafish neurogenesis. We demonstrated that Rest function is essential to repress a fraction of neural genes during early development and in non-neural adult tissues. However, impairment of Rest function does not affect early development and patterning of zebrafish embryos. In these embryos, germ layer specification and early neural patterning are not perturbed, neurogenesis is not affected. Epistatic analysis of the Rest function in a Notch mediated neurogenic background revealed no interaction between Notch pathway and Rest function during neurogenesis. In a more focused study, we also revealed less migrating olig2+ OPCs in the dorsal spinal cord in 2- and 3-day-old *rest* embryos but not older larvae.

A subset of neural genes that are direct targets of Rest were de-repressed in MZrest$^{-/-}$ mutants (Fig 5.4). *snap25b* is expressed almost undetectable levels at sphere stage where blastomeres are still pluripotent and it is highly upregulated in differentiated neurons. In MZrest$^{-/-}$ mutants, in which Rest mediated repression is relieved, expression levels of the snap25b is greatly de-repressed up to 262 fold. Similarly, *bdnf* is expressed only at low levels in pluripotent blastomeres but its expression is up-regulated in MZrest$^{-/-}$ at sphere stage. Interestingly, a fraction of RE1 containing genes' expression levels were not changed at that stage. On the other hand, only a subset of RE1 containing genes such as *snap25a, snap25b,* and *grin1a* is de-repressed but not the other genes we examined in this study at 8 somites. The effects of the loss of Rest function on RE1 containing gene expression levels were not observed after 24 hpf. In summary, the degree of the different neural gene de-repression upon Rest deficiency differs at different stages suggesting that Rest mediated repression function is gene and context dependent *in-vivo*. Moreover, similar to *in-vitro* observations [176], Rest probably fine-tunes temporal expression of the neural genes during development and provides neural plasticity during neurogenesis *in-vivo*.

The distinct patterns of de-repression of the Rest target genes in MZrest$^{-/-}$ mutants indicate that expression levels of these genes are controlled by more complex mechanisms than simple Rest mediated repression. Redundant regulatory elements and the chromatin structure of the Rest target site can also mediate the extent of the regulation

entailed by Rest function. This observation is consistent with other *in-vitro* and biochemical studies [169, 170, 172, 173, 176, 177, 202, 206, 253, 254, 263-265] proposing presence of other regulatory elements present on the gene (cis-regulatory) and in the cellular context (trans-regulatory) to control the extent of Rest mediated repression. For example, if the gene has a redundant cis-acting regulatory element besides RE1 motif, de-repression due to loss of Rest function may not be detected while another gene lacking that additional cis-regulatory element can be upregulated in *rest* mutants. Similarly, lack of activators can also prevent the de-repression of certain genes but not the others. Thus, the nature of the redundant regulatory elements may control the relative output of the Rest mediated repression differently in different gene and cellular contexts *in-vivo*.

In-vitro studies established that Rest functions as repressor of neural genes in non-neural tissues [206]. Here, we provide the first *in-vivo* evidence for a role of Rest in long term repression of neural gene *snap25b* in non-neural tissues. *snap25b* in adult rest$^{-/-}$ non-neural tissues such as pancreas, ovaries and liver is greatly de-repressed. However, if Rest provides long term repression of *snap25b* in non-neural tissue, some degree of de-repression should also be detected in non-neural tissues in MZrest$^{-/-}$ at pre-adult larvae. Thus, failure to detect de-repression of snap25b in non-neural tissues of the MZrest$^{-/-}$ larvae is an extremely intriguing observation. Again, the regulation difference between pre-adult and adult stages can be attributed to presence of distinctive redundant silencing systems. Alternatively, the high baseline expression levels of the *snap25b* in neural tissue of 8 and 19-day-old larvae may obscure subtle de-repression of *snap25b* in non-neural tissues.

We employed three independent approaches to eliminate or reduce the function of Rest to analyze Rest function on regulation of RE1 containing target gene expression: Generation of MZ*rest*^{SBU29}, microinjection of dnRest and *rest* morpholinos to the embryos. Overall, the function of Rest as transcriptional repressor is confirmed in all three approaches however closer examination of the gene expression levels revealed subtle differences. For example, in *rest* mutants, snap25b levels were upregulated at both sphere and 8 somites while it is upregulated only at 8 somites in the dnRest injected

embryos. Similarly, *bdnf* is induced at 8 somites in the *rest* morphants but not *rest* mutants (Fig 5.7).

The phenotypic difference between all three approaches is expected since each approach works differently to modulate the levels of Rest function. dnRest binds RE1 sites, blocking both Rest and other factors from the RE1 site whereas injection of *rest* ATG or splice MO diminishes the amount of functionally translated Rest protein, leaving the RE1 site unmasked. Since RE1 site is not blocked by functional protein, other RE1 dependent regulatory systems can still operate in morphants but not in dnRest injected embryos. Rest function is eliminated from the $rest^{-/-}$ mutants in a similar fashion to morphants. The biggest difference between these two approaches, though, is the degree of penetrance. In mutants, the gene is knocked-out completely while in morphants, even in ideal conditions, gene cannot be knocked-out completely. Therefore, instead of using these three approaches independently to assess the function of Rest in gene regulation, they must be used together in a complimentary fashion.

Homozygous deletion of NRSF/REST in mice is embryonic lethal by E11.5. These embryos exhibit severe developmental defects including growth retardation, and apoptosis[206]. Similarly, in Xenopus, overexpression of dnRest caused expansion of neural plate, diminished prospective epidermal markers and disrupted ectoderm and neural crest patterning [207]. In contrast, zebrafish mutants lacking functional Rest activity have more subtle phenotype. This difference can be attributed to possible redundant silencing systems, discussed earlier, present in zebrafish. Interestingly, although the zebrafish genome is duplicated, there is only one copy of the *rest* gene. However, the presence of a "redundant RE1 binding silencer" is still a possibility. To test that hypothesis, gel shift assay (EMSA) was performed using double stranded (DS) RE1 site as bait. Our preliminary results indicate that DS RE1 fragment is still "shifted" by a (redundant) "RE1 binding protein" in *rest* mutants. However, better controlled analysis is required to confirm the presence of another RE1- mediated repressor in zebrafish.

We observed de-repression of a subset of RE1 containing genes in *rest* mutants. However, we did not detect any defects in germ layer specification or patterning. In Xenopus, Rest modulates BMP mediated ectoderm patterning [207]. Moreover, although

there are conflicting reports, Rest is essential for ES cell self-renewal and maintenance [212]. On the other hand, germ line specification and early patterning are not affected when Rest mediated repression is relieved in zebrafish. More importantly, loss of Rest function did not overtly affect the neural differentiation in the non-neural tissue in *rest* mutants. This observation suggests that Rest functions to repress the neural terminal differentiation genes but not to specify cell fate. It is demonstrated that progression of neural differentiation and identity is partially controlled by REST and degradation of Rest is key step in differentiation of neural precursors [176]. However, loss of Rest function in the progenitors does not necessarily lead to robust expression of terminal differentiation genes *in-vitro* and *in-vivo* to change cell fates [206, 266, 267]; other redundant control mechanisms, such as lack of activators and presence of supressors, may prevent terminal differentiation progression. Thus, we proposed that effects of the *rest* knockout will be enhanced if another negative neurogenesis regulator is removed. To test that hypothesis, we removed the Rest function from *mindbomb* (*mib*) embryos. *mib* is a neurogenic mutant which lack Notch regulated lateral inhibition [258]. Interestingly, loss of Rest function did not enhance the neurogenic phenotype of *mib* suggesting that there is no interaction between Notch pathway and Rest function during neurogenesis.

Although a subset of Rest target genes is de-repressed in *rest* mutants, overall neurogenesis is not visibly affected. Therefore, we examined the subtle differences in neural phenotypes in *rest* mutants. In chick, overexpression of Rest also did not overtly affect neurogenesis but caused axon guidance defects in developing chick spinal cord [209] suggesting that Rest function is essential for proper development of sub-population of neural phenotypes *in-vivo*. This proposal is supported by our results which indicated reduced number of migrating *olig2*+ OPCs in the spinal cord. It is also important to note that neural phenotype defects were later recovered in *rest* mutants, indicating the presence of redundant regulators which mediate the progression of OPC differentiation and migration later in development.

OPC differentiation is progressively regulated by differential gene expression. For example, while OPC precursors are *ngn2*+; *olig2*+, repression of *ngn2* from the precursors is critical for initiating OPC differentiation [260-262]. Possibly, Rest may

mediate the plasticity of the OPC differentiation by regulating *ngn2* levels in the precursors and the differentiated OPCs. As a result of the *rest* mutation, *ngn2* repression may fail in the OPC precursors and OPC differentiation could not be initiated. Besides *ngn2*, 127 additional exclusive Rest target genes are defined in OPC precursors to regulate differentiation. Even though further analysis is necessary to determine how Rest regulates the number of the migrating OPCs *in-vivo*, it is clear that Rest function is critical for progression of the phenotypes essential for proper neural function in the nervous system.

We also studied another ZFN induced *rest* mutation, $rest^{SBU30}$, which lacks residues 58-71 in Rest repressor (Fig 5.1). Because $Rest^{SBU30}$ still has the DNA binding domains, we propose that this mutation is hypomorphic. However, we demonstrated that residues 58-71 are not essential for proper Rest mediated repression. This observation is consistent with the previously reported minimal Sin3B binding site of the mouse Rest protein [268]. In that study, NRSF/REST residues 38-57 is shown to be the minimal Sin3B repressor binding domain and is required for proper Sin3B interaction with N-terminus of NRSF/REST protein [268]. These residues are highly conserved between species and in zebrafish, residues 18-38, which are still present in $rest^{SBU30}$ mutants, are homologous to residues 38-57 in mouse counterpart. On the other hand, another study reported that residues 76-83, which are homologous to residues 54-61 in zebrafish, are necessary for the repression activity of the N-terminus repression domain of Rest [190]. Interestingly, these residues are deleted in $rest^{SBU30}$ mutants, suggesting $Rest^{SBU30}$ lacks the N-terminus dependent repressor activity according to this report [190]. However, it still has the Co-Rest binding repressor domain, which can partially compensate the loss of N-terminus dependent repressor activity.

5.3.1 Targeted mutagenesis with zinc finger nucleases is practical in zebrafish

We used ZFNs to introduce targeted genetic lesions at *rest* gene in zebrafish genome. In previous reports, which utilize ZFNs to disrupt the gene of interest, zebrafish developmental geneticists collaborated with groups who are experts in zinc finger

behavior and specificity because designing target specific zinc fingers is too laborious and cumbersome and requires special expertise to construct libraries and select the "active" ZFNs [1-3]. As an alternative, we used "modular assembly" strategy which involves assembly of pre-characterized zinc fingers to form an array targeting specified DNA sequences. Although the overall efficiency of the modular assembly is as low as 6% in human cells, zinc fingers that exclusively target GXX sub-sites are reported to have success rates of 36% [246].

We also bypassed the labor intensive affinity selection assays and we prescreened the efficiency of the ZFNs *in-vivo*. Typically, construction of target specific libraries and selection of target ZFNs by affinity selection takes 2-4 months when established protocols are followed. Modular assembly strategy takes only few days to design and select "active" ZFNs for the target gene. Although the success rate of the ZFNs designed in this study is lower (16%) than that of designed using more complicated engineering approaches, easiness and rapidness of the "modular approach" provide great advantage over other ZFN engineering methods. In this study, we demonstrated that the modular design of zinc finger nucleases was effective in disrupting the zebrafish *rest* locus.

Antisense morpholino oligos are widely used to block translation or disrupt splicing. However, the function of maternal protein already present in the egg cannot be blocked by morpholinos. That makes impossible to study the early function of the maternal effect gene using morpholinos. Now, ZFN technology can easily be used to eliminate gene function of suspected maternal-effect genes in zebrafish. For example, in this study, we established very early function of Rest which could not be studied in *rest* morphants utilizing ZFN induced *rest* mutants (Fig 5.6).

5.4 Materials and methods

5.4.1 Adult fish and embryo maintenance

Adult zebrafish strains and embryos obtained from natural crossings were maintained at 28.5°C. Developmental stages of the embryos were determined according to Kimmel *et. al*. [5].

5.4.2 ZFN construction and mRNA synthesis

The ZiFiT software program (http://www.zincfingers.org/software-tools.htm) was used to identify potential ZFN target sites. Conventional cloning strategies were employed to construct each array from clones in the Addgene Zinc Finger kit (www.addgene.com). Each ZF array is then cloned into KpnI/BamHI site of FokI-RR or FokI-DD vectors, which are also purchased from Addgene. Capped sense ZFN mRNA was synthesized using mMESSAGE mMACHINE Kit (Ambion, Austin, TX).

5.4.3 Screening "active" ZFNs *in-vivo*/mutation analysis

10-25 pg of ZFN mRNA is injected into blastomeres of one-cell-stage embryos. Genomic DNA is extracted from whole embryos following the protocol previously described [107] at 24hpf. PCR primers used to screen "active" ZFNs embryos are:

66 site GGATCTTCCTGCCGGATCT /TGCTGTATTCTGATGCAGACG

181/184 site F CTGAGGGGAAGCAGATGATG/TGTCCATGCTGTATCTCACGA

The amplification product of each PCR reaction is ~100 bp with the ZFN target site in the center. PCR products then run on 2-2.5% agarose gel. "Active" ZFN pair produces mutant allele whose size is different than that of wild type.

5.4.4 Sequence analysis of mutations induced by ZFNs

Genomic DNA is extracted from either single embryo at 24 hours following ZFN injection or fin-clips from ZFN injected adult fish to analyze somatic mutations induced by ZFNs. Genomic DNA of the offspring of the ZFN injected fish is extracted for germ line mutation analysis. PCR primers used to clone mutant sites are same with "screening"

primers. PCR fragments were digested with BamHI and SacII and cloned into pCS2+ vector. Positive clones were sequenced with Sp6 primer.

5.4.5 Relative quantitation of gene expression by real-time PCR

Total RNA was extracted from adult tissues or pools of 5 wild type and MZ*rest* embryos using the Trizol reagent (Invitrogen, Carlsbad, CA). SuperScript II Reverse Transcriptase (Invitrogen, Carlsbad, CA) was used to synthesize first strand cDNA from 0.5 ng of total RNA. Real time PCR was carried out using Lightcycler 480 (Roche) in 15 μL of final volume using 2X FastStart SYBR Green Master (Roche, Indianapolis, IN). Total RNA amount of each sample is normalized to relative amount of *β-actin* transcripts in each pool. In each experiment, 3 pools of control and experimental samples were run in duplicates; Ct values of each pool are averaged and relative amounts of gene expression were calculated using relative standard curve prepared for each primer set in each particular real time PCR run.

5.4.6 Whole mount in-situ hybridization

In situ hybridizations were performed according to Thisse et. al. [102]. Digoxigenin labeled probes for *in situ* hybridization were synthesized using T7, T3 or Sp6 RNA polymerase (Roche, Indianapolis, IN). Hybridized probes were detected using NBT/BCIP system (Roche, Indianapolis, IN). Stained embryos were re-fixed in 4% PFA and either stored in 100% methanol or cleared in Benzyl benzoate/benzyl alcohol solution (2:1) and mounted in Canada balsam/methyl salicylate (2.5% v/v) or flat mounted in 70% glycerol. Embryos were viewed with Zeiss Axioplan microscope, digitally photographed with Zeiss Axiocam camera. Images were processed and assembled with Zeiss Axiovision and Adobe Photoshop.

Chapter 6: Conclusions and Future Directions

Together, our results are largely in agreement with previous biochemical, *in-vivo* and *in-vitro* reports on Rest function. Here, we demonstrated that Rest acts as a transcription repressor of the neural genes in a gene, cellular context dependent manner during development. Moreover, we provided the first *in-vivo* evidence for a role of Rest in long term repression of neural gene *snap25b* in adult non-neural tissues. Although mice and Xenopus lacking Rest function exhibit severe developmental problems [206, 207], *rest* mutation displays very subtle defects which are not apparent morphologically indicating that Rest function is not necessary for early zebrafish development. Moreover, our data suggested that Rest is not involved in neurogenesis, but it maintains repression of the neural specific terminal differentiation gene in non-neural tissues.

In-vitro studies provided great insight to the function of Rest in neural and non-neural tissue. Here, we provided additional understanding of the role played by Rest *in-vivo.* Our observations will alleviate understanding intriguing, sometimes conflicting roles of Rest.

6.1: Future Directions

6.1.1 Biochemical validation of *rest* mutation

We used ZFNs to introduce targeted genetic lesions at *rest* gene in zebrafish genome to assess the function of Rest in gene regulation during early development. Sequence analysis of the ZFN mediated germ line mutations revealed multiple sequence changes (4nt, Δ6nt; Δ7nt; Δ39nt). The majority of our studies utilized an allele that encoded a 7nt deletion in the first exon of *rest*. Because the mutation produces a frameshift that eliminates the DNA binding domain, this mutation is predicted to be a null.

We observed de-repression of a subset of RE1 containing genes in *rest* mutants indicating that Rest mediated repression is relieved in *rest* mutants in a subset of genes. This observation supports our prediction of loss of functional Rest in *rest* mutants. However, this prediction should be further biochemically validated. More importantly, Rest deficiency should also be confirmed by Western blot analysis. We predict that *restΔ7* mutation lacks both DNA binding domain and the C-terminus repressor domain (Fig 5.1). Western blot analysis using Rest antibodies raised against either DNA binding domain or the C-terminus repressor domain can establish the presence (or absence, in the case of *rest* mutants) of the Rest protein in the cells. Because commercially available Rest antibodies cross-react with numerous zebrafish proteins, we generated zRest polyclonal antibody raised against C-terminus of the zebrafish Rest. Our preliminary experiments demonstrated loss of Rest protein in *rest* mutants (data not shown) however further analysis is needed to confirm this observation. The biggest setback of using western blot analysis to study the Rest function is that Rest is a low abundance protein, making it extremely difficult to detect endogenous Rest levels. To surmount this problem, nuclear extracts, which should contain larger fraction of total Rest protein, can be used.

In a complimentary approach, electrophoretic mobility shift assay (EMSA) can be used to validate the loss of Rest function in *rest* mutants. In this assay, double stranded RE1 site can be used as a bait to study Rest-RE1 interaction. We hypothesized that if functional Rest is lost in *rest* mutants, the RE1 "shift" caused by endogenous Rest

interaction will be lost in rest mutants. Interestingly, however, we still see the RE1 "shift" in *rest* mutants although this observation is very inconsistent implying a possible background effect. Further analysis with better controls is needed to confirm this observation.

Rest interacting proteins are well established in *in-vitro* studies. Co-immunoprecipitation (Co-IP) with the Rest interacting proteins can also provide insight into the absence (or presence) of functional Rest in *rest* mutants. To further validate the loss of Rest function in *rest* mutants, chromatin immunoprecipitation (ChIP) can also be employed (discussed in section 6.1.2).

6.1.2 Global analysis of Rest target genes

It is estimated that there are ~25,000 REST binding sites in human genome [178] while ~10,000 REST binding sites are estimated in mouse genome [177]. On the other hand computational analysis estimates ~810 RE1 sites regulating ~4200 genes in zebrafish [184], (Ian Wood, personal communication). Further biochemical analysis is needed to test the functionality of these "predicted" sites.

ChIPSAGE (SACO), ChIP-chip and ChIP-Seq analysis is employed to predict RE1 sites in human and mouse genome [177, 178, 183]. However, zebrafish anti-Rest antibody is not specific enough to analyze Rest target sites using these methods. Alternatively, differences in transcript levels of the whole transcriptome between wild type and *rest* mutant embryos can be studied by deep RNA sequencing (RNA-Seq). RNA-Seq is a high-throughput sequencing technique to measure the absolute mRNA levels of the each gene in the total RNA pool. Using this technique, possible Rest targets can be directly uncovered by comparing transcripts in wild type and *rest* mutants. Further computational analysis is also required to determine the exact Rest binding locations (RE1 sites) on these genes. Consequently, the impact of Rest loss of function on expression levels of the RNA-Seq- identified genes must also be confirmed by qRT-PCR. ChIP analysis will be also essential to confirm the functionality of the RE1 sites. After Rest specific binding sites are established, ChIP analysis can be used to test whether RE1 sites are occupied by functional Rest in *rest* mutants.

6.1.3 Crosstalk between Rest and other signaling pathways

In Xenopus, inhibition of REST function expands neural plate, interferes with ectoderm and neural crest patterning, and diminishes prospective epidermal markers [207]. Overall, these observations mimic a BMP decrease defects in the embryo and the BMP overexpression seems to eliminate these developmental problems [207] suggesting that Xenopus Rest has a role in promoting BMP function. The interaction between BMP signaling and Rest function in zebrafish is another avenue for investigation. Our preliminary experiments demonstrated that BMP signaling activation by Alk4, an activin receptor, overexpression is dampened in *rest* mutants. This observation suggests that zebrafish Rest also has a role in regulating BMP signaling however further experiments are necessary to resolve that aspect of Rest function.

The canonical Wnt pathway directly regulates REST expression in chick spinal cord and human embryonic carcinoma cells [269, 270]. REST in turn regulates Wnt signaling components, which are Rest target genes in ES cells [183]. Moreover, Rest corepressor CoRest expression is also regulated by Wnt components [271]. The details of Rest-Wnt signaling association should be further analyzed in zebrafish.

6.1.4 Analyzing Rest function in miRNA regulation

MicroRNAs (MiRNAs) are involved in regulation of cell fate determination, tissue differentiation and maintenance by negatively regulating target protein levels by increasing mRNA turnover and inhibiting translation [272, 273]. Expression of miR-124a, miR-132, miR-9, miR153 is regulated by Rest [182, 274]. Global analysis of Rest binding sites revealed that some RE1 sites are located in close proximity to miRNAs [177, 183]. Identification of RE1 sites regulating miRNA expression in zebrafish will add another level of understanding of the Rest mediated gene silencing.

References:

1. Meng, X., et al., *Targeted gene inactivation in zebrafish using engineered zinc-finger nucleases.* Nat Biotechnol, 2008. **26**(6): p. 695-701.
2. Doyon, Y., et al., *Heritable targeted gene disruption in zebrafish using designed zinc-finger nucleases.* Nat Biotechnol, 2008. **26**(6): p. 702-8.
3. Foley, J.E., et al., *Rapid mutation of endogenous zebrafish genes using zinc finger nucleases made by Oligomerized Pool ENgineering (OPEN).* PLoS One, 2009. **4**(2): p. e4348.
4. Saga, Y. and H. Takeda, *The making of the somite: molecular events in vertebrate segmentation.* Nat Rev Genet, 2001. **2**(11): p. 835-45.
5. Kimmel, C.B., et al., *Stages of embryonic development of the zebrafish.* Dev Dyn, 1995. **203**(3): p. 253-310.
6. Collier, J.R., et al., *A cell cycle model for somitogenesis: mathematical formulation and numerical simulation.* J Theor Biol, 2000. **207**(3): p. 305-16.
7. Cooke, J. and E.C. Zeeman, *A clock and wavefront model for control of the number of repeated structures during animal morphogenesis.* J Theor Biol, 1976. **58**(2): p. 455-76.
8. Flint, O.P., et al., *Control of somite number in normal and amputated mutant mouse embryos: an experimental and a theoretical analysis.* J Embryol Exp Morphol, 1978. **45**: p. 189-202.
9. Jaeger, J. and B.C. Goodwin, *A cellular oscillator model for periodic pattern formation.* J Theor Biol, 2001. **213**(2): p. 171-81.
10. Kaern, M., M. Menzinger, and A. Hunding, *Segmentation and somitogenesis derived from phase dynamics in growing oscillatory media.* J Theor Biol, 2000. **207**(4): p. 473-93.
11. Kerszberg, M. and L. Wolpert, *A clock and trail model for somite formation, specialization and polarization.* J Theor Biol, 2000. **205**(3): p. 505-10.
12. Keynes, R.J. and C.D. Stern, *Mechanisms of vertebrate segmentation.* Development, 1988. **103**(3): p. 413-29.
13. Polezhaev, A.A., *A mathematical model of the mechanism of vertebrate somitic segmentation.* J Theor Biol, 1992. **156**(2): p. 169-81.
14. Schnell, S. and P.K. Maini, *Clock and induction model for somitogenesis.* Dev Dyn, 2000. **217**(4): p. 415-20.
15. Palmeirim, I., et al., *Avian hairy gene expression identifies a molecular clock linked to vertebrate segmentation and somitogenesis.* Cell, 1997. **91**(5): p. 639-48.
16. Jouve, C., et al., *Notch signalling is required for cyclic expression of the hairy-like gene HES1 in the presomitic mesoderm.* Development, 2000. **127**(7): p. 1421-9.
17. Bessho, Y., et al., *Dynamic expression and essential functions of Hes7 in somite segmentation.* Genes Dev, 2001. **15**(20): p. 2642-7.
18. Leimeister, C., et al., *Oscillating expression of c-Hey2 in the presomitic mesoderm suggests that the segmentation clock may use combinatorial signaling through multiple interacting bHLH factors.* Dev Biol, 2000. **227**(1): p. 91-103.

19. Henry, C.A., et al., *Two linked hairy/Enhancer of split-related zebrafish genes, her1 and her7, function together to refine alternating somite boundaries.* Development, 2002. **129**(15): p. 3693-704.
20. Holley, S.A., et al., *her1 and the notch pathway function within the oscillator mechanism that regulates zebrafish somitogenesis.* Development, 2002. **129**(5): p. 1175-83.
21. Oates, A.C. and R.K. Ho, *Hairy/E(spl)-related (Her) genes are central components of the segmentation oscillator and display redundancy with the Delta/Notch signaling pathway in the formation of anterior segmental boundaries in the zebrafish.* Development, 2002. **129**(12): p. 2929-46.
22. Jiang, Y.J., et al., *Notch signalling and the synchronization of the somite segmentation clock.* Nature, 2000. **408**(6811): p. 475-9.
23. Prince, V.E., et al., *Zebrafish lunatic fringe demarcates segmental boundaries.* Mech Dev, 2001. **105**(1-2): p. 175-80.
24. Forsberg, H., F. Crozet, and N.A. Brown, *Waves of mouse Lunatic fringe expression, in four-hour cycles at two-hour intervals, precede somite boundary formation.* Curr Biol, 1998. **8**(18): p. 1027-30.
25. McGrew, M.J., et al., *The lunatic fringe gene is a target of the molecular clock linked to somite segmentation in avian embryos.* Curr Biol, 1998. **8**(17): p. 979-82.
26. Aulehla, A. and R.L. Johnson, *Dynamic expression of lunatic fringe suggests a link between notch signaling and an autonomous cellular oscillator driving somite segmentation.* Dev Biol, 1999. **207**(1): p. 49-61.
27. Aulehla, A., et al., *Wnt3a plays a major role in the segmentation clock controlling somitogenesis.* Dev Cell, 2003. **4**(3): p. 395-406.
28. Ishikawa, A., et al., *Mouse Nkd1, a Wnt antagonist, exhibits oscillatory gene expression in the PSM under the control of Notch signaling.* Mech Dev, 2004. **121**(12): p. 1443-53.
29. Suriben, R., D.A. Fisher, and B.N. Cheyette, *Dact1 presomitic mesoderm expression oscillates in phase with Axin2 in the somitogenesis clock of mice.* Dev Dyn, 2006. **235**(11): p. 3177-83.
30. Dequeant, M.L., et al., *A complex oscillating network of signaling genes underlies the mouse segmentation clock.* Science, 2006. **314**(5805): p. 1595-8.
31. Artavanis-Tsakonas, S., K. Matsuno, and M.E. Fortini, *Notch signaling.* Science, 1995. **268**(5208): p. 225-32.
32. Artavanis-Tsakonas, S., M.D. Rand, and R.J. Lake, *Notch signaling: cell fate control and signal integration in development.* Science, 1999. **284**(5415): p. 770-6.
33. Greenwald, I., *LIN-12/Notch signaling: lessons from worms and flies.* Genes Dev, 1998. **12**(12): p. 1751-62.
34. Bruckner, K., et al., *Glycosyltransferase activity of Fringe modulates Notch-Delta interactions.* Nature, 2000. **406**(6794): p. 411-5.
35. Moloney, D.J., et al., *Fringe is a glycosyltransferase that modifies Notch.* Nature, 2000. **406**(6794): p. 369-75.
36. Panin, V.M., et al., *Fringe modulates Notch-ligand interactions.* Nature, 1997. **387**(6636): p. 908-12.

37. Zhang, N. and T. Gridley, *Defects in somite formation in lunatic fringe-deficient mice.* Nature, 1998. **394**(6691): p. 374-7.
38. Wong, P.C., et al., *Presenilin 1 is required for Notch1 and DII1 expression in the paraxial mesoderm.* Nature, 1997. **387**(6630): p. 288-92.
39. van Eeden, F.J., et al., *Mutations affecting somite formation and patterning in the zebrafish, Danio rerio.* Development, 1996. **123**: p. 153-64.
40. Takke, C. and J.A. Campos-Ortega, *her1, a zebrafish pair-rule like gene, acts downstream of notch signalling to control somite development.* Development, 1999. **126**(13): p. 3005-14.
41. Oka, C., et al., *Disruption of the mouse RBP-J kappa gene results in early embryonic death.* Development, 1995. **121**(10): p. 3291-301.
42. Kusumi, K., et al., *The mouse pudgy mutation disrupts Delta homologue Dll3 and initiation of early somite boundaries.* Nat Genet, 1998. **19**(3): p. 274-8.
43. Hrabe de Angelis, M., J. McIntyre, 2nd, and A. Gossler, *Maintenance of somite borders in mice requires the Delta homologue DII1.* Nature, 1997. **386**(6626): p. 717-21.
44. Evrard, Y.A., et al., *lunatic fringe is an essential mediator of somite segmentation and patterning.* Nature, 1998. **394**(6691): p. 377-81.
45. Conlon, R.A., A.G. Reaume, and J. Rossant, *Notch1 is required for the coordinate segmentation of somites.* Development, 1995. **121**(5): p. 1533-45.
46. Dunwoodie, S.L., et al., *Axial skeletal defects caused by mutation in the spondylocostal dysplasia/pudgy gene Dll3 are associated with disruption of the segmentation clock within the presomitic mesoderm.* Development, 2002. **129**(7): p. 1795-806.
47. Jen, W.C., et al., *Periodic repression of Notch pathway genes governs the segmentation of Xenopus embryos.* Genes Dev, 1999. **13**(11): p. 1486-99.
48. Jen, W.C., et al., *The Notch ligand, X-Delta-2, mediates segmentation of the paraxial mesoderm in Xenopus embryos.* Development, 1997. **124**(6): p. 1169-78.
49. Dornseifer, P., C. Takke, and J.A. Campos-Ortega, *Overexpression of a zebrafish homologue of the Drosophila neurogenic gene Delta perturbs differentiation of primary neurons and somite development.* Mech Dev, 1997. **63**(2): p. 159-71.
50. Ozbudak, E.M. and J. Lewis, *Notch signalling synchronizes the zebrafish segmentation clock but is not needed to create somite boundaries.* PLoS Genet, 2008. **4**(2): p. e15.
51. Sieger, D., D. Tautz, and M. Gajewski, *The role of Suppressor of Hairless in Notch mediated signalling during zebrafish somitogenesis.* Mech Dev, 2003. **120**(9): p. 1083-94.
52. Geling, A., et al., *A gamma-secretase inhibitor blocks Notch signaling in vivo and causes a severe neurogenic phenotype in zebrafish.* EMBO Rep, 2002. **3**(7): p. 688-94.
53. Gajewski, M., et al., *Anterior and posterior waves of cyclic her1 gene expression are differentially regulated in the presomitic mesoderm of zebrafish.* Development, 2003. **130**(18): p. 4269-78.
54. Julich, D., et al., *beamter/deltaC and the role of Notch ligands in the zebrafish somite segmentation, hindbrain neurogenesis and hypochord differentiation.* Dev Biol, 2005. **286**(2): p. 391-404.

55. Holley, S.A., R. Geisler, and C. Nusslein-Volhard, *Control of her1 expression during zebrafish somitogenesis by a delta-dependent oscillator and an independent wave-front activity.* Genes Dev, 2000. **14**(13): p. 1678-90.
56. Itoh, M., et al., *Mind bomb is a ubiquitin ligase that is essential for efficient activation of Notch signaling by Delta.* Dev Cell, 2003. **4**(1): p. 67-82.
57. Durbin, L., et al., *Anteroposterior patterning is required within segments for somite boundary formation in developing zebrafish.* Development, 2000. **127**(8): p. 1703-13.
58. Lewis, J., *Autoinhibition with transcriptional delay: a simple mechanism for the zebrafish somitogenesis oscillator.* Curr Biol, 2003. **13**(16): p. 1398-408.
59. Giudicelli, F., et al., *Setting the tempo in development: an investigation of the zebrafish somite clock mechanism.* PLoS Biol, 2007. **5**(6): p. e150.
60. Yamaguchi, T.P., R.A. Conlon, and J. Rossant, *Expression of the fibroblast growth factor receptor FGFR-1/flg during gastrulation and segmentation in the mouse embryo.* Dev Biol, 1992. **152**(1): p. 75-88.
61. Sawada, A., et al., *Zebrafish Mesp family genes, mesp-a and mesp-b are segmentally expressed in the presomitic mesoderm, and Mesp-b confers the anterior identity to the developing somites.* Development, 2000. **127**(8): p. 1691-702.
62. Yamaguchi, T.P., et al., *fgfr-1 is required for embryonic growth and mesodermal patterning during mouse gastrulation.* Genes Dev, 1994. **8**(24): p. 3032-44.
63. Reifers, F., et al., *Fgf8 is mutated in zebrafish acerebellar (ace) mutants and is required for maintenance of midbrain-hindbrain boundary development and somitogenesis.* Development, 1998. **125**(13): p. 2381-95.
64. Dubrulle, J., M.J. McGrew, and O. Pourquie, *FGF signaling controls somite boundary position and regulates segmentation clock control of spatiotemporal Hox gene activation.* Cell, 2001. **106**(2): p. 219-32.
65. Sawada, A., et al., *Fgf/MAPK signalling is a crucial positional cue in somite boundary formation.* Development, 2001. **128**(23): p. 4873-80.
66. Perantoni, A.O., et al., *Inactivation of FGF8 in early mesoderm reveals an essential role in kidney development.* Development, 2005. **132**(17): p. 3859-71.
67. Nagano, T., et al., *Shisa2 promotes the maturation of somitic precursors and transition to the segmental fate in Xenopus embryos.* Development, 2006. **133**(23): p. 4643-54.
68. Anderson, W.G., J.M. Conlon, and N. Hazon, *Characterization of the endogenous intestinal peptide that stimulates the rectal gland of Scyliorhinus canicula.* Am J Physiol, 1995. **268**(6 Pt 2): p. R1359-64.
69. Keegan, B.R., et al., *The elongation factors Pandora/Spt6 and Foggy/Spt5 promote transcription in the zebrafish embryo.* Development, 2002. **129**(7): p. 1623-32.
70. Bortvin, A. and F. Winston, *Evidence that Spt6p controls chromatin structure by a direct interaction with histones.* Science, 1996. **272**(5267): p. 1473-6.
71. Swanson, M.S. and F. Winston, *SPT4, SPT5 and SPT6 interactions: effects on transcription and viability in Saccharomyces cerevisiae.* Genetics, 1992. **132**(2): p. 325-36.

72. Hartzog, G.A., et al., *Evidence that Spt4, Spt5, and Spt6 control transcription elongation by RNA polymerase II in Saccharomyces cerevisiae.* Genes Dev, 1998. **12**(3): p. 357-69.
73. Saunders, A., et al., *Tracking FACT and the RNA polymerase II elongation complex through chromatin in vivo.* Science, 2003. **301**(5636): p. 1094-6.
74. Adkins, M.W. and J.K. Tyler, *Transcriptional activators are dispensable for transcription in the absence of Spt6-mediated chromatin reassembly of promoter regions.* Mol Cell, 2006. **21**(3): p. 405-16.
75. Kaplan, C.D., L. Laprade, and F. Winston, *Transcription elongation factors repress transcription initiation from cryptic sites.* Science, 2003. **301**(5636): p. 1096-9.
76. Hubbard, E.J., Q. Dong, and I. Greenwald, *Evidence for physical and functional association between EMB-5 and LIN-12 in Caenorhabditis elegans.* Science, 1996. **273**(5271): p. 112-5.
77. Henry, C.A., et al., *Somites in zebrafish doubly mutant for knypek and trilobite form without internal mesenchymal cells or compaction.* Curr Biol, 2000. **10**(17): p. 1063-6.
78. Tsai, S.F., et al., *Cloning of cDNA for the major DNA-binding protein of the erythroid lineage through expression in mammalian cells.* Nature, 1989. **339**(6224): p. 446-51.
79. Krauss, S., et al., *Expression of the zebrafish paired box gene pax[zf-b] during early neurogenesis.* Development, 1991. **113**(4): p. 1193-206.
80. Henry, C.A., et al., *Roles for zebrafish focal adhesion kinase in notochord and somite morphogenesis.* Dev Biol, 2001. **240**(2): p. 474-87.
81. Hens, M.D. and D.W. DeSimone, *Molecular analysis and developmental expression of the focal adhesion kinase pp125FAK in Xenopus laevis.* Dev Biol, 1995. **170**(2): p. 274-88.
82. Polte, T.R., A.J. Naftilan, and S.K. Hanks, *Focal adhesion kinase is abundant in developing blood vessels and elevation of its phosphotyrosine content in vascular smooth muscle cells is a rapid response to angiotensin II.* J Cell Biochem, 1994. **55**(1): p. 106-19.
83. Henry, C.A., et al., *Interactions between muscle fibers and segment boundaries in zebrafish.* Dev Biol, 2005. **287**(2): p. 346-60.
84. Topczewska, J.M., et al., *The winged helix transcription factor Foxc1a is essential for somitogenesis in zebrafish.* Genes Dev, 2001. **15**(18): p. 2483-93.
85. Cortes, F., et al., *Cadherin-mediated differential cell adhesion controls slow muscle cell migration in the developing zebrafish myotome.* Dev Cell, 2003. **5**(6): p. 865-76.
86. Gray, M., et al., *Zebrafish deadly seven functions in neurogenesis.* Dev Biol, 2001. **237**(2): p. 306-23.
87. Oxtoby, E. and T. Jowett, *Cloning of the zebrafish krox-20 gene (krx-20) and its expression during hindbrain development.* Nucleic Acids Res, 1993. **21**(5): p. 1087-95.
88. Kim, C.H., et al., *Zebrafish elav/HuC homologue as a very early neuronal marker.* Neurosci Lett, 1996. **216**(2): p. 109-12.

89. Pawson, T., *Protein modules and signalling networks.* Nature, 1995. **373**(6515): p. 573-80.
90. Clark-Adams, C.D. and F. Winston, *The SPT6 gene is essential for growth and is required for delta-mediated transcription in Saccharomyces cerevisiae.* Mol Cell Biol, 1987. **7**(2): p. 679-86.
91. Malone, E.A., J.S. Fassler, and F. Winston, *Molecular and genetic characterization of SPT4, a gene important for transcription initiation in Saccharomyces cerevisiae.* Mol Gen Genet, 1993. **237**(3): p. 449-59.
92. Kaplan, C.D., et al., *Spt5 and spt6 are associated with active transcription and have characteristics of general elongation factors in D. melanogaster.* Genes Dev, 2000. **14**(20): p. 2623-34.
93. Winkler, M., T. aus Dem Siepen, and T. Stamminger, *Functional interaction between pleiotropic transactivator pUL69 of human cytomegalovirus and the human homolog of yeast chromatin regulatory protein SPT6.* J Virol, 2000. **74**(17): p. 8053-64.
94. Nishiwaki, K., T. Sano, and J. Miwa, *emb-5, a gene required for the correct timing of gut precursor cell division during gastrulation in Caenorhabditis elegans, encodes a protein similar to the yeast nuclear protein SPT6.* Mol Gen Genet, 1993. **239**(3): p. 313-22.
95. Tenney, K., et al., *Drosophila Rtf1 functions in histone methylation, gene expression, and Notch signaling.* Proc Natl Acad Sci U S A, 2006. **103**(32): p. 11970-4.
96. Bray, S., H. Musisi, and M. Bienz, *Bre1 is required for Notch signaling and histone modification.* Dev Cell, 2005. **8**(2): p. 279-86.
97. Wood, A., et al., *The Paf1 complex is essential for histone monoubiquitination by the Rad6-Bre1 complex, which signals for histone methylation by COMPASS and Dot1p.* J Biol Chem, 2003. **278**(37): p. 34739-42.
98. Costa, P.J. and K.M. Arndt, *Synthetic lethal interactions suggest a role for the Saccharomyces cerevisiae Rtf1 protein in transcription elongation.* Genetics, 2000. **156**(2): p. 535-47.
99. Tsukiyama, T. and C. Wu, *Chromatin remodeling and transcription.* Curr Opin Genet Dev, 1997. **7**(2): p. 182-91.
100. Gates, M.A., et al., *A genetic linkage map for zebrafish: comparative analysis and localization of genes and expressed sequences.* Genome Res, 1999. **9**(4): p. 334-47.
101. Takke, C., et al., *her4, a zebrafish homologue of the Drosophila neurogenic gene E(spl), is a target of NOTCH signalling.* Development, 1999. **126**(9): p. 1811-21.
102. Thisse, C., et al., *Structure of the zebrafish snail1 gene and its expression in wild-type, spadetail and no tail mutant embryos.* Development, 1993. **119**(4): p. 1203-15.
103. Bassett, D.I., et al., *Dystrophin is required for the formation of stable muscle attachments in the zebrafish embryo.* Development, 2003. **130**(23): p. 5851-60.
104. Parsons, M.J., et al., *Zebrafish mutants identify an essential role for laminins in notochord formation.* Development, 2002. **129**(13): p. 3137-46.
105. Henry, C.A. and S.L. Amacher, *Zebrafish slow muscle cell migration induces a wave of fast muscle morphogenesis.* Dev Cell, 2004. **7**(6): p. 917-23.

106. Crawford, B.D., et al., *Activity and Distribution of Paxillin, Focal Adhesion Kinase, and Cadherin Indicate Cooperative Roles during Zebrafish Morphogenesis.* Mol Biol Cell, 2003. **14**(8): p. 3065-81.
107. Sirotkin, H.I., et al., *bozozok and squint act in parallel to specify dorsal mesoderm and anterior neuroectoderm in zebrafish.* Development, 2000. **127**(12): p. 2583-92.
108. Bottcher, R.T. and C. Niehrs, *Fibroblast growth factor signaling during early vertebrate development.* Endocr Rev, 2005. **26**(1): p. 63-77.
109. Amaya, E., T.J. Musci, and M.W. Kirschner, *Expression of a dominant negative mutant of the FGF receptor disrupts mesoderm formation in Xenopus embryos.* Cell, 1991. **66**(2): p. 257-70.
110. Borland, C.Z., J.L. Schutzman, and M.J. Stern, *Fibroblast growth factor signaling in Caenorhabditis elegans.* Bioessays, 2001. **23**(12): p. 1120-30.
111. Coumoul, X. and C.X. Deng, *Roles of FGF receptors in mammalian development and congenital diseases.* Birth Defects Res C Embryo Today, 2003. **69**(4): p. 286-304.
112. Sutherland, D., C. Samakovlis, and M.A. Krasnow, *branchless encodes a Drosophila FGF homolog that controls tracheal cell migration and the pattern of branching.* Cell, 1996. **87**(6): p. 1091-101.
113. Thisse, B. and C. Thisse, *Functions and regulations of fibroblast growth factor signaling during embryonic development.* Dev Biol, 2005. **287**(2): p. 390-402.
114. Krens, S.F., et al., *Distinct functions for ERK1 and ERK2 in cell migration processes during zebrafish gastrulation.* Dev Biol, 2008. **319**(2): p. 370-83.
115. Furthauer, M., et al., *Fgf signalling controls the dorsoventral patterning of the zebrafish embryo.* Development, 2004. **131**(12): p. 2853-64.
116. Huang, H., et al., *Amotl2 is essential for cell movements in zebrafish embryo and regulates c-Src translocation.* Development, 2007. **134**(5): p. 979-88.
117. Sheng, G., M. dos Reis, and C.D. Stern, *Churchill, a zinc finger transcriptional activator, regulates the transition between gastrulation and neurulation.* Cell, 2003. **115**(5): p. 603-13.
118. Londin, E.R., et al., *Expression and regulation of the zinc finger transcription factor Churchill during zebrafish development.* Gene Expr Patterns, 2007. **7**(6): p. 645-50.
119. Snir, M., et al., *Xenopus laevis POU91 protein, an Oct3/4 homologue, regulates competence transitions from mesoderm to neural cell fates.* Embo J, 2006. **25**(15): p. 3664-74.
120. Kimelman, D. and A. Maas, *Induction of dorsal and ventral mesoderm by ectopically expressed Xenopus basic fibroblast growth factor.* Development, 1992. **114**(1): p. 261-9.
121. LaBonne, C. and M. Whitman, *Mesoderm induction by activin requires FGF-mediated intracellular signals.* Development, 1994. **120**(2): p. 463-72.
122. Londin, E.R., L. Mentzer, and H.I. Sirotkin, *Churchill regulates cell movement and mesoderm specification by repressing Nodal signaling.* BMC Dev Biol, 2007. **7**: p. 120.

123. Lee, B.M., et al., *Embryonic neural inducing factor churchill is not a DNA-binding zinc finger protein: solution structure reveals a solvent-exposed beta-sheet and zinc binuclear cluster.* J Mol Biol, 2007. **371**(5): p. 1274-89.
124. Remacle, J.E., et al., *New mode of DNA binding of multi-zinc finger transcription factors: deltaEF1 family members bind with two hands to two target sites.* Embo J, 1999. **18**(18): p. 5073-84.
125. Verschueren, K., et al., *SIP1, a novel zinc finger/homeodomain repressor, interacts with Smad proteins and binds to 5'-CACCT sequences in candidate target genes.* J Biol Chem, 1999. **274**(29): p. 20489-98.
126. Postigo, A.A., *Opposing functions of ZEB proteins in the regulation of the TGFbeta/BMP signaling pathway.* Embo J, 2003. **22**(10): p. 2443-52.
127. Postigo, A.A., et al., *Regulation of Smad signaling through a differential recruitment of coactivators and corepressors by ZEB proteins.* Embo J, 2003. **22**(10): p. 2453-62.
128. Comijn, J., et al., *The two-handed E box binding zinc finger protein SIP1 downregulates E-cadherin and induces invasion.* Mol Cell, 2001. **7**(6): p. 1267-78.
129. Cooke, J., *Somite abnormalities caused by short heat shocks to pre-neurula stages of Xenopus laevis.* J Embryol Exp Morphol, 1978. **45**: p. 283-94.
130. Pourquie, O., *The segmentation clock: converting embryonic time into spatial pattern.* Science, 2003. **301**(5631): p. 328-30.
131. Pourquie, O., *Vertebrate somitogenesis.* Annu Rev Cell Dev Biol, 2001. **17**: p. 311-50.
132. Dale, K.J. and O. Pourquie, *A clock-work somite.* Bioessays, 2000. **22**(1): p. 72-83.
133. Giudicelli, F. and J. Lewis, *The vertebrate segmentation clock.* Curr Opin Genet Dev, 2004. **14**(4): p. 407-14.
134. Cinquin, O., *Understanding the somitogenesis clock: what's missing?* Mech Dev, 2007. **124**(7-8): p. 501-17.
135. Dale, J.K., et al., *Periodic notch inhibition by lunatic fringe underlies the chick segmentation clock.* Nature, 2003. **421**(6920): p. 275-8.
136. Qiu, X., et al., *Sequence and embryonic expression of three zebrafish fringe genes: lunatic fringe, radical fringe, and manic fringe.* Dev Dyn, 2004. **231**(3): p. 621-30.
137. Sato, Y., K. Yasuda, and Y. Takahashi, *Morphological boundary forms by a novel inductive event mediated by Lunatic fringe and Notch during somitic segmentation.* Development, 2002. **129**(15): p. 3633-44.
138. Serth, K., et al., *Transcriptional oscillation of lunatic fringe is essential for somitogenesis.* Genes Dev, 2003. **17**(7): p. 912-25.
139. Takada, S., et al., *Wnt-3a regulates somite and tailbud formation in the mouse embryo.* Genes Dev, 1994. **8**(2): p. 174-89.
140. Delfini, M.C., et al., *Control of the segmentation process by graded MAPK/ERK activation in the chick embryo.* Proc Natl Acad Sci U S A, 2005. **102**(32): p. 11343-8.

141. Wahl, M.B., et al., *FGF signaling acts upstream of the NOTCH and WNT signaling pathways to control segmentation clock oscillations in mouse somitogenesis.* Development, 2007. **134**(22): p. 4033-41.
142. Furthauer, M., C. Thisse, and B. Thisse, *A role for FGF-8 in the dorsoventral patterning of the zebrafish gastrula.* Development, 1997. **124**(21): p. 4253-64.
143. Maruhashi, M., et al., *Involvement of SIP1 in positioning of somite boundaries in the mouse embryo.* Dev Dyn, 2005. **234**(2): p. 332-8.
144. Delalande, J.M., et al., *Zebrafish sip1a and sip1b are essential for normal axial and neural patterning.* Dev Dyn, 2008. **237**(4): p. 1060-9.
145. Yamamoto, A., et al., *Zebrafish paraxial protocadherin is a downstream target of spadetail involved in morphogenesis of gastrula mesoderm.* Development, 1998. **125**(17): p. 3389-97.
146. Weinberg, E.S., et al., *Developmental regulation of zebrafish MyoD in wild-type, no tail and spadetail embryos.* Development, 1996. **122**(1): p. 271-80.
147. Durbin, L., et al., *Eph signaling is required for segmentation and differentiation of the somites.* Genes Dev, 1998. **12**(19): p. 3096-109.
148. Furthauer, M., et al., *sprouty4 acts in vivo as a feedback-induced antagonist of FGF signaling in zebrafish.* Development, 2001. **128**(12): p. 2175-86.
149. Draper, B.W., P.A. Morcos, and C.B. Kimmel, *Inhibition of zebrafish fgf8 pre-mRNA splicing with morpholino oligos: a quantifiable method for gene knockdown.* Genesis, 2001. **30**(3): p. 154-6.
150. Nitta, K.R., et al., *XSIP1 is essential for early neural gene expression and neural differentiation by suppression of BMP signaling.* Dev Biol, 2004. **275**(1): p. 258-67.
151. van Grunsven, L.A., et al., *XSip1 neuralizing activity involves the co-repressor CtBP and occurs through BMP dependent and independent mechanisms.* Dev Biol, 2007. **306**(1): p. 34-49.
152. Groves, J.A., C.L. Hammond, and S.M. Hughes, *Fgf8 drives myogenic progression of a novel lateral fast muscle fibre population in zebrafish.* Development, 2005. **132**(19): p. 4211-22.
153. Sun, X., et al., *Targeted disruption of Fgf8 causes failure of cell migration in the gastrulating mouse embryo.* Genes Dev, 1999. **13**(14): p. 1834-46.
154. Ciruna, B. and J. Rossant, *FGF signaling regulates mesoderm cell fate specification and morphogenetic movement at the primitive streak.* Dev Cell, 2001. **1**(1): p. 37-49.
155. Yang, X., et al., *Cell movement patterns during gastrulation in the chick are controlled by positive and negative chemotaxis mediated by FGF4 and FGF8.* Dev Cell, 2002. **3**(3): p. 425-37.
156. Allfrey, V.G., R. Faulkner, and A.E. Mirsky, *Acetylation and Methylation of Histones and Their Possible Role in the Regulation of Rna Synthesis.* Proc Natl Acad Sci U S A, 1964. **51**: p. 786-94.
157. Kuo, M.H. and C.D. Allis, *Roles of histone acetyltransferases and deacetylases in gene regulation.* Bioessays, 1998. **20**(8): p. 615-26.
158. Cheung, P., C.D. Allis, and P. Sassone-Corsi, *Signaling to chromatin through histone modifications.* Cell, 2000. **103**(2): p. 263-71.

159. Sung, P., S. Prakash, and L. Prakash, *The RAD6 protein of Saccharomyces cerevisiae polyubiquitinates histones, and its acidic domain mediates this activity.* Genes Dev, 1988. **2**(11): p. 1476-85.
160. Stevely, W.S. and L.A. Stocken, *Phosphorylation of rat-thymus histone.* Biochem J, 1966. **100**(2): p. 20C-1C.
161. Shiio, Y. and R.N. Eisenman, *Histone sumoylation is associated with transcriptional repression.* Proc Natl Acad Sci U S A, 2003. **100**(23): p. 13225-30.
162. Kouzarides, T., *Histone methylation in transcriptional control.* Curr Opin Genet Dev, 2002. **12**(2): p. 198-209.
163. Gill, G., *SUMO and ubiquitin in the nucleus: different functions, similar mechanisms?* Genes Dev, 2004. **18**(17): p. 2046-59.
164. Wolffe, A.P. and M.A. Matzke, *Epigenetics: regulation through repression.* Science, 1999. **286**(5439): p. 481-6.
165. Urnov, F.D. and A.P. Wolffe, *Above and within the genome: epigenetics past and present.* J Mammary Gland Biol Neoplasia, 2001. **6**(2): p. 153-67.
166. Chong, J.A., et al., *REST: a mammalian silencer protein that restricts sodium channel gene expression to neurons.* Cell, 1995. **80**(6): p. 949-57.
167. Schoenherr, C.J. and D.J. Anderson, *The neuron-restrictive silencer factor (NRSF): a coordinate repressor of multiple neuron-specific genes.* Science, 1995. **267**(5202): p. 1360-3.
168. Schoenherr, C.J., A.J. Paquette, and D.J. Anderson, *Identification of potential target genes for the neuron-restrictive silencer factor.* Proc Natl Acad Sci U S A, 1996. **93**(18): p. 9881-6.
169. Bessis, A., et al., *The neuron-restrictive silencer element: a dual enhancer/silencer crucial for patterned expression of a nicotinic receptor gene in the brain.* Proc Natl Acad Sci U S A, 1997. **94**(11): p. 5906-11.
170. Kallunki, P., G.M. Edelman, and F.S. Jones, *Tissue-specific expression of the L1 cell adhesion molecule is modulated by the neural restrictive silencer element.* J Cell Biol, 1997. **138**(6): p. 1343-54.
171. Kraner, S.D., et al., *Silencing the type II sodium channel gene: a model for neural-specific gene regulation.* Neuron, 1992. **9**(1): p. 37-44.
172. Lonnerberg, P., et al., *Cell type-specific regulation of choline acetyltransferase gene expression. Role of the neuron-restrictive silencer element and cholinergic-specific enhancer sequences.* J Biol Chem, 1996. **271**(52): p. 33358-65.
173. Mieda, M., T. Haga, and D.W. Saffen, *Expression of the rat m4 muscarinic acetylcholine receptor gene is regulated by the neuron-restrictive silencer element/repressor element 1.* J Biol Chem, 1997. **272**(9): p. 5854-60.
174. Mori, N., et al., *A common silencer element in the SCG10 and type II Na+ channel genes binds a factor present in nonneuronal cells but not in neuronal cells.* Neuron, 1992. **9**(1): p. 45-54.
175. Wood, I.C., A. Roopra, and N.J. Buckley, *Neural specific expression of the m4 muscarinic acetylcholine receptor gene is mediated by a RE1/NRSE-type silencing element.* J Biol Chem, 1996. **271**(24): p. 14221-5.
176. Ballas, N., et al., *REST and its corepressors mediate plasticity of neuronal gene chromatin throughout neurogenesis.* Cell, 2005. **121**(4): p. 645-57.

177. Otto, S.J., et al., *A new binding motif for the transcriptional repressor REST uncovers large gene networks devoted to neuronal functions.* J Neurosci, 2007. **27**(25): p. 6729-39.
178. Bruce, A.W., et al., *Genome-wide analysis of repressor element 1 silencing transcription factor/neuron-restrictive silencing factor (REST/NRSF) target genes.* Proc Natl Acad Sci U S A, 2004. **101**(28): p. 10458-63.
179. Palm, K., et al., *Neuronal expression of zinc finger transcription factor REST/NRSF/XBR gene.* J Neurosci, 1998. **18**(4): p. 1280-96.
180. Wood, I.C., et al., *Interaction of the repressor element 1-silencing transcription factor (REST) with target genes.* J Mol Biol, 2003. **334**(5): p. 863-74.
181. Calderone, A., et al., *Ischemic insults derepress the gene silencer REST in neurons destined to die.* J Neurosci, 2003. **23**(6): p. 2112-21.
182. Conaco, C., et al., *Reciprocal actions of REST and a microRNA promote neuronal identity.* Proc Natl Acad Sci U S A, 2006. **103**(7): p. 2422-7.
183. Johnson, D.S., et al., *Genome-wide mapping of in vivo protein-DNA interactions.* Science, 2007. **316**(5830): p. 1497-502.
184. Johnson, R., et al., *Evolution of the vertebrate gene regulatory network controlled by the transcriptional repressor REST.* Mol Biol Evol, 2009. **26**(7): p. 1491-507.
185. Bruce, A.W., et al., *Functional diversity for REST (NRSF) is defined by in vivo binding affinity hierarchies at the DNA sequence level.* Genome Res, 2009. **19**(6): p. 994-1005.
186. Johnson, R., et al., *REST regulates distinct transcriptional networks in embryonic and neural stem cells.* PLoS Biol, 2008. **6**(10): p. e256.
187. Andres, M.E., et al., *CoREST: a functional corepressor required for regulation of neural-specific gene expression.* Proc Natl Acad Sci U S A, 1999. **96**(17): p. 9873-8.
188. Grimes, J.A., et al., *The co-repressor mSin3A is a functional component of the REST-CoREST repressor complex.* J Biol Chem, 2000. **275**(13): p. 9461-7.
189. Huang, Y., S.J. Myers, and R. Dingledine, *Transcriptional repression by REST: recruitment of Sin3A and histone deacetylase to neuronal genes.* Nat Neurosci, 1999. **2**(10): p. 867-72.
190. Naruse, Y., et al., *Neural restrictive silencer factor recruits mSin3 and histone deacetylase complex to repress neuron-specific target genes.* Proc Natl Acad Sci U S A, 1999. **96**(24): p. 13691-6.
191. Roopra, A., et al., *Transcriptional repression by neuron-restrictive silencer factor is mediated via the Sin3-histone deacetylase complex.* Mol Cell Biol, 2000. **20**(6): p. 2147-57.
192. Nakagawa, Y., et al., *Class II HDACs mediate CaMK-dependent signaling to NRSF in ventricular myocytes.* J Mol Cell Cardiol, 2006. **41**(6): p. 1010-22.
193. Zhang, Y., et al., *SAP30, a novel protein conserved between human and yeast, is a component of a histone deacetylase complex.* Mol Cell, 1998. **1**(7): p. 1021-31.
194. Alland, L., et al., *Identification of mammalian Sds3 as an integral component of the Sin3/histone deacetylase corepressor complex.* Mol Cell Biol, 2002. **22**(8): p. 2743-50.

195. Fleischer, T.C., U.J. Yun, and D.E. Ayer, *Identification and characterization of three new components of the mSin3A corepressor complex.* Mol Cell Biol, 2003. **23**(10): p. 3456-67.
196. Hassig, C.A., et al., *Histone deacetylase activity is required for full transcriptional repression by mSin3A.* Cell, 1997. **89**(3): p. 341-7.
197. Kuzmichev, A., et al., *Role of the Sin3-histone deacetylase complex in growth regulation by the candidate tumor suppressor p33(ING1).* Mol Cell Biol, 2002. **22**(3): p. 835-48.
198. You, A., et al., *CoREST is an integral component of the CoREST- human histone deacetylase complex.* Proc Natl Acad Sci U S A, 2001. **98**(4): p. 1454-8.
199. Shi, Y., et al., *Histone demethylation mediated by the nuclear amine oxidase homolog LSD1.* Cell, 2004. **119**(7): p. 941-53.
200. Roopra, A., et al., *Localized domains of G9a-mediated histone methylation are required for silencing of neuronal genes.* Mol Cell, 2004. **14**(6): p. 727-38.
201. Tachibana, M., et al., *Set domain-containing protein, G9a, is a novel lysine-preferring mammalian histone methyltransferase with hyperactivity and specific selectivity to lysines 9 and 27 of histone H3.* J Biol Chem, 2001. **276**(27): p. 25309-17.
202. Lunyak, V.V., et al., *Corepressor-dependent silencing of chromosomal regions encoding neuronal genes.* Science, 2002. **298**(5599): p. 1747-52.
203. Shi, Y., et al., *Coordinated histone modifications mediated by a CtBP co-repressor complex.* Nature, 2003. **422**(6933): p. 735-8.
204. Ooi, L., et al., *BRG1 chromatin remodeling activity is required for efficient chromatin binding by repressor element 1-silencing transcription factor (REST) and facilitates REST-mediated repression.* J Biol Chem, 2006. **281**(51): p. 38974-80.
205. Guardavaccaro, D., et al., *Control of chromosome stability by the beta-TrCP-REST-Mad2 axis.* Nature, 2008. **452**(7185): p. 365-9.
206. Chen, Z.F., A.J. Paquette, and D.J. Anderson, *NRSF/REST is required in vivo for repression of multiple neuronal target genes during embryogenesis.* Nat Genet, 1998. **20**(2): p. 136-42.
207. Olguin, P., et al., *RE-1 silencer of transcription/neural restrictive silencer factor modulates ectodermal patterning during Xenopus development.* J Neurosci, 2006. **26**(10): p. 2820-9.
208. Armisen, R., et al., *Repressor element-1 silencing transcription/neuron-restrictive silencer factor is required for neural sodium channel expression during development of Xenopus.* J Neurosci, 2002. **22**(19): p. 8347-51.
209. Paquette, A.J., S.E. Perez, and D.J. Anderson, *Constitutive expression of the neuron-restrictive silencer factor (NRSF)/REST in differentiating neurons disrupts neuronal gene expression and causes axon pathfinding errors in vivo.* Proc Natl Acad Sci U S A, 2000. **97**(22): p. 12318-23.
210. Gates, K.P., et al., *The transcriptional repressor REST/NRSF modulates hedgehog signaling.* Dev Biol, 2010. **340**(2): p. 293-305.
211. Loh, Y.H., et al., *The Oct4 and Nanog transcription network regulates pluripotency in mouse embryonic stem cells.* Nat Genet, 2006. **38**(4): p. 431-40.

212. Singh, S.K., et al., *REST maintains self-renewal and pluripotency of embryonic stem cells.* Nature, 2008. **453**(7192): p. 223-7.
213. Buckley, N.J., et al., *Is REST a regulator of pluripotency?* Nature, 2009. **457**(7233): p. E5-6; discussion E7.
214. Jorgensen, H.F., et al., *Is REST required for ESC pluripotency?* Nature, 2009. **457**(7233): p. E4-5; discussion E7.
215. Jorgensen, H.F., et al., *REST selectively represses a subset of RE1-containing neuronal genes in mouse embryonic stem cells.* Development, 2009. **136**(5): p. 715-21.
216. Yamada, Y., et al., *Rest promotes the early differentiation of mouse ESCs but is not required for their maintenance.* Cell Stem Cell, 2010. **6**(1): p. 10-5.
217. Jorgensen, H.F. and A.G. Fisher, *Can controversies be put to REST?* Nature, 2010. **467**(7311): p. E3-4; discussion E5.
218. Kemp, D.M., J.C. Lin, and J.F. Habener, *Regulation of Pax4 paired homeodomain gene by neuron-restrictive silencer factor.* J Biol Chem, 2003. **278**(37): p. 35057-62.
219. Kania, G., et al., *Differentiation of mouse embryonic stem cells into pancreatic and hepatic cells.* Methods Enzymol, 2003. **365**: p. 287-303.
220. Blom, T., et al., *Molecular genetic analysis of the REST/NRSF gene in nervous system tumors.* Acta Neuropathol, 2006. **112**(4): p. 483-90.
221. Westbrook, T.F., et al., *A genetic screen for candidate tumor suppressors identifies REST.* Cell, 2005. **121**(6): p. 837-48.
222. Fuller, G.N., et al., *Many human medulloblastoma tumors overexpress repressor element-1 silencing transcription (REST)/neuron-restrictive silencer factor, which can be functionally countered by REST-VP16.* Mol Cancer Ther, 2005. **4**(3): p. 343-9.
223. Coulson, J.M., *Transcriptional regulation: cancer, neurons and the REST.* Curr Biol, 2005. **15**(17): p. R665-8.
224. Zuccato, C., et al., *Huntingtin interacts with REST/NRSF to modulate the transcription of NRSE-controlled neuronal genes.* Nat Genet, 2003. **35**(1): p. 76-83.
225. Marullo, M., et al., *Analysis of the repressor element-1 silencing transcription factor/neuron-restrictive silencer factor occupancy of non-neuronal genes in peripheral lymphocytes from patients with Huntington's disease.* Brain Pathol, 2010. **20**(1): p. 96-105.
226. Zuccato, C., et al., *Widespread disruption of repressor element-1 silencing transcription factor/neuron-restrictive silencer factor occupancy at its target genes in Huntington's disease.* J Neurosci, 2007. **27**(26): p. 6972-83.
227. Packer, A.N., et al., *The bifunctional microRNA miR-9/miR-9* regulates REST and CoREST and is downregulated in Huntington's disease.* J Neurosci, 2008. **28**(53): p. 14341-6.
228. Lepagnol-Bestel, A.M., et al., *DYRK1A interacts with the REST/NRSF-SWI/SNF chromatin remodelling complex to deregulate gene clusters involved in the neuronal phenotypic traits of Down syndrome.* Hum Mol Genet, 2009. **18**(8): p. 1405-14.

229. Tahiliani, M., et al., *The histone H3K4 demethylase SMCX links REST target genes to X-linked mental retardation.* Nature, 2007. **447**(7144): p. 601-5.
230. Coulson, J.M., et al., *A splice variant of the neuron-restrictive silencer factor repressor is expressed in small cell lung cancer: a potential role in derepression of neuroendocrine genes and a useful clinical marker.* Cancer Res, 2000. **60**(7): p. 1840-4.
231. Palm, K., M. Metsis, and T. Timmusk, *Neuron-specific splicing of zinc finger transcription factor REST/NRSF/XBR is frequent in neuroblastomas and conserved in human, mouse and rat.* Brain Res Mol Brain Res, 1999. **72**(1): p. 30-9.
232. Lawinger, P., et al., *The neuronal repressor REST/NRSF is an essential regulator in medulloblastoma cells.* Nat Med, 2000. **6**(7): p. 826-31.
233. Ayer, D.E., Q.A. Lawrence, and R.N. Eisenman, *Mad-Max transcriptional repression is mediated by ternary complex formation with mammalian homologs of yeast repressor Sin3.* Cell, 1995. **80**(5): p. 767-76.
234. Murphy, M., et al., *Transcriptional repression by wild-type p53 utilizes histone deacetylases, mediated by interaction with mSin3a.* Genes Dev, 1999. **13**(19): p. 2490-501.
235. Reiner, A., et al., *Differential loss of striatal projection neurons in Huntington disease.* Proc Natl Acad Sci U S A, 1988. **85**(15): p. 5733-7.
236. Formisano, L., et al., *Ischemic insults promote epigenetic reprogramming of mu opioid receptor expression in hippocampal neurons.* Proc Natl Acad Sci U S A, 2007. **104**(10): p. 4170-5.
237. Lloyd, A., et al., *Targeted mutagenesis using zinc-finger nucleases in Arabidopsis.* Proc Natl Acad Sci U S A, 2005. **102**(6): p. 2232-7.
238. Wright, D.A., et al., *High-frequency homologous recombination in plants mediated by zinc-finger nucleases.* Plant J, 2005. **44**(4): p. 693-705.
239. Urnov, F.D., et al., *Genome editing with engineered zinc finger nucleases.* Nat Rev Genet, 2010. **11**(9): p. 636-46.
240. Porteus, M.H., *Mammalian gene targeting with designed zinc finger nucleases.* Mol Ther, 2006. **13**(2): p. 438-46.
241. Beumer, K., et al., *Efficient gene targeting in Drosophila with zinc-finger nucleases.* Genetics, 2006. **172**(4): p. 2391-403.
242. Alwin, S., et al., *Custom zinc-finger nucleases for use in human cells.* Mol Ther, 2005. **12**(4): p. 610-7.
243. Bibikova, M., et al., *Targeted chromosomal cleavage and mutagenesis in Drosophila using zinc-finger nucleases.* Genetics, 2002. **161**(3): p. 1169-75.
244. Morton, J., et al., *Induction and repair of zinc-finger nuclease-targeted double-strand breaks in Caenorhabditis elegans somatic cells.* Proc Natl Acad Sci U S A, 2006. **103**(44): p. 16370-5.
245. Bibikova, M., et al., *Enhancing gene targeting with designed zinc finger nucleases.* Science, 2003. **300**(5620): p. 764.
246. Ramirez, C.L., et al., *Unexpected failure rates for modular assembly of engineered zinc fingers.* Nat Methods, 2008. **5**(5): p. 374-5.

247. Arnone, M.I. and E.H. Davidson, *The hardwiring of development: organization and function of genomic regulatory systems.* Development, 1997. **124**(10): p. 1851-64.
248. Edlund, T. and T.M. Jessell, *Progression from extrinsic to intrinsic signaling in cell fate specification: a view from the nervous system.* Cell, 1999. **96**(2): p. 211-24.
249. Sasai, Y., *Identifying the missing links: genes that connect neural induction and primary neurogenesis in vertebrate embryos.* Neuron, 1998. **21**(3): p. 455-8.
250. Mani, M., et al., *Design, engineering, and characterization of zinc finger nucleases.* Biochem Biophys Res Commun, 2005. **335**(2): p. 447-57.
251. Hurt, J.A., et al., *Highly specific zinc finger proteins obtained by directed domain shuffling and cell-based selection.* Proc Natl Acad Sci U S A, 2003. **100**(21): p. 12271-6.
252. Joung, J.K., E.I. Ramm, and C.O. Pabo, *A bacterial two-hybrid selection system for studying protein-DNA and protein-protein interactions.* Proc Natl Acad Sci U S A, 2000. **97**(13): p. 7382-7.
253. Ballas, N., et al., *Regulation of neuronal traits by a novel transcriptional complex.* Neuron, 2001. **31**(3): p. 353-65.
254. Belyaev, N.D., et al., *Distinct RE-1 silencing transcription factor-containing complexes interact with different target genes.* J Biol Chem, 2004. **279**(1): p. 556-61.
255. Cheong, A., et al., *Downregulated REST transcription factor is a switch enabling critical potassium channel expression and cell proliferation.* Mol Cell, 2005. **20**(1): p. 45-52.
256. Kuwahara, K., et al., *NRSF regulates the fetal cardiac gene program and maintains normal cardiac structure and function.* EMBO J, 2003. **22**(23): p. 6310-21.
257. Ogawa, E., et al., *Fibronectin signaling stimulates BNP gene transcription by inhibiting neuron-restrictive silencer element-dependent repression.* Cardiovasc Res, 2002. **53**(2): p. 451-9.
258. Louvi, A. and S. Artavanis-Tsakonas, *Notch signalling in vertebrate neural development.* Nat Rev Neurosci, 2006. **7**(2): p. 93-102.
259. Park, H.C., et al., *olig2 is required for zebrafish primary motor neuron and oligodendrocyte development.* Dev Biol, 2002. **248**(2): p. 356-68.
260. Zhou, Q. and D.J. Anderson, *The bHLH transcription factors OLIG2 and OLIG1 couple neuronal and glial subtype specification.* Cell, 2002. **109**(1): p. 61-73.
261. Zhou, Q., G. Choi, and D.J. Anderson, *The bHLH transcription factor Olig2 promotes oligodendrocyte differentiation in collaboration with Nkx2.2.* Neuron, 2001. **31**(5): p. 791-807.
262. Park, H.C., J. Shin, and B. Appel, *Spatial and temporal regulation of ventral spinal cord precursor specification by Hedgehog signaling.* Development, 2004. **131**(23): p. 5959-69.
263. Timmusk, T., et al., *Brain-derived neurotrophic factor expression in vivo is under the control of neuron-restrictive silencer element.* J Biol Chem, 1999. **274**(2): p. 1078-84.

264. Kallunki, P., et al., *Silencer elements modulate the expression of the gene for the neuron-glia cell adhesion molecule, Ng-CAM.* J Biol Chem, 1995. **270**(36): p. 21291-8.
265. Kallunki, P., G.M. Edelman, and F.S. Jones, *The neural restrictive silencer element can act as both a repressor and enhancer of L1 cell adhesion molecule gene expression during postnatal development.* Proc Natl Acad Sci U S A, 1998. **95**(6): p. 3233-8.
266. Okamoto, S., K. Sherman, and S.A. Lipton, *Absence of binding activity of neuron-restrictive silencer factor is necessary, but not sufficient for transcription of NMDA receptor subunit type 1 in neuronal cells.* Brain Res Mol Brain Res, 1999. **74**(1-2): p. 44-54.
267. Bergsland, M., et al., *The establishment of neuronal properties is controlled by Sox4 and Sox11.* Genes Dev, 2006. **20**(24): p. 3475-86.
268. Nomura, M., et al., *The neural repressor NRSF/REST binds the PAH1 domain of the Sin3 corepressor by using its distinct short hydrophobic helix.* J Mol Biol, 2005. **354**(4): p. 903-15.
269. Willert, J., et al., *A transcriptional response to Wnt protein in human embryonic carcinoma cells.* BMC Dev Biol, 2002. **2**: p. 8.
270. Nishihara, S., L. Tsuda, and T. Ogura, *The canonical Wnt pathway directly regulates NRSF/REST expression in chick spinal cord.* Biochem Biophys Res Commun, 2003. **311**(1): p. 55-63.
271. de la Calle-Mustienes, E., J. Modolell, and J.L. Gomez-Skarmeta, *The Xiro-repressed gene CoREST is expressed in Xenopus neural territories.* Mech Dev, 2002. **110**(1-2): p. 209-11.
272. Hornstein, E. and N. Shomron, *Canalization of development by microRNAs.* Nat Genet, 2006. **38 Suppl**: p. S20-4.
273. Kloosterman, W.P. and R.H. Plasterk, *The diverse functions of microRNAs in animal development and disease.* Dev Cell, 2006. **11**(4): p. 441-50.
274. Mortazavi, A., et al., *Comparative genomics modeling of the NRSF/REST repressor network: from single conserved sites to genome-wide repertoire.* Genome Res, 2006. **16**(10): p. 1208-21.